Aus der Neurologischen Klinik und Poliklinik

der Universität Würzburg

Direktor: Professor Dr. med. Jens Volkmann

Mapping and Neutralization of Antibodies against Neurofascin, Contactin 1, Contactin associated protein 1 and Cortactin

Inauguraldissertation

zur Erlangung der Doktorwürde der

Medizinischen Fakultät

der

Julius-Maximilians-Universität Würzburg

vorgelegt von

Katharina Karch

aus Würzburg

Würzburg, Januar 2022

Referentin:	Prof. Dr. med. Claudia Sommer
Korreferentin:	Prof. Dr. Carmen Villmann
Dekan:	Prof. Dr. med. Matthias Frosch
Tag der mündlichen Prüfung:	18.07.2022

Die Promovendin ist Ärztin

Dedicated to My Parents

Table of Contents

1 Introduction

1.1 Immune-mediated Polyneuropathies

1.1.1 General Information

Polyneuropathies (PNPs) are defined as generalized diseases of the peripheral nervous system (PNS) (1). Prevalence is estimated between 2.5 – 8 % in general population (2). Diabetic and alcohol associated PNPs are the most frequent subgroups, followed by immune-mediated PNPs (2). Several diseases belong to the latter subgroup, like the Guillain-Barré syndrome (GBS) or the chronic inflammatory demyelinating polyradiculoneuropathy (CIDP) (2). Both rank among the orphan diseases (3-5). In contrast to CIDP, which has a disease progression over more than two months, GBS is an acute neuropathy with a monophasic course of disease (2). Both diseases are characterized by unique features.

1.1.2 Guillain-Barré Syndrome

GBS is the most common cause of acute flaccid paralysis these days (2, 4). The clinical picture is characterized by acute progressive pareses, sensory deficits and areflexia (2, 4). Some patients suffer from respiratory insufficiency (2, 4). The involvement of the autonomic nervous system can also lead to cardiac arrythmia or dysfunction of bladder and intestine (2, 4). The patients often have a prior infection with Campylobacter jejuni, a bacterium of the gastrointestinal tract, but also infections with Mycoplasma pneumoniae or with distinct viruses (e.g. with cytomegalovirus, Zika virus, Epstein-Barr virus or influenza viruses) are described (2, 4, 6). This suggests immune stimulation playing an important role in the pathomechanism of the disease (4). Regarding the eventual outcome, clinical improvement can be observed in most of the patients, especially among children (2, 4). In 20% of the cases deficits remain; the mortality rate ranges between 5% and 15%, affecting mostly elderly patients with acute and severe course (2, 4).

1.1.3 Chronic Inflammatory Demyelinating Polyradiculoneuropathy

CIDP can follow a chronic-progredient or relapsing course (2, 3). Beside demyelination and elevated protein level in the cerebrospinal fluid, response to immunotherapy is a diagnostic criterion according to the European Federation of Neurological Societies (EFNS) and Peripheral Nerve Society guideline (3, 7). Tendon reflexes are attenuated

or absent. Distal as well as proximal weakness or pareses and sensory disorders characterize the typical form of CIDP (2, 3).

1.2 Autoantibodies in Immune-mediated Polyneuropathies

1.2.1 Autoantibodies against Nodal and Paranodal Proteins

Lately, autoantibodies against proteins of the nodal and paranodal region have been described in patients with immune-mediated neuropathies like CIDP or GBS. In particular, these antibodies were directed against different isoforms of Neurofascin (NF), against Contactin 1 (CNTN1) or Contactin associated protein 1 (Caspr1) (2, 3, 8-14). The mentioned proteins play an important role in the formation of the node of Ranvier (15).

1.2.2 Structure of the Node of Ranvier

In the PNS, the myelin sheath covering the axon is formed by Schwann cells (16). It is interrupted by gaps, called nodes of Ranvier. In this region a high density of voltage-gated sodium channels mediates saltatory conduction (8). Several proteins have been identified to be critical for the formation, maintenance and physiological function (Figure 1):

One of these proteins is NF, a cell adhesion molecule (15). Alternative splicing results in the expression of different isoforms, including NF140, NF155 and NF186 (15, 17). NF140 displays highest expression during embryonic development. Expression then declines and may increase again in response to demyelination (18). Its function was proposed to be largely similar to NF186 (18). NF155 and NF186 are the major isoforms in the mature nervous system (15). NF186 is a neuronal protein, interacting with gliomedin, expressed in Schwann cell microvilli (15, 17). This interaction was proposed to support the attachment of the myelin sheath to the axon (15). In addition, NF186 is linked to Ankyrin-G, a component of the cytoskeleton (17). Neuronal cell adhesion molecule (NrCAM) is also part of this nodal complex (15), leading all in all to a clustering of sodium channels (15, 17).

In contrast to NF186, NF155 is a glial protein, localized in Schwann cells (15). It interacts with CNTN1 in the paranodal region, next to the node of Ranvier (15, 17). Together with Caspr1, this complex is indispensable for keeping the paranodal loop near the axon, as well as for the separation of the potassium channels, localized in the juxtaparanode region, from the sodium channels in the nodal area (8, 15).

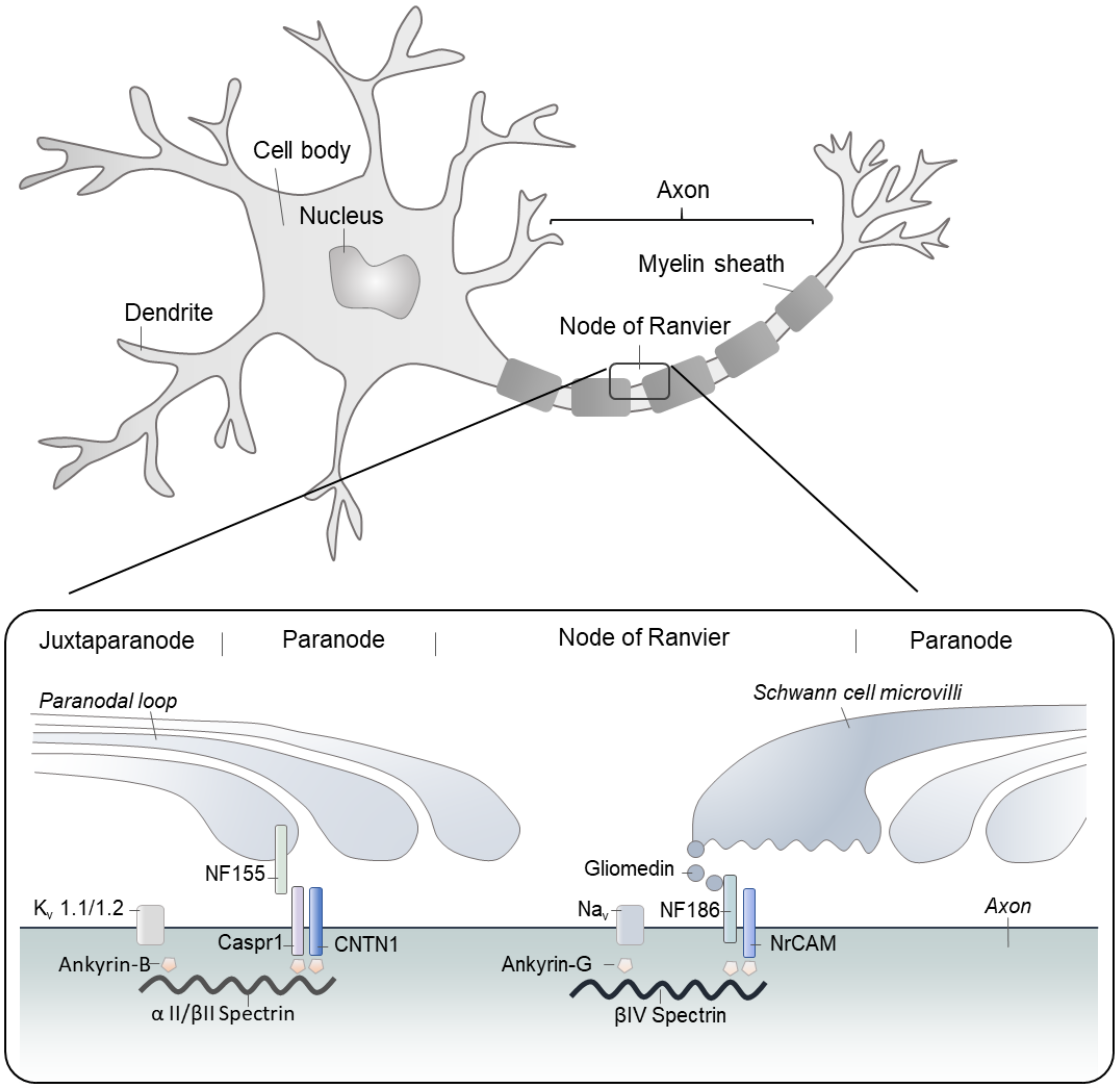

Figure 1 Simplified Illustration of the Node of Ranvier in the Peripheral Nervous System

At the top a neuron is shown (19), in the lower part the region of the node of Ranvier is displayed augmented (based on Kira et al. (15) and Vural et al. (20)).
Caspr1 = Contactin associated protein 1; CNTN1 = Contactin 1; K_v = potassium channel; Na_v = voltage-gated sodium channel; NF = Neurofascin; NrCAM = Neuronal cell adhesion molecule

1.2.3 Crucial Role of Certain Proteins for Saltatory Conduction

In mice, loss of NF155 leads to loss of CNTN1 and Caspr1 from the paranodal complex (21). As a result, the nerve conduction velocity is reduced and potassium channels invade the nodal region (15, 21). Furthermore, passive transfer experiments in animal models revealed that anti-NF155 IgG4 antibodies led to a decreased NF155 protein level, impeded paranodal formation and a reduced conduction velocity can be observed (22). This provides evidence of the pathogenic role of anti-NF155 IgG4 antibodies (22). A loss of NF186 caused either a loss of other components of the node

of Ranvier (21), leading to a migration of the paranodal loop to the node as well as to reduced concentration of sodium channels, finally reduced conduction velocity results (15, 23).

Injection of IgG3 of patients with autoantibodies against CNTN1 to Lewis rats induced an acute conduction block (24). Beside the motor conduction deficits, Manso et al. (25) described a loss of paranodal specialization by passive transfer of anti-CNTN1 IgG4. These findings indicate the pathogenicity of anti-CNTN1 antibodies (24, 25). Loss or change of CASPR1 also results in reduced conduction velocity (23).

This underlines the crucial role of the proteins for saltatory conduction. Autoantibody binding to these proteins impairs this conduction and leads to neurological symptoms like motor deficits (17, 21, 22, 24, 25). The molecular pathomechanisms are widely unknown.

1.2.4 Prevalence of (Para-) Nodal Autoantibodies

Patients with detectable autoantibodies against nodal or paranodal proteins represent a minority amongst people suffering from CIDP or GBS (3, 8). However, the percentage of those vary within a wide range (3): 2.2% - 8.7% patients with anti-CNTN1 antibodies among CIDP patients are described (10, 26-28) , 4% - 18% with anti-NF155 antibodies (14, 29-31) and less than 2% with antibodies against NF140 or NF186 (13). Anti-Caspr1 antibodies were detected in 3% of patients with CIDP in one study (8, 11). There might be several possible explanations for the high variety among different cohorts or geographical regions, e.g. genetic reasons or the different sensitivities of the applied diagnostic tests (3, 8).

1.2.5 (Para-) Nodopathy

Among patients with immune-mediated neuropathies, the ones with autoantibodies against nodal or paranodal proteins differ from the ones without (3, 8, 15, 20). They show a distinct clinical phenotype: acute onset, the focus is more on the severe motoric deficits than on sensory disorders and many of them with anti-NF or anti-CNTN1 antibodies suffer from action tremor (10, 11, 14, 26, 27, 29, 31). Regarding the treatment, especially patients with antibodies from the IgG4 subtype have a poor response to intravenous immunoglobulin, contrary to the typical phenotype of immune-mediated neuropathies (10, 11, 14, 26, 29, 32).

Another discrepancy was found within the pathomechanism (7, 11, 26, 27, 31): in nerve biopsies, there were no signs of inflammation or demyelination, the latter one even being

a diagnostic criterium for CIDP. The myelin sheath mainly stayed unaffected, instead the disorder takes place at the nodes or paranodes and elongation of the node of Ranvier results (11, 26, 31, 33, 34). Autoantibody presence leads to an impaired adhesion and axonal detachment of the myelin sheath and hence widened myelin loops (11, 15, 26, 31, 33, 34). Dispersion of the potassium and sodium channels takes place, the unique structure of the node of Ranvier is getting destroyed, eventually leading to impaired saltatory conduction (11, 15, 26, 31, 33, 34).
Because of these characteristics, which distinguish this subgroup from the classical immune-mediated neuropathies, they are nowadays termed nodopathy and paranodopathy (8, 34, 35).

1.2.6 Epitope-specific Clinical Phenotypes

Stengel et al. (36) described IgG subclass and epitope specific clinical phenotypes for anti-NF associated neuropathies. Anti-NF155-specific antibodies recognized the Fn3Fn4 domain and were mostly IgG4. Patients with these antibodies showed a subacute onset and the motor symptoms tended to be more severe than the sensory. Additionally, tremor was described. On the other hand, anti-NF associated neuropathies with autoantibodies binding the common Ig-domain were mainly IgG3 and persons affected suffered from a fulminant course of disease, tetraplegia or even almost locked-in syndrome and showed involvement of the cranial nerve. Another case report of one patient with IgG3 autoantibodies recognizing NF155, NF186 and NF140 described equal symptoms: tetraplegia and almost locked-in syndrome (37). Delmont et al. (13) compared patients with autoantibodies binding to NF186 and NF140 with patients harboring anti-NF155 autoantibodies. The clinical presentation differed between these two groups.
First, these results indicate that phenotype and severity of the disease depend on the epitopes recognized by the autoantibodies (36). Second, these data point out that the detection and characterization of autoantibodies can facilitate adequate patient therapy. Probably due to the low prevalence of CIDP and GBS, only few cases of immune neuropathies have been described. Future studies will have to decipher how the clinical picture is associated with the epitopes that are recognized by the autoantibodies (36).

1.2.7 Need to Establish Further Test Methods

Recently, in consequence of the associated characteristic clinical picture of (para-) nodopathies and the poor response to the first line therapy of typical immune-mediated neuropathies, the German Society of Neurology added the recommendation to their

guidelines to search for paranodal and nodal antibodies in suspect cases of PNPs (1). However, with a prevalence of less than 5 cases per 100 000, CIDP and GBS are currently ranked as orphan diseases (3-5). Only in a minority of this already small group nodal or paranodal autoantibodies can be detected (3, 20, 23). Thus, there is a strong need to develop further detecting methods, confirmed in the following.

It was proposed that nodal and paranodal autoantibodies not only have diagnostic utility, but are also pathogenic (9, 22-25). This is consistent with the frequently better response to plasma exchange (PE) or rituximab than to intravenous immunoglobulin (20, 32). PE leading to a fast reversal of electrophysical blockade can be better explained with removed or neutralized autoantibodies that block saltatory conduction than with remyelination (23). In addition, in a study with three anti-NF155 antibody-positive CIPD patients, decreased autoantibody level was accompanied by clinical improvement (38). Moreover, for other autoimmune diseases it could be shown that neutralization of the pathogenic autoantibodies leads to improvement of the phenotype in animal models (39). Different response to therapy was not only described in patients with and without autoantibodies (see 1.2.5). It was also proposed that response to treatment could be correlated to specific epitope patterns (39). Therefore, knowledge of the presence of autoantibodies or even of the specific autoantigen target would influence treatment decisions.

Testing sera from patients with CIDP or GBS for binding to nodal or paranodal region on teased sciatic nerves from mice revealed that 30% of CIDP and more than 40% of GBS patients showed a binding to these areas (9). More often than not the specific autoantigen could not be detected. This underlines that there may be several additional autoimmune targets in the nodes and paranodes. The discovery of novel autoantibody targets would not only accelerate the diagnosis, it would also make it safer and allow further classification into subgroups.

Taken together, studying these autoantigens and corresponding autoantibodies can open many possibilities:

(i) faster and safer diagnosis
(ii) classification into subgroups
(iii) proper treatment
(iv) disease monitoring (40)
(v) therapy response monitoring (40, 41)
(vi) antigen specific therapy (see 1.4.4) (39-41)
(vii) identification of novel autoantigens

Furthermore, discovery and characterization of nodal and paranodal antibodies facilitates the future development of robust and broadly applicable diagnostic tools.

1.3 Myasthenia Gravis

1.3.1 Characteristics

Myasthenia gravis (MG) is an autoimmune disease of the neuromuscular junction (Figure 2) (42). Prevalence ranges between 150 and 250 per one million (42). Causative are antibodies against the acetylcholine receptor (AChR), less frequently against the muscle-specific kinase (MuSK) or lipoprotein receptor-related protein 4 (LRP4) (42-44). Patients suffer from weakness of the skeletal muscles, which fatigue unusual fast (42).The symptoms are less severe in the morning than in the evening, with variability each day (42). The most frequently affected muscles are ocular muscles (42). The disease can be restricted to this muscle group but can also be generalized (42, 45). Beside the typical clinical picture, the detection of autoantibodies against the described targets is an important diagnostic criterion (42).

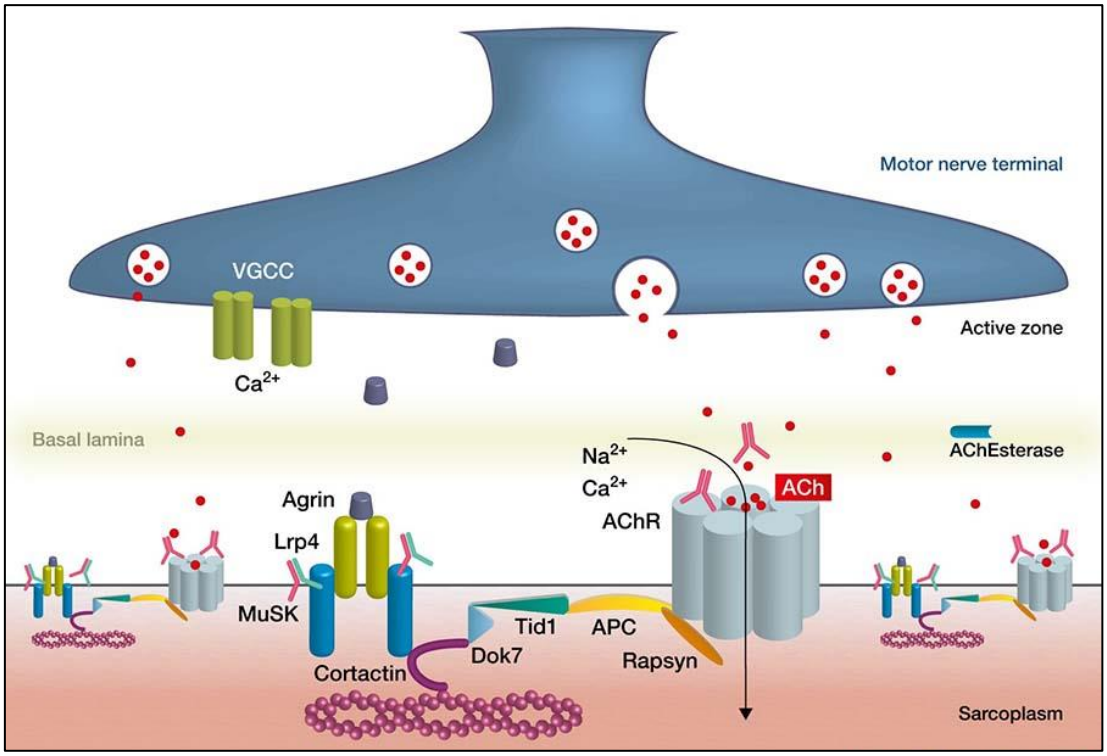

Figure 2 Neuromuscular Junction

Source: Illa et al. (43), used by permission of the author. © Hospital de la Santa Creu i Sant Pau. Endplate proteins are the targets of autoantibodies in myasthenia gravis (MG), e.g. AChR, MuSK or Cortactin. Cortactin promotes clustering of AChR (42, 43). Ach = acetylcholine; AChR = acetylcholine receptor; APC = adenomatous polyposis coli; Dok7 = downstream of tyrosine kinase 7; Lrp4 = lipoprotein receptor-related protein 4; MuSK = muscle-specific kinase; Tid1 = tumorous imaginal disc 1; VGCC = voltage-gated calcium channel

1.3.2 Double-seronegative Myasthenia Gravis

Among patients with generalized MG, about 80% have autoantibodies against AChR, up to 8% against MuSK (43, 44). Within the remaining, no antibodies against these two antigens are detectable (43). This subgroup is called double-seronegative myasthenia gravis (dSNMG) (43). By now, several autoantibodies against other proteins than AChR or MuSK have been detected among some of these patients, but not in all (45). The current lack of biomarkers and knowledge on the autoantibodies strongly impedes diagnosis and treatment in the group of seronegative patients (45).

1.3.3 Autoantibodies against Cortactin in Patients with dSNMG

In 2014, Gallardo et. al (46) described Cortactin as a potential new target in patients with dSNMG. Nearly 20% of people diagnosed with dSNMG showed antibodies against this antigen, as against only 4.8% of $AChR^+$ MG and 5% of the healthy controls (46).
Cortactin is a protein of the neuromuscular junction, interacting with MuSK, LRP4 and Agrin, and promoting the clustering of AChR (43) (Figure 2).
dSNMG patients with antibodies against Cortactin show distinct characteristics, which separate them from MG patients with AChR antibodies, among them: enhanced frequency of ocular or mild generalized forms, disease onset at younger age and often lack of bulbar signs (45). As Cortactin autoantibodies were also described in other neuromuscular autoimmune disorders as well as in healthy controls, the pathogenic role in MG patients is not yet clear (45). Nevertheless, detection of this biomarker in patients with dSNMG helps to diagnose autoimmune MG and find an appropriate treatment like immunosuppressive therapies (43, 45, 46). Especially in patients with ocular dSNMG, Cortactin as a routinely tested target might be supporting, as – in contrast to generalized MG – about one half of this group have no detectable AChR antibodies (43, 45). Moreover, pharmacological and electrophysiological tests used for differential diagnosis of ptosis and diplopia are not always definite, pointing out the relevance of such a biomarker (45).
All in all, a test for the detection of Cortactin antibodies would facilitate the diagnosis and treatment decision of MG.

1.4 Autoantibody Detection and Characterization in Microarray Format

1.4.1 Development of Antibody Detection Methods

Human antibodies were initially detected in radioimmunoassays, first described in the 1960s (47), and enzyme-linked immunosorbent assay (ELISA), first described in the

1970s (48-50). ELISA can be performed in many variants, including an indirect version to detect specific antibodies (51). For this purpose, wells are coated with antigen, blocked, incubated with antibody or anti-sera, washed, incubated with an enzyme-linked secondary antibody and washed again (51). By the adding of substrate, bindings can be detected.

Another method for autoantibody detection are peptide microarrays. In the 1990s, first fully synthetic approaches for the display of biomolecules were described (52, 53). Among them the so-called SPOT-synthesis, a method to produce peptide sequences for binding experiments and, consequently, to study protein-protein interactions at the molecular level (53). Automatization of the array production, further miniaturization and the integration of the production and evaluation workflows established peptide microarrays as state-of-the-art method for the detection and characterization of antibodies in vitro as well as in physiological samples (54-56).

1.4.2 Advantages of Peptide Microarrays

The success of ELISA may be explained amongst others by the sensitivity, the reproducibility and the various modified versions adapted for the specific target of investigation (51). Anyway, using peptide microarrays has some advantages over ELISA (57). A multiplex analysis can be done in high-throughput, a large number of probes like sera can be tested on arrays displaying several antigens at once. This offers the possibility to discover new autoantigens from a research perspective (57). Furthermore, identified autoantibodies can be characterized regarding their binding epitope in a very high resolution, up to a single amino acid resolution (57). Whereas the expression, purification and validation of the antigens required for ELISA is elaborate, the synthesis of the peptides used for the microarrays can be done fully automatic, being relatively economical, and the produced peptides are very stable (51, 57, 58). The sensitivity of microarrays is proposed considerably higher compared to ELISA, the amount of required patient sample relatively low (58, 59).

1.4.3 Microarrays applied in Multiple Sclerosis Research

Over decades, the potential of antigen and peptide arrays for autoantibody profiling has been proven (40, 41, 57). For multiple sclerosis (MS), an inflammatory disease of the central nervous system, microarrays have been successful used to identify subgroup specific serum autoantibody pattern (59). To specify the received autoantibody reactivity, Quintana et al. (59) preincubated the sera with the respective unbound peptide. A similar

method of validation was established in this thesis (see 2.3.4). Furthermore, a nontargeted approach using arrays with protein fragments aiming to explore the autoantibody repertoire in MS has been conducted (60). Based on these findings, a novel autoantibody target was identified (61).

Once autoantigens are discovered, the binding epitope can be fine mapped with the help of peptide microarrays. In MS research, high-density peptide arrays have already been used for profiling autoantibody reactivities (62, 63). Hereby, an adapted peptide library design allows a single amino acid resolution.

1.4.4 Microarray Application in this Thesis

Likewise in the described MS research, peptide microarrays can be used for the issues explained in 1.2.7 and 1.3.3. Sera of patients with immune-mediated neurological diseases like CIDP, GBS or MG can be tested on peptide microarrays for autoantibodies against several antigens simultaneously. Novel antigens could be identified and identified targets could be further characterized according to the binding epitope in a setting with higher density. Together, this provides the possibility to classify further subgroups of autoimmune diseases related with different clinical phenotype and different prognosis. This finally leads to faster and safer diagnosis. Therapeutic potential of autoantibody neutralization can be evaluated with the knowledge of the exact binding epitope, leading to antigen-specific, individualized therapy (40, 41). For other autoimmune diseases, it has already been shown that a targeted neutralization of pathogenic autoantibodies leads to clinical improvement in animal models (39). Furthermore, monitoring of disease progression, epitope spreading (41, 57, 58) and therapy response (40, 41) could be conducted with the gained information about the autoantibody binding epitope.

Taken together, peptide microarray can be used and developed as a diagnostic tool, in research issues as well as in point-of-care diagnostic. Many studies have been conducted using protein or peptide arrays as a screening tool. However, their current applications are limited by high false-positive rates. Consequently, technical verification and validation of the results is essential and particular attention should be paid to this point (57). To establish a way of validating the received output within the same peptide microarray method is the central point of this thesis. The value of methods investigating the autoantibody specificity has already been proposed (57).

2 Materials and Methods

2.1 Ethic Vote

The ethics committee of the medical faculty of the Julius-Maximilians-University Würzburg has permitted the use of patient sera within this project (no. 278/13 and 222/20).

2.2 Materials

2.2.1 Equipment and Consumables

Important equipment used in this thesis is listed in Table 1. Consumables are tabulated in Table 2.

Table 1 List of Equipment

Device	Source	Product name
Balances	A&D Company, Ltd.	FZ-300i
Centrifuge Rotor	Thermo Scientific Thermo Scientific	TX-400 M20
Centrifuges	Benchmark Labnet VWR	MyFuge Mini Prism R Mega Star 1.6R
Imaging system	Azure	c400
Laboratory bottles	Simax	GL45; 100, 250, 500, 1000ml
Liquid dispenser	Brand	Dispensette S
Magnetic stirrer	Carl Roth	MH 15
Measuring cylinders	VWR	25, 50, 100, 250, 500, 1000 ml
Microarray contact printer	Intavis	SlideSpotter
Orbital Shaker	Scientific Industries	Mini-100 Orbital-Genie
Peptide synthesizer	Intavis	MultiPep RSi
pH-meter	VWR	pHenomenal pH 1100 L
Pipette	Rainin Eppendorf	Pipet-Lite LTS Pipette L-1000XLS+ Pipet-Lite LTS Pipette L-200XLS+ Pipet-Lite LTS Pipette L-20XLS+ Pipet-Lite LTS Pipette L-2XLS+ Research plus, 0,1-2,5 µl, E-1860

Pipette (multichannel)	Brand	Transferpette S-12
Pipette (stepper)	Eppendorf	Multipette M4
Pipette controller	Brand	Accu-jet pro
Serological pipette	Sarstedt	5, 10, 25 ml
Shaker/incubator	Eppendorf VWR	Thermo Mixer C Thermal Shake lite
Slide tray plates	MoBiTec	4 well
Tube roller	Phoenix	RS-TR-5
Vacuum pump	VWR	Mini diaphragm vacuum pump
Vortex	Scientific Industries	Vortex-Genie 2

Table 2 List of Consumables

Consumable	Source	Product Name/Additional information
Conical tubes	Sarsted	15, 50 ml
Gloves	VWR	NITRILE Light
Pipette tips	Biozym Eppendorf	SurPhob; 20, 200, 1000 µl epT.I.P.S. 0.1-10µl
Pipette tips (stepper)	Eppendorf	Combitips advanced; 5, 10, 25, 50 ml
Reaction tubes	Sarstedt	0.2, 0.5, 1.5, 2, 5 ml
Well plates	Eppendorf Intavis	Deepwell plate 96/100 µl 384 well plate

2.2.2 Key Resources

Table 3 shows a survey of the key reagents and resources used within methods of this thesis.

Table 3 List of Key Resources

Reagent or resource	Source	Identifier
Antibodies, primary:		
Anti-Caspr1 antibody	Abcam	ab34151
Anti-CNTN1 antibody	Abcam	ab66265
Anti-Cortactin antibody	OriGene	TA590298
Anti-NF antibody	Abcam	ab31457

Antibodies, secondary: Goat Anti-rabbit IgG, HRP-linked Goat anti-human IgG, HRP-linked	 Cell Signaling Technology ThermoFisher Scientific/Invitrogen	 7074 31410
Cellulose paper: Whatman Grade 50	GE Healthcare	1450-916
Detection Reagents: SuperSignal West Femto Maximum Sensitivity Substrate	Thermo Scientific	34095
Peptides: CNTN1_017 CNTN1_018 CNTN1_036 Caspr1_090 Caspr1_091 Caspr1_018 NF183_083 NF140_065 NF155_071 NF155_072 NF155_032 Cort_008 Cort_012 Cort_013 Cort_018 Cort_027	Dr. Shuang-Yan Wang, RVZ Würzburg	N.A.
Red dye for CelluSpot Markers	Intavis	54. 115
Sera: Patient 1-5, Healthy Control 1-3	Universitätsklinikum Würzburg, Neurologische Klinik	N.A.
Slides: White coated slides (CelluSpot blank slides)	Intavis	54.112

2.2.3 Chemicals

Chemicals including buffer ingredients, solvents as well as other reagents were purchased from Iris, Sigma-Aldrich, Carl Roth or VWR.

2.2.4 Software

Software used to carry out experiments, analyze the data and illustrate the results is specified in Table 4.

Table 4 List of Software

Software	Reference
Array Analyze	https://www.activemotif.com/
ClustalOmega, Multi Sequence Alignment	https://www.ebi.ac.uk/Tools/msa/clustalo/
Laura	Intavis
Microsoft Office	https://products.office.com/de-de
MultiPep	Intavis
OriginPro 2019	https://www.originlab.com/
Paint.net	https://www.getpaint.net/
UniProt	https://www.uniprot.org/

2.3 Methods

2.3.1 Autoantigen Display in Microarray Format

2.3.1.1 Library Design

The antigens of interest were included in the peptide library like described in Table 5. Corresponding amino acid sequences were subdivided into peptides with a length of 25 amino acids (AA), overlapping in ten AA and differing in 15 from the relative peptide before (Figure 3). Signal sequence is not included. Each peptide got a specific name, consisting of the protein name and a sequential number, e.g. CNTN1_021. For a more detailed presentation of the library see Table A1 - Table A6. Further description of the microarrays including the numbering of the spots is pointed out in 2.3.1.3.

Table 5 Overview of the Displayed Antigens

Antigens were subdivided into peptides having a length of 25 AA, offset at 15 AA, overlapping in 10 AA. The last two displayed peptides of each antigen may overlap in more than 10 AA. As the isoforms of NF have parts of the sequence in common, for NF140 and NF155 only the peptide fragments that differ from NF186 library are included, explaining their shorter library. For the antibodies anti-CNTN1 (ab66265) and anti-NF (ab31457) a positive control is included on E01 and E02 (anti-CNTN1_1 and anti-CNTN1_2) or rather on K01 and K02 (anti-NF_1 and anti-NF_2) (see Table A1 and Table A5). The positive control peptides for CNTN1 are overlapping in 5 AA. CNTN1 and Caspr1 are displayed on a common microarray (slides called “CC”) as well as NF186, NF140, NF150 and Cortactin are displayed together (slides called “NC”).

Antigene	Source	Length*	n	Spots	Library**
CNTN1 **(Human)**	Uniprot ID Q12860-1, residue 21-1018	25	66	A01-C18	WSY-010-Reprinted II
Caspr1 **(Human)**	Uniprot ID P78357-1, residue 20-1384	25	91	G01-J19	WSY-010-Reprinted II
NF186 **(Human)**	Uniprot ID O94856-1, residue 25-1347	25	88	A01-D16	WSY-010-Reprinted I
NF140 **(Human)**	Uniprot ID A0A386QWI1-1, residue 805-1054	25	16	E01-E16	WSY-010-Reprinted I
NF155 **(Human)**	Uniprot ID O94856-3, residue 25-1160	25	75	F01-I03	WSY-010-Reprinted I
Cortactin **(Human)**	Uniprot ID Q14247-1, residue 1-550	25	36	M01-N12	WSY-010-Reprinted I

* length of the peptides ** internally name of the library

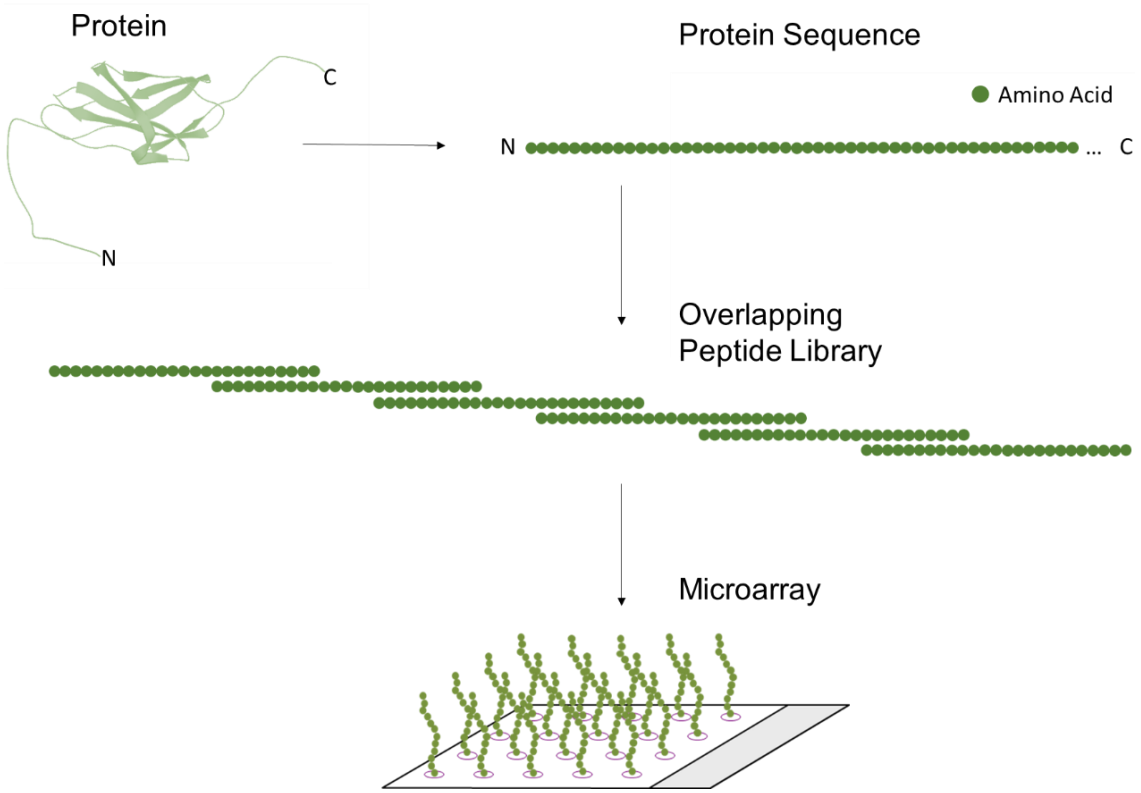

Figure 3 Overlapping Library Design

The outlined protein is CNTN1 (Uniprot ID Q12860-1, (64)). The amino acid sequence of the protein is divided into overlapping peptides with a length of 25 AA: overlapping in 10 AA from the peptide before and after. The peptides are synthesized and then printed on chips (2.3.1.2, 2.3.1.3).

2.3.1.2 Peptide Synthesis

Peptides were synthesized and worked-up by Dr. Shuang-Yan Wang and Sonja Kachler, using µSPOT, a modified variant of the SPOT synthesis principle (53, 65, 66). In brief, peptides are synthesized on 9-Fluorenylmethyl-oxycarbonyl (Fmoc)-β-alanine-functionalized cellulose with the help of a liquid handling robot (MultiPep RSi, Intavis). Up to 1536 peptides can concurrently be synthesized by this Fmoc-based automated Solid-Phase Peptide Synthesis (SPPS) (65). The dissolved peptides are transferred into 384 well plates.

2.3.1.3 Printing

Subsequently, the peptides are printed as peptide-cellulose conjugates (PCCs) in microscope slide format (7.5 cm x 2.5 cm) using a Slide Spotting Robot. This approach provides peptide microarrays displaying 768 peptides in a format of 2 x 16 x 24 PPCs, a duplicate of 384 spots. The spots are numbered from A01 to P24 on each duplicate, the letter naming the row, the number describing the column. Red points surrounding the

peptides act as a marker (Figure 4). After printing, the 384 well plates with the dissolved peptides are stored at -80°C and the slides were left to dry for at least three hours at room temperature (RT).

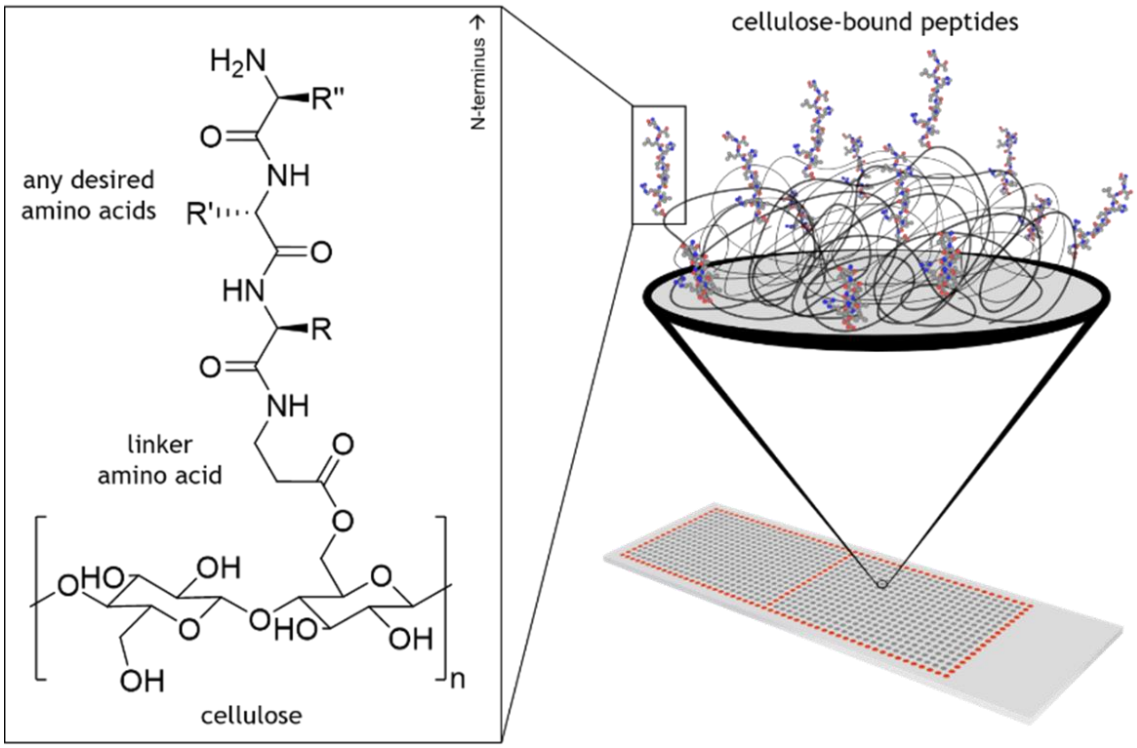

Figure 4 Microarray Format

On each spot specific peptide-cellulose conjugates (PCCs) are printed, all in all a duplicate of 384 PCCs on one slide. As they are invisible, red points are printed for orientation. On the left it is shown how the peptides are linked to cellulose. Figure provided by Mark Löbel (RVZ Würzburg).

2.3.2 Mapping in Microarray Format

2.3.2.1 General Proceeding

Figure 5 gives an overview of the assay. To avoid unspecific binding, the microarrays were blocked with 3 ml 1% (w/v) bovine serum albumin (BSA; Carl Roth) in 1 × phosphate-buffered saline (PBS; 137 mM NaCl, 2.7 mM KCl, 10 mM Na_2HPO_4, 1.8 mM KH_2PO_4, pH 7.4) for 15 minutes on shaker plate at ~50 rounds per minute and RT. Afterwards, the slides were incubated for the same time on the rotator with 2.3 – 3.0 ml of different dilutions of primary antibody or patient sera. For the primary antibodies, the concentration ranges between 1:10 000 and 1:250 000, for the patient sera between 1:100 and 1:5 000. This is followed by washing steps: incubation with 3 ml buffer (1% BSA in 1 × PBS) for 5 minutes, two or three times. Subsequently, the slides were incubated with the same amount of secondary antibody specific for the primary

antibody, diluted 1:10 000. For this thesis, goat anti-rabbit IgG (Cell Signaling Technology, #7074) and goat anti-human IgG (ThermoFisher Scientific/Invitrogen, 31410) were used as secondary antibodies, both connected to horseradish peroxidase (HRP). After this, the slides were washed again with 3 ml buffer for 5 minutes, two or three times.

In every experimental series there is at least one control slide running, being not incubated with primary antibody or patient sera. Instead of this step, incubation with buffer takes place. The rest stays the same. Table 6 shows the summarized steps.

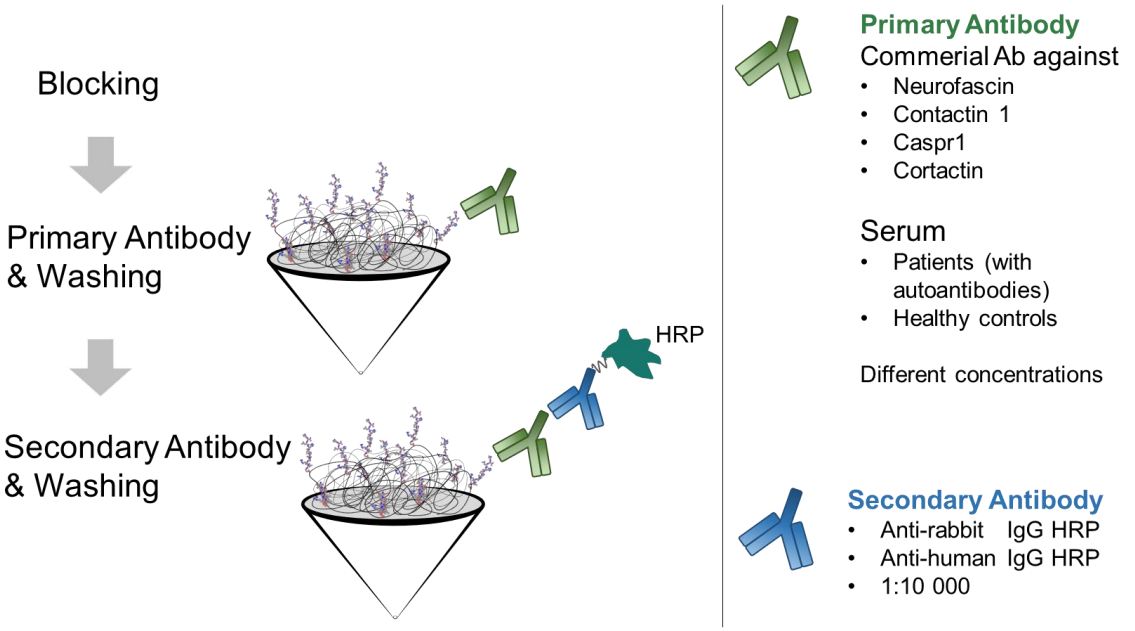

Figure 5 Schema of Assay in Microarray Format

After Blocking, the slides were incubated with primary and secondary antibody, with washing steps in between and in the end.

Table 6 Assay in Microarray Format: Workflow

All steps at room temperature; blocking, incubation and washing always on shaker plate. Buffer = 1% BSA in 1 × PBS

No.	Step	Reagent	Solvent	V [ml]	t [min]	Repeats
1	Blocking	/	buffer	3	15	/
2	Incubation	Primary antibody/Sera	buffer	2.3 - 3	15	/
3	Washing	/	buffer	3	5	2-3 ×
4	Incubation	Secondary antibody	buffer	3	15	/
5	Washing	/	buffer	3	5	2-3 ×

2.3.2.2 Mapping of Patient Sera

For the mapping of sera, the peptides of the NF libraries were printed on the microarrays (slides “NC”, see Table 5). Sera of patients and healthy controls were diluted 1:500, 1:1 500 and 1:4 500. 2.3 ml of the solutions were taken to incubate the slides. As secondary antibody goat anti-human IgG HRP-linked (ThermoFisher Scientific/Invitrogen, 31410) was chosen, diluted 1:10 000.

2.3.2.3 Mapping of Commercial Antibodies

Four polyclonal IgG antibodies raised in rabbit were studied, enumerated in Table 7. Initially, the antibodies were tested at 1:10 000 to 1:250 000 dilution, while the secondary antibody (goat anti-rabbit IgG HRP-linked, Cell Signaling Technology, #7074) was kept at 1:10 000 (Data not shown). Best results were achieved with primary antibody concentration 1:10 000 and 1:50 000. Accordingly, the screen was conducted n=3 using primary antibody concentration 1:10 000, 1:25 000 and 1:50 000 as specified in 3.2. Dilution of the secondary antibody stayed at 1:10 000. The control slides were not incubated with primary antibody.

For the experimental runs with anti-CNTN1 and anti-Caspr1, the slides “CC” were used, with the CNTN1 library (Table A1) as well as the Caspr1 library (Table A2) printed on the surface (see Table 5). Incubation with anti-NF or anti-Cortactin took place on the microarrays “NC”, displaying the libraries of NF (Table A3 – Table A5) and Cortactin (Table A6).

Table 7 List of Primary Antibodies used for Fine Mapping and Neutralization

Antibody	Source, Identifier	Host species	Clonality	Iso-type	Immunogen
Anti-CNTN1	Abcam, ab66265	rabbit	polyclonal	IgG	residues 250-350 of mouse CNTN1 (ab74597)
Anti-Caspr1	Abcam, ab34151	rabbit	polyclonal	IgG	residues 1350 to C-Terminus of Mouse Caspr1 (ab34150)
Anti-NF	Abcam, ab31457	rabbit	polyclonal	IgG	residues 1150 to C-Terminus of mouse NF (ab33377)
Anti-Cortactin	OriGene, TA590298	rabbit	polyclonal	IgG	residues 175-274 of human Cortactin (NM_005231)

2.3.3 Chemiluminescent Detection of Binding Events

For detection of binding events, the slides were incubated with 200 µl of SuperSignal West Femto Maximum Sensitivity Substrate, containing Luminol and Peroxide. On the spots with bonded antibodies, HRP, attached to secondary antibody, can catalyze a reaction on which photons are radiated (67), detectable with Azure c400 imaging system. Washing steps with 0.1 % tris-buffered saline with Tween20 (0.5M Tris, 1.5M NaCl, 1ml Tween 20 (0.1%) for 1l, H_2O, pH 7.5) after finishing the assay reduce unspecific binding and often lead to clearer results.
This chemiluminescent detection is very sensitive and can be done in high-throughput. The pictures output by the machine are evaluated with Array Analyze.

2.3.4 On-chip Validation of Binding Events

2.3.4.1 Principle and Value of On-chip Neutralization

Once the epitopes targeted by the antibody are identified, competition assays are both useful and necessary to explore the specificity of the antibody. The value of this method was already proposed (57). A way to integrate this validation within the same methods and working steps already used for mapping was designed in this thesis and is described in the following.
The peptides that showed the strongest signals and therefore the strongest binding to the antibody were resynthesized as cleavable conjugates. Preincubation of the corresponding antibody with excess of the putative binding peptides is expected to neutralize the antibodies. Consequently, corresponding binding signals should disappear. A reduction of antibody binding by on-chip neutralization with the identified target would confirm autoantibody specificity (57). To be able doing this validation within the same method provides flexibility according to novel targeted peptides as well as economic and time-related advantages.
Various critical parameters had to be thought of: It had to be ensured that the synthesized peptide fragments are pure and soluble. The adequate concentration range for the peptide to incubate with primary antibody had to be calculated and, subsequently, the required amount from synthesis. The ideal neutralization would be an economic approach and therefore the synthesis should be feasible in high-throughput using the identical nano scale synthesis that was used for production of the initial microarray. Furthermore, since peptide epitope/antibody affinities are unknown, peptides were used in excess over the antibodies.

2.3.4.2 High-throughput Peptide Synthesis

The additional peptides used for this method could be produced in parallel to the peptides used for the slides and in nanomolar scale. Hence, there was no need to buy purified peptides as it was possible to synthesize them in high-throughput within the same methods used for the peptide microarrays, with Fmoc-based automated SPPS.
On SPPS and by cleaving the peptides from cellulose there is unavoidable a loss of material, so the output is estimated around 40% from the original ~1 200 nmol per peptide fragment. Accordingly, the amount of substance might be about 500 nmol. This was dissolved in 90 µl buffer (1% BSA in 1 × PBS) and 10 µl dimethyl sulfoxide.

2.3.4.3 Neutralization in Solution

For the experiments, the dissolved peptides were diluted 1:50 up to 1:125 000, resulting in final concentrations of 100 µmol/l to 40 nmol/l. First, the diluted primary antibody was incubated with different concentrations of the peptide in relation 1:1 (1.2 ml of both reagents) for 30 minutes at 4°C on the shaker by 650 pm. After blocking (see 2.3.2.1) the composition of peptide and antibody is incubated on the slides for 15 min at RT. Additionally, there were two control slides: one incubated with 1.2 ml of the primary antibody dilution mixed with 1.2 ml buffer, the other slide with 2.4 ml buffer. The following steps are identical with the assay described before: two or three washing steps, incubation with secondary antibody (goat anti-rabbit IgG HRP-linked, Cell Signaling Technology, #7074, diluted 1:10 000) before the wells are washed again. The whole setting is illustrated in Figure 6.
Signals corresponding to the binding between the antibody and the specific peptide on the microarray are expected to be neutralized: antibodies binding to the peptide fragments in solution are not available anymore for interaction with the respective immobilized peptides on the slides. At the same time this would be evidence of the interplay between the antibody and the distinct epitope.

In detail, the assays were conducted as described in the following. In a first experimental row, each of the four antibodies was diluted 1:50 000 and got incubated with one of the corresponding peptides diluted 1:50, 1:500 and 1:5 000 (~100 µmol/l, ~10 µmol/l, ~1 µmol/l) (Figure A7 - Figure A14). The neutralization was distinct clearer to notice with the higher concentrated peptides and the signal slowly showed up again by using the 1:5 000 diluted peptide solution. Consequently, the following assays were run with a 1:120 (~42 µmol/l) dilution of the 16 synthesized peptides, primary antibody

concentration stayed at 1:50 000. The experiments were conducted three times and standard deviations were calculated. This validated output is demonstrated in 3.3.

In order to show that the signal of the primary antibody is getting stronger again with lower amount of the neutralizing peptide, another experimental run (n=1) was done with peptide NF155_072 (see 3.3.5). Concentration of anti-NF (ab31457) stayed constant at 1:25 000, whereas for the peptide fragment a dilution series was prepared, starting with 1:50 (~100 µmol/l), going over 1:2 500 (~2 µmol/l) and ending with 1:125 000 (~40 nmol/l). One slide got incubated with primary antibody on its own, without soluble peptide. Another control slide with neither anti-NF nor peptide, just secondary antibody (goat anti-rabbit IgG HRP-linked, Cell Signaling Technology, #7074, diluted 1:10 000), was included as well.

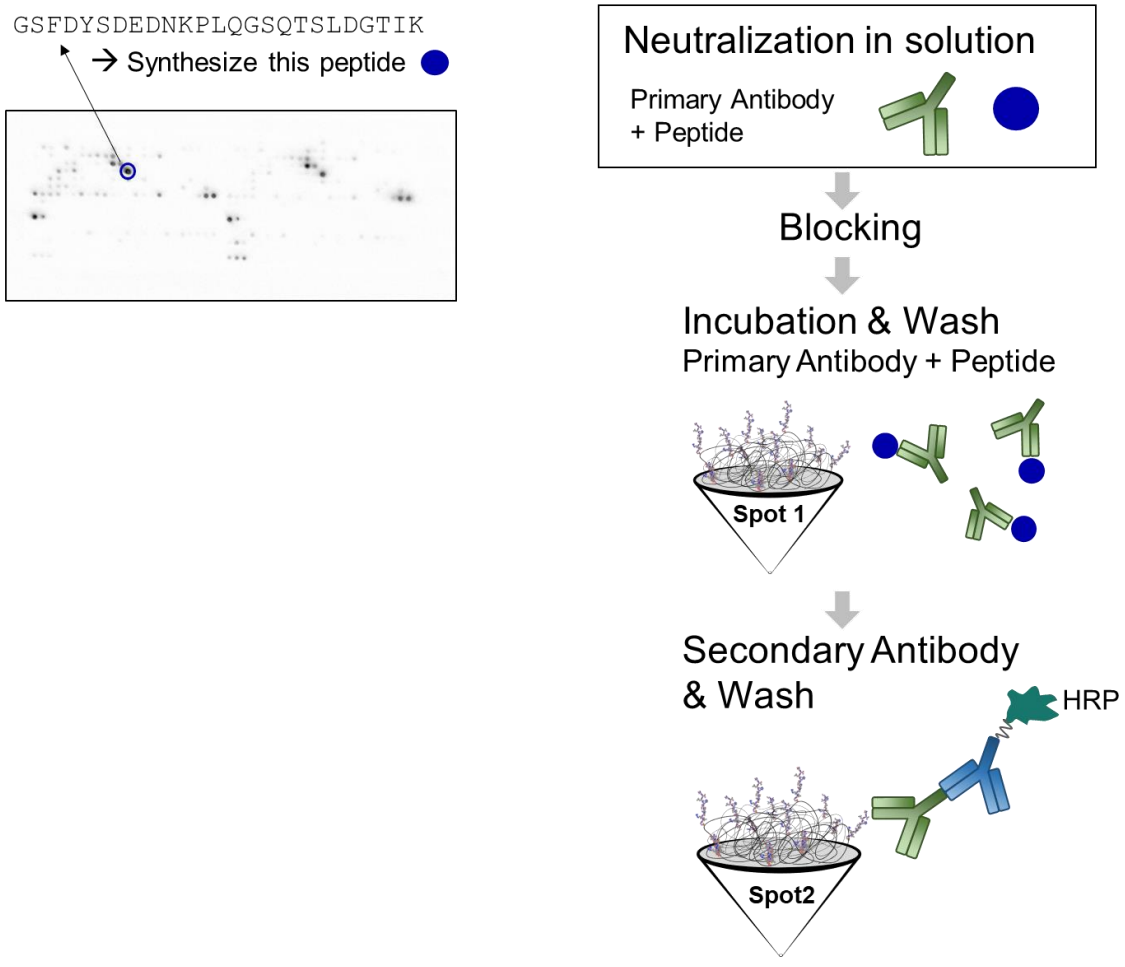

Figure 6 Validation of Binding Events: Neutralization in Solution

On the left a picture received from Azure c400 imaging system is shown. A peptide with strong binding to the antibody according to the strong, black signal is chosen and resynthesized. It is taken for incubation with primary antibody in solution, in expectation of neutralizing the signal. The following steps are the same as pictured in Figure 5.

3 Results

3.1 Microarray-based Characterization of Patient Sera

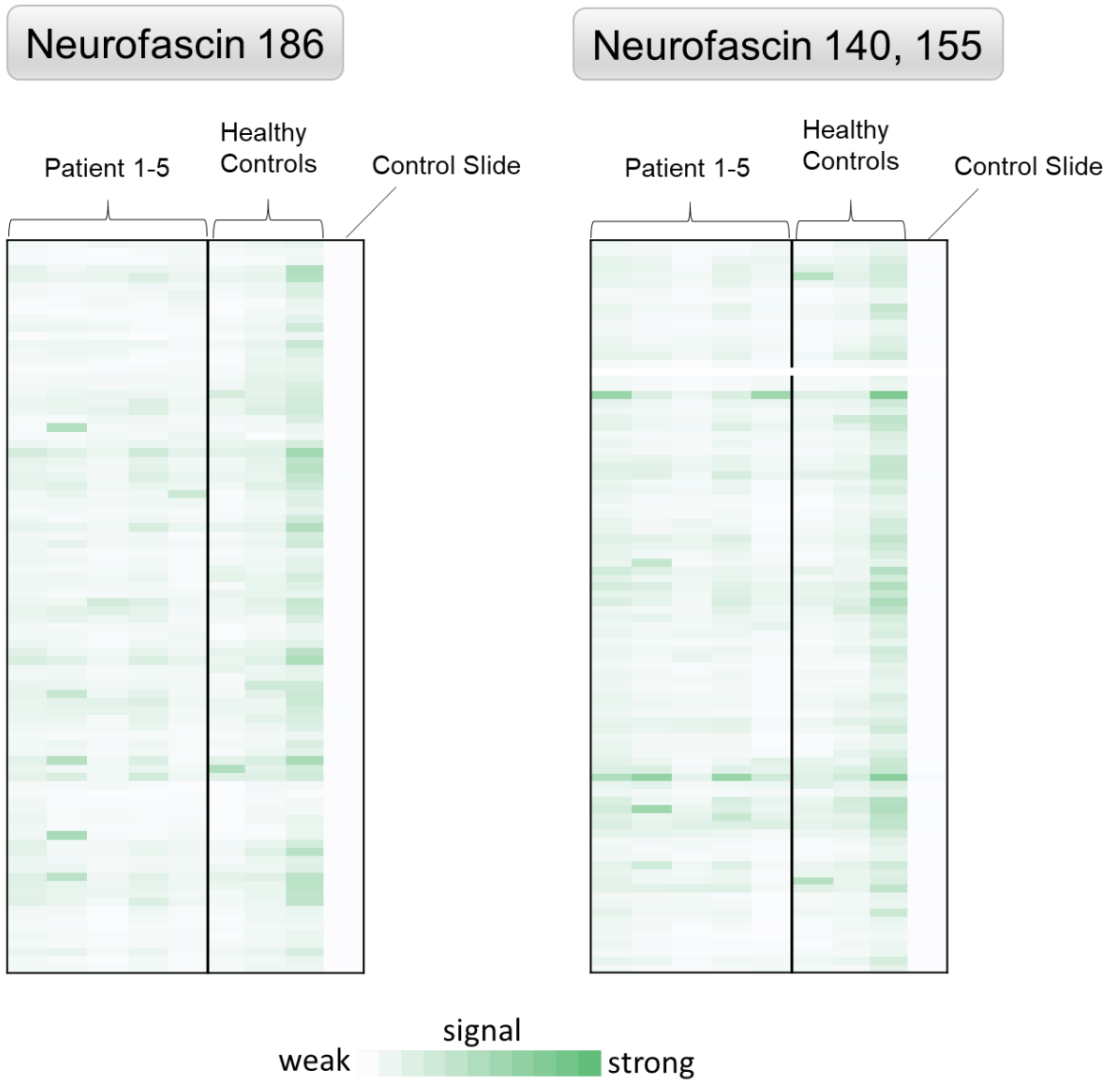

Figure 7 Binding of Antibodies in Patient Sera to NF Peptide Libraries visualized by Chemiluminescence

Results of the 1:500 diluted patient sera are shown. Each column stands for one sample, from left to right: patient 1-5, healthy control 1-3, control slide. Each row stands for one specific epitope from the NF library (Table A3 - Table A5). On the left part of the figure, the library for NF186 is illustrated, on the right for NF140 and NF155. The darker the color of one field is, the stronger is the binding between autoantibodies in this serum and the specific peptide on the slide. The binding signals are sample specific and reproducible. On the control slides almost no signal was measured. Note that the chosen experimental setup does not allow for unambiguous identification of the actual binding epitope.

Five patient sera with autoantibodies against NF detected by ELISA at the University Hospital Würzburg, Department of Neurology, were tested on in-house produced autoantigen microarrays. The patients were diagnosed with immune-mediated neuropathies, more precisely with CIDP. Patient 1 - 4 had detectable NF155 - specific antibodies, Patient 5 anti-pan-NF autoantibodies, directed against NF155, NF186 and NF140. Three healthy control sera were tested as well.
The assay was performed as described in 2.3.2.2. The results are shown in Figure 7 (for raw data see Figure A1). The binding signals were sample specific and reproducible even at dilutions higher than corresponding ELISAs (12, 36), resulting in lowered sample consumption. Yet, the significance of these results is not clear. The aim of this thesis is to develop an approach which would unambiguously identify signals received from the microarrays representing the specific epitope. Using commercially available antibodies I demonstrate fine mapping and binding site validation using on-chip neutralization (2.3.4, 3.3).

3.2 Fine Mapping of Commercial Antibodies

The results of fine mapping for the four commercial antibodies (see Table 7) are specified in the following paragraphs. Raw data are displayed in Figure A2 – Figure A6.

3.2.1 Fine Mapping of Anti-CNTN1 (ab66265)

The assays were performed as per description (2.3.2.3). Figure 8 shows the binding intensity received from imaging system and charted in this graph. On the left part of the figure the signals from the whole library are illustrated. The right zoomed-in part focuses on the regions with the strongest intensity average. Three epitopes of the library show a clear binding signal: CNTN1_017 and CNTN1_018 and the positive control 2 (labeled anti-CNTN1_2 in the graph). The more diluted the antibody is, the weaker the signal gets. The control slide shows no binding for these spots. Neither the peptide fragments before and after CNTN1_017 and CNTN1_018 show a signal, nor the positive control 1. Accordingly, the microarray data suggests that the amino acid fragment “RKVLEPMPST” (bold AA in Figure 8 and Figure 9) is an essential part of the binding epitope. The identified binding epitope is part of the approx. 100 amino acid fragment that was used for raising the antibodies (Figure 8, AA marked blue).

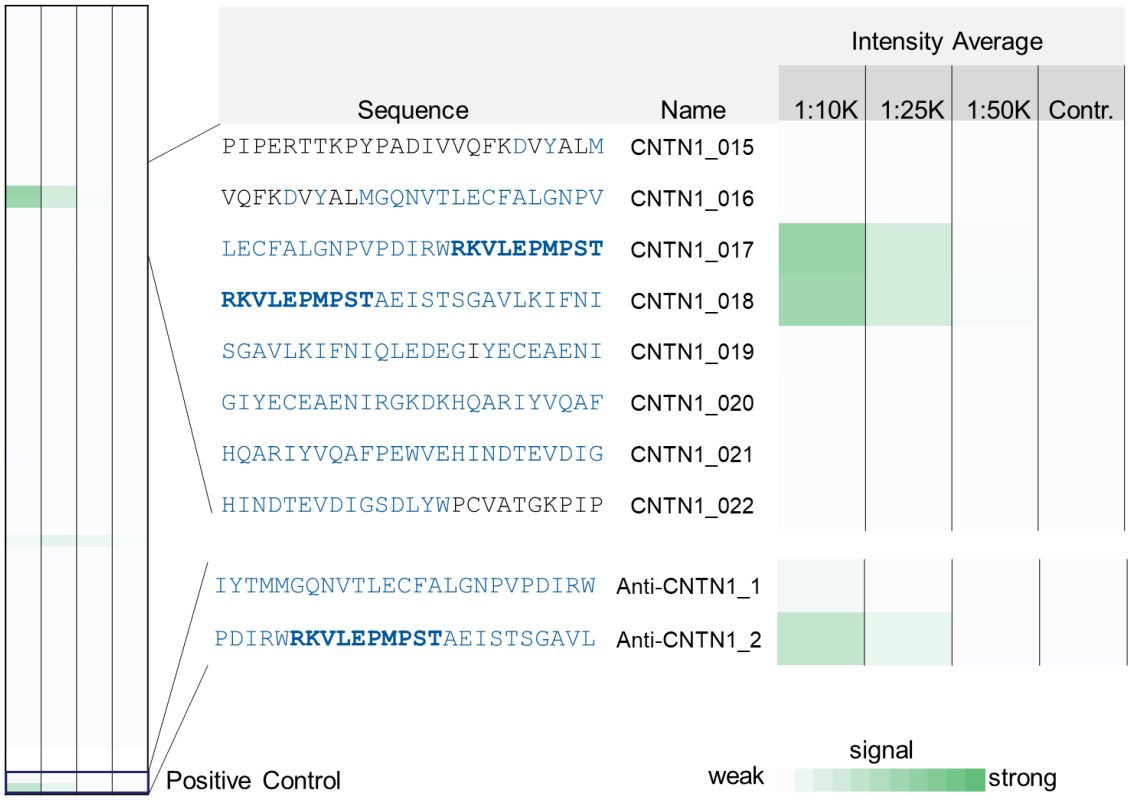

Figure 8 Epitope Mapping of Anti-CNTN1 (ab66265)

On the left the whole library for CNTN1 (Table A1) is shown, with every row representing one specific epitope. In the end of the library a positive control is included. The columns from left to right show the results for the different primary antibody concentrations: 1:10 000, 1:25 000, 1:50 000 and for the control slide on the very right. The right part of the picture allows a closer look at the region of the antigen against which the primary antibody was raised, symbolized by the blue letters. The bold AA seem to play a key role for the interplay with primary antibody.

In Figure 9, the raw data for primary antibody concentration 1:10 000 are displayed and the results are transferred in a bar graph together with the standard deviation from n=3 measurements. On the x-scale the spots of the CNTN1 library are shown (positive control excluded), on the y-scale the intensity average of the signals received from the assay, normalized to black dots standing for the strongest possible signal with the intensity 1.0. It is clearly recognizable that anti-CNTN1 binds mainly to CNTN1_017 and CNTN1_018. The corresponding spots on the slides are marked, their sequence is written down. These two spots with the strongest binding were synthesized again for subsequent experiments (3.3.1), as well as the peptide CNTN1_036, acting as negative control.

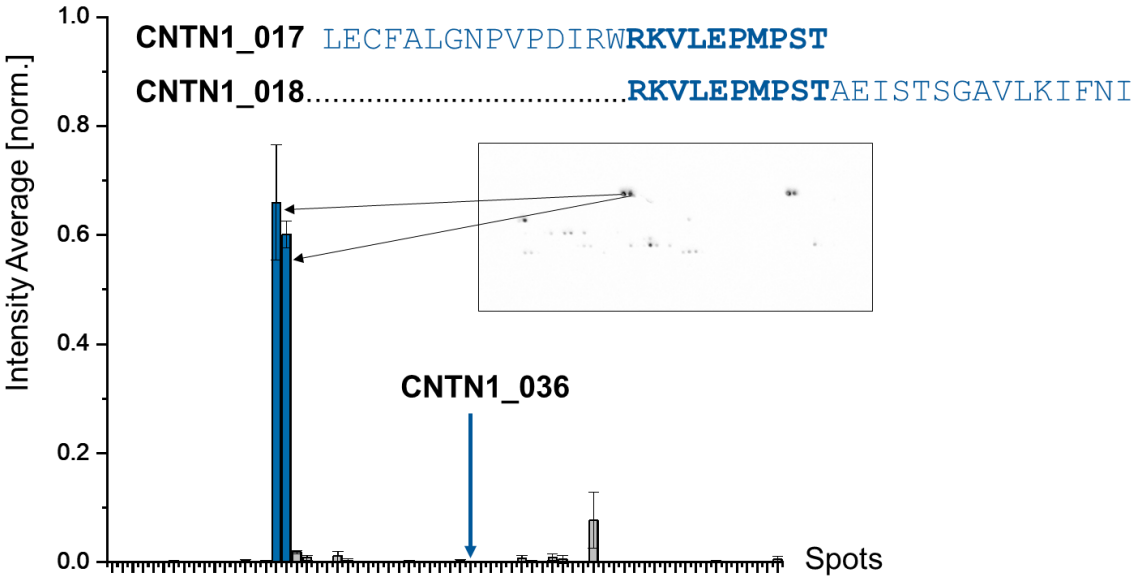

Figure 9 Chart of Anti-CNTN1 (ab66265) Fine Mapping

Results for primary antibody concentration 1:10 000. The intensity average on the y-scale is normalized to black dots. On the x-scale the CNTN1 library (excluding positive control) is shown with every peptide represented by one spot. The standard deviation is demonstrated by bars. For the peptides corresponding with the strongest binding (blue colored bars), the amino acid sequence is given. One spot with low signal is marked as well and taken as negative control for following tests described in 3.3.1. On the included raw data, the two hits region is marked.

3.2.2 Fine Mapping of Anti-Caspr1 (ab34151)

Incubation of the Caspr1 peptide library (slides “CC”, see Table 5) with anti-Caspr1 (ab34151) is shown in Figure 10 and Figure 11.

Figure 10 displays on the left the intensity average of the whole Caspr1 library (Table A2), whereas the right part represents the sector where the binding took place. The commercial antibody was raised against the three last spots of the library, represented by the blue written AA. Indeed, the strongest signal was received from the latest peptides, but only from the latest two. These two peptide fragments are even overlapping in 20 AA, as they are on the end of the library. Binding Signals for Caspr1_090 and Caspr1_091 suggest that residues “APTPAPAPGPRDQNLPQILE” (bold in Figure 10 and Figure 11) are an essential part of the binding epitope.

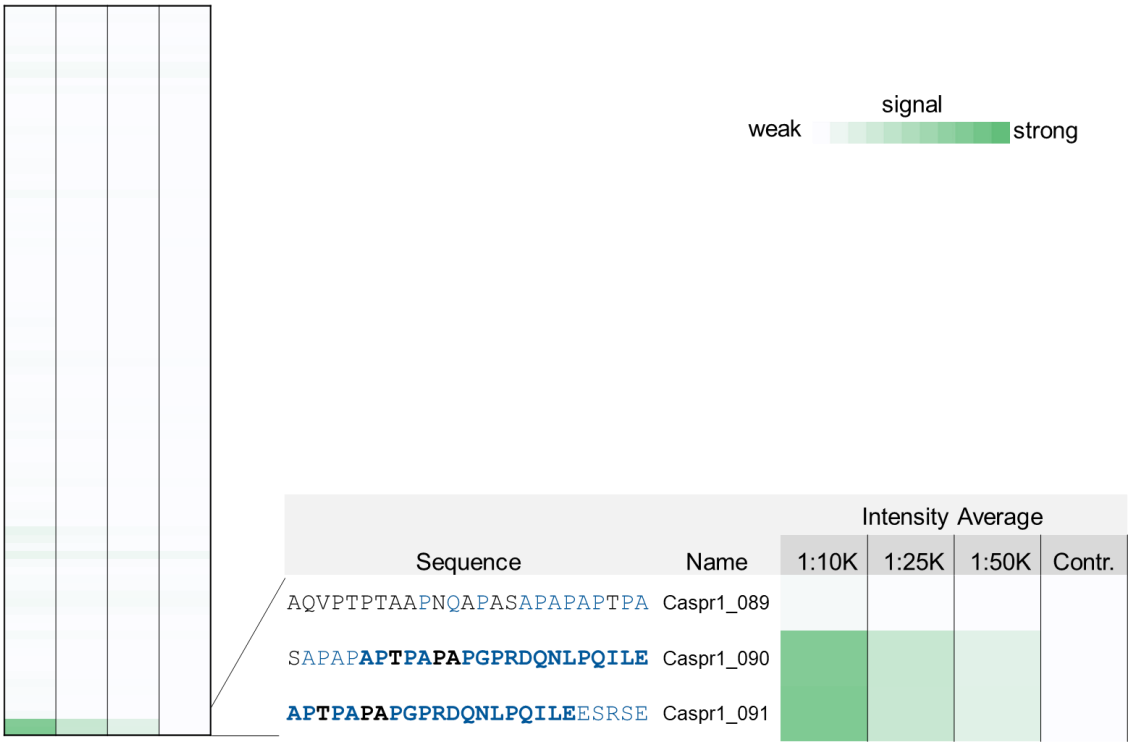

Figure 10 Epitope Mapping of Anti-Caspr1 (ab34151)

On the left the whole library for Caspr1 is represented with every raw standing for one specific epitope. The columns show the results for the different primary antibody concentrations (from left to right: 1:10 000, 1:25 000, 1:50 000) and for the control slide on the very right. The enhanced part of the picture gives a closer look to the region of the antigen against which the primary antibody was raised, symbolized by the blue colored letters. AA written in bold seem to be crucial for binding.

Figure 11 shows the results of the 1:10 000 diluted anti-Caspr1. The epitope responsible for the binding with the antibody can be easily described: Caspr1_090 and Caspr1_091 have the highest signal intensity by far.

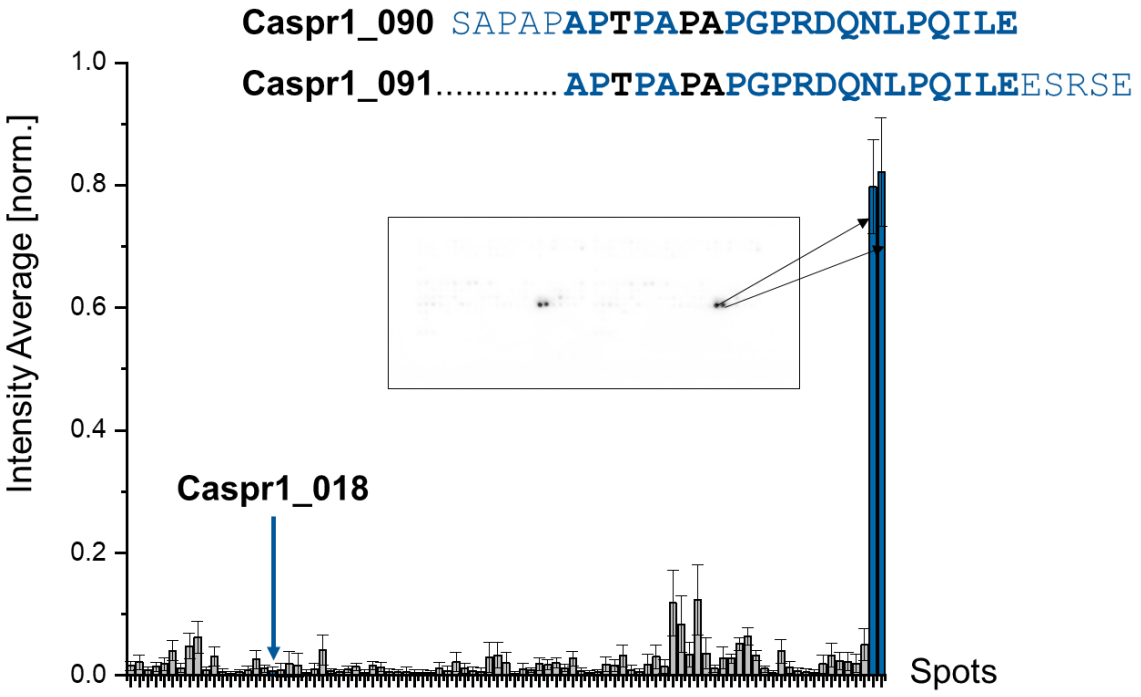

Figure 11 Chart of Anti-Caspr1 (ab34151) Fine Mapping

Results for primary antibody concentration 1:10 000. A picture of the original output is included. Normalized intensity average on the y-scale, Caspr1 library on the x-scale. Error bars demonstrate standard deviation. The last two balks represent the intensity of the spots with the strongest binding to the antibody, also marked on the peptide microarray. Their amino acid sequence is given. Another peptide (Caspr1_018) is labeled and taken in the following for validation (3.3.2).

3.2.3 Fine Mapping of Anti-NF (ab31457)

Anti-pan-NF antibody (ab31457) used in this thesis is raised against the common C-Terminus of the isoforms NF186, 155 and NF140. Except the signal sequence, the whole protein NF186 is printed on the slides. For the other two isoforms, only the peptide fragments that differs from NF186 library were collected in the library, so the identical spots are just synthesized and printed once (see Table 5). A positive control is integrated at the end of NF library. The slides (“NC”) got incubated with anti-pan-NF. Figure 12 gives an overview of the results, the signals received from the whole NF library are shown.

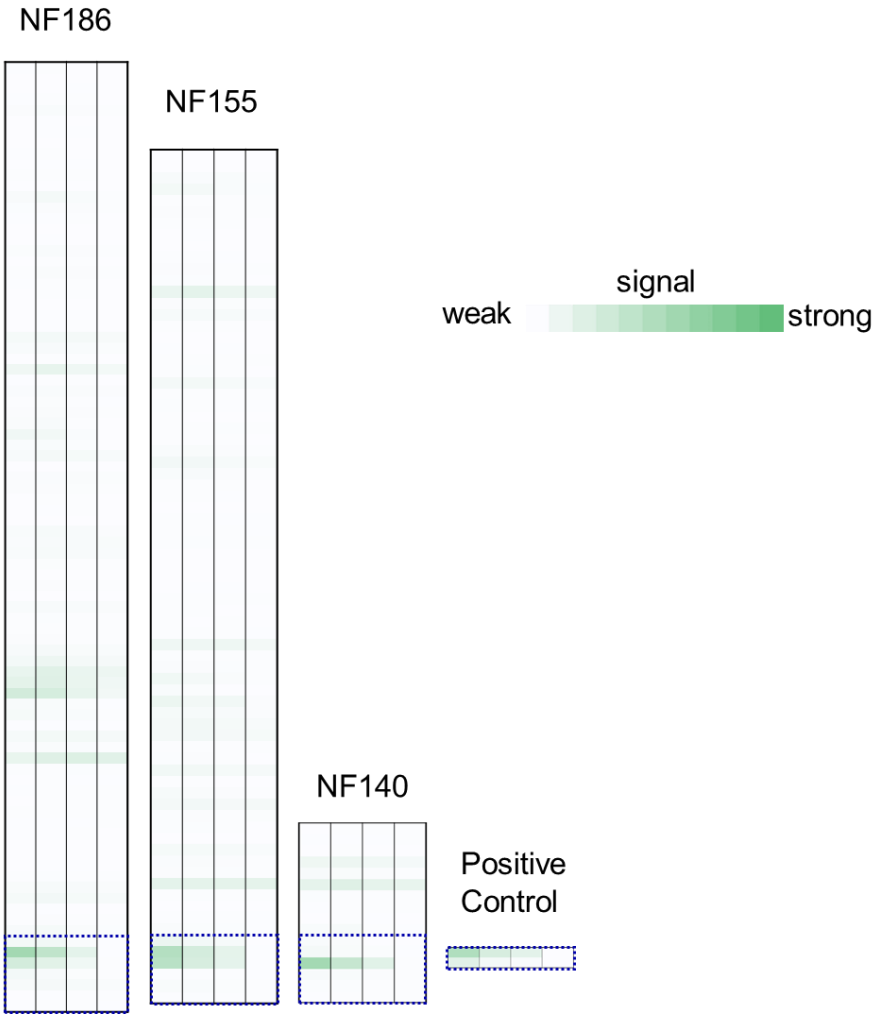

Figure 12 Overview of Anti-NF (ab31457) Fine Mapping

Overview of the NF library, with every row representing one distinct epitope (see Table A3 – Table A5). For the isoforms as well as for the positive control four columns are shown, standing for the primary antibody concentrations (from left to right: 1:10 000, 1:25 000, 1:50 000) and for the control slide on the very right. The framed regions are illustrated more detailed in Figure 13.

The key region of the library is illustrated in Figure 13 more detailed. The part of the sequence, anti-NF was raised against, is colored blue. Binding signals from all isoforms as well as from the positive control were mainly received from spots containing the amino acid fragment “DYSDEDNKPL” (written bold in Figure 13 and Figure 14), suggesting this epitope being crucial for the interplay.

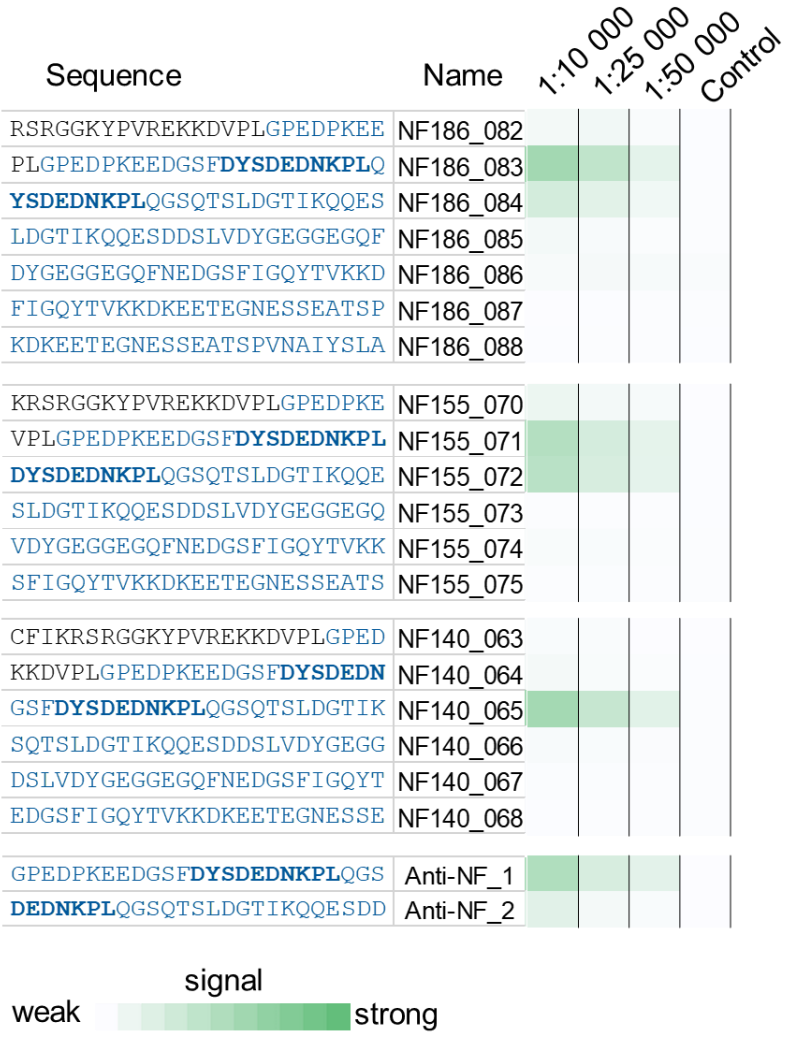

Figure 13 Details of Anti-NF (ab31457) Fine Mapping

This figure shows the regions where the binding took place. The three isoforms of NF as well as a positive control (Anti-NF_1 and Anti-NF_2) are included. The blue colored AA stand for the ones the primary antibody was raised against. Data indicates that the bold AA are necessary for binding.

The results for the assays with the highest primary antibody concentration are represented in a chart (Figure 14). The bars of the peptide fragments with the highest signal are shown in blue. By a comparison of the sequences it becomes clear that residues “DYSDEDNKPL” (written bold) are an essential part of the recognized binding epitope.

For validation, NF186_083, NF155_071, NF155_072 and NF140_065 are produced again with SPPS, equally NF155_032. The latter gives almost no signal and is taken as negative control (3.3.3).

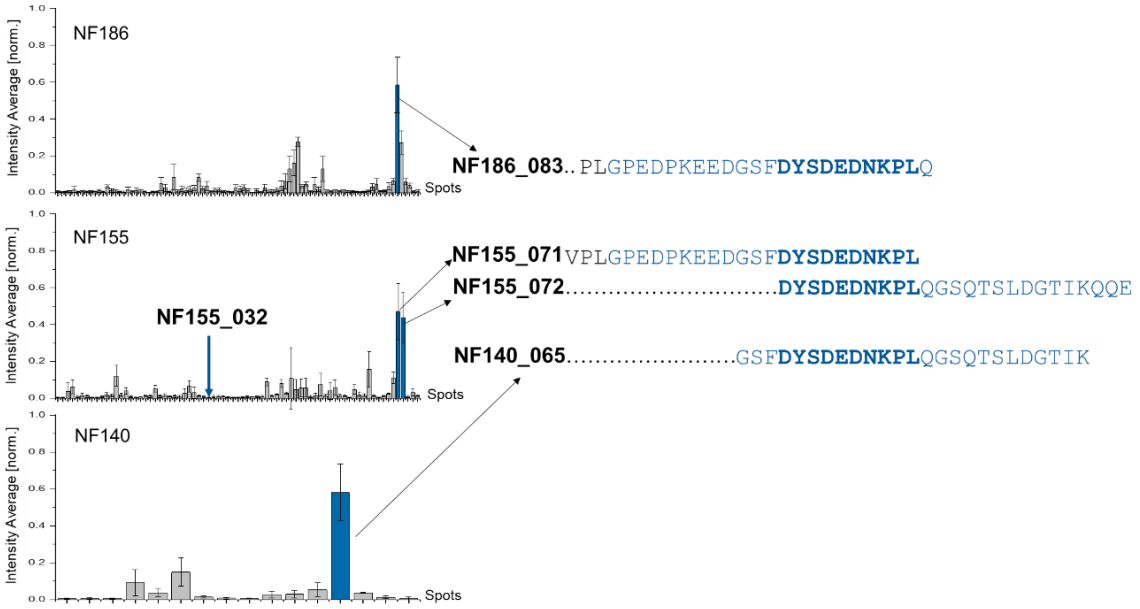

Figure 14 Chart of Anti-NF (ab31457) Fine Mapping

The charts show the results for primary antibody concentration 1:10 000. Normalized intensity average on the y-scale, the library of the respective NF isoform on the x-scale, with every spot representing one distinct epitope (positive control excluded). The upper chart demonstrates the signals received from NF186 library, in the middle NF155 library is shown and in the lower part the library of NF140. Standard deviation is demonstrated by bars. For the spots with the strongest signal (blue colored bars), the amino acid sequence of the peptide is given. NF155_032 is also marked, given low signal and taken for negative control in validation like described in 3.3.3.

3.2.4 Fine Mapping of Anti-Cortactin (TA590298)

Cortactin is an antigen with many repeats in his sequence (see Table A6). In Figure 15 the results of incubation with anti-Cortactin (TA590298) are shown together with an overview of the whole library and the relevant region as zoom-in. Signals were dose-dependent and no signal was received from the control slide. The AA the antibody was raised against are written in blue. The output indicates that the binding mainly takes place at only a part of this sequence, but additionally on outlying spots. This can be explained by the repeats within the antigen:

The sequences of the four peptide fragments with the strongest binding – highlighted in Figure 15 – are compared in Figure 16. They have a short epitope in common, with slightly individual differences. The shared sequence might be responsible for the interplay. As this common epitope can be also found in other spots in modified variants, extenuated signals are likewise received from these peptide fragments.

Cort_008, Cort_012, Cort_013, Cort_018 and Cort_027 are synthesized again for further experiments (3.3.4).

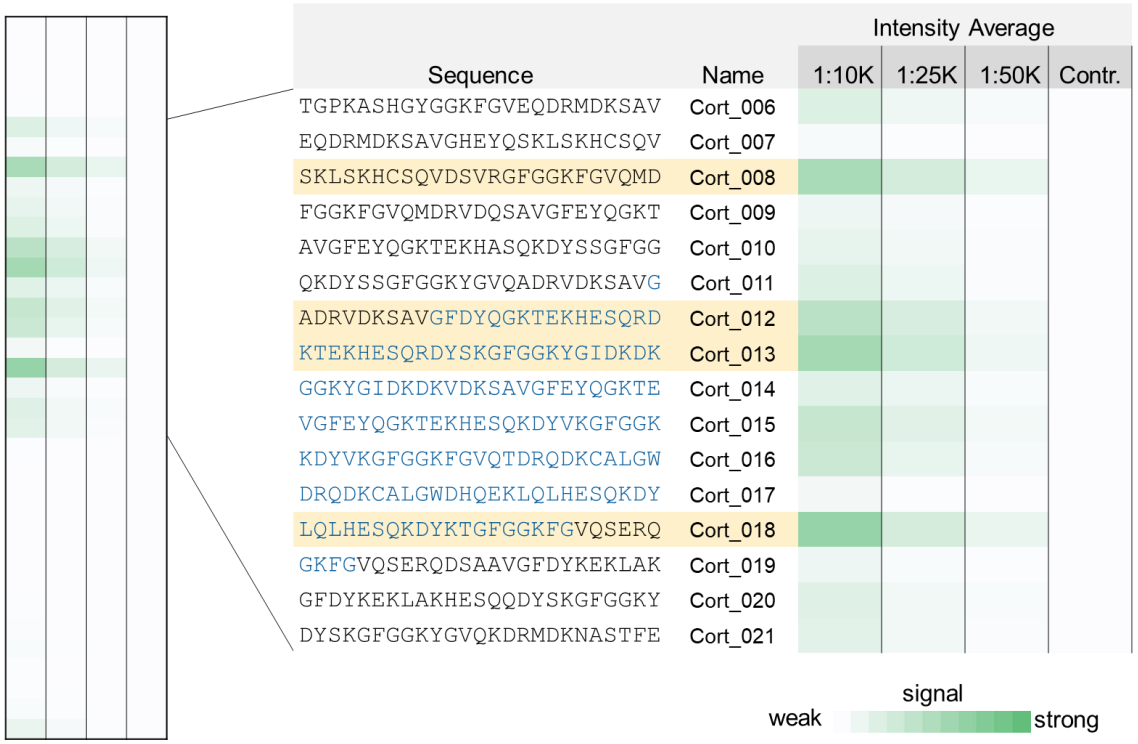

Figure 15 Epitope Mapping of Anti-Cortactin (TA590298)

On the left part of the figure Cortactin library is shown, with every row representing one specific epitope. Primary antibody concentrations 1:10 000, 1:25 000, 1:50 000 and the control slide are shown by the columns from left to right. The region with detectable signals is enlarged on the right. The blue marked AA stand for the sequence against which the primary antibody was raised against, the highlighted peptides are the ones with the strongest binding to the antibody. Their sequences are compared in Figure 16.

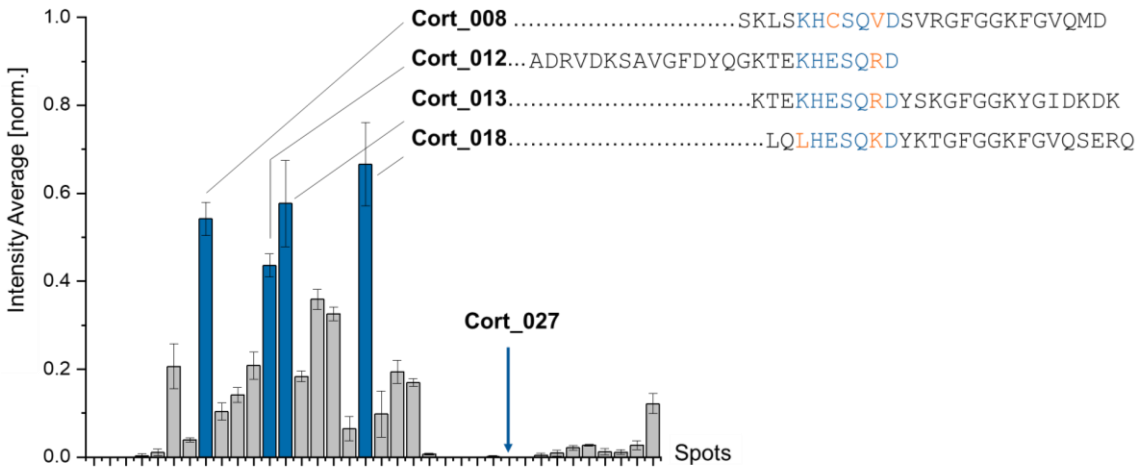

Figure 16 Chart of Anti-Cortactin (TA590298) Fine Mapping

Primary antibody concentration 1:10 000 gives the results shown in this chart. Normalized intensity average on y-scale, Cortactin library on x-scale. Standard deviation is demonstrated by bars. The spots with the strongest signal are blue colored and labeled with the related amino acid sequence. The common AA of these peptides are written in blue, those with slightly variability in between the shared sequence are orange marked. Cort_027 gives low signal and is chosen for validation (3.3.4).

3.3 Neutralization of Commercial Antibodies

Binding signals were validated via on-chip-neutralization using newly synthesized peptides (technical description in 2.3.4). The peptides chosen for this validation are marked in 3.2 for the respective antigens. The results are demonstrated in the following, raw data are displayed in Figure A15 - Figure A18.

3.3.1 Neutralization of Anti-CNTN1 (ab66265)

Figure 17 Neutralization of CNTN1 Binding Events

The CNTN1 library (Table A1) is represented on the left, one specific epitope corresponding to one row. In the end a positive control is included. The columns from left to right show the results for incubation of the 1:50 00 diluted antibody with the 1:120 diluted peptides CNTN1_017 (first column), CNTN1_018 (second column), CNTN1_036 (third column). The fourth column demonstrates the results received from the antibody without peptide, the very right column stands for the control slide with neither primary antibody nor peptide (just secondary antibody).
The right part of the figure shows the results for the key region of the library more detailed. The blue highlighted AA in the sequence are the ones the primary antibody was raised against. The epitope responsible for the binding is written in bold.

CNTN1_017 and CNTN1_018 showed the strongest signal at fine mapping of anti-CNTN1 (see 3.2.1). Therefore, these two peptide fragments were taken for validation. CNTN1_036 was used as negative control as almost no signal was received from this spot. The incubation of the first two peptides with anti-CNTN1 (ab66265) led to an

extenuated or even a disappearing signal, whereas the negative control peptide hardly weakened the intensity (Figure 17). CNTN1_017 neutralizes the signal of both binding spots. Incubation with CNTN1_018 prevents the antibody from binding to this epitope on the microarrays, represented by the fading signal. Nevertheless, under these conditions there is still an interaction between spot CNTN1_017 and the antibody, even though a weaker one, indicating a stronger binding of anti-CNTN1 to CNTN1_017 over CNTN1_018.

Figure 18 shows the results transferred to a chart. The grey bars demonstrate the intensity average received from primary antibody without any peptide. After incubation with CNTN1_017 the signal disappeared, CNTN1_018 extenuates the intensity far more compared to the negative control, especially for spot CNTN1_018.

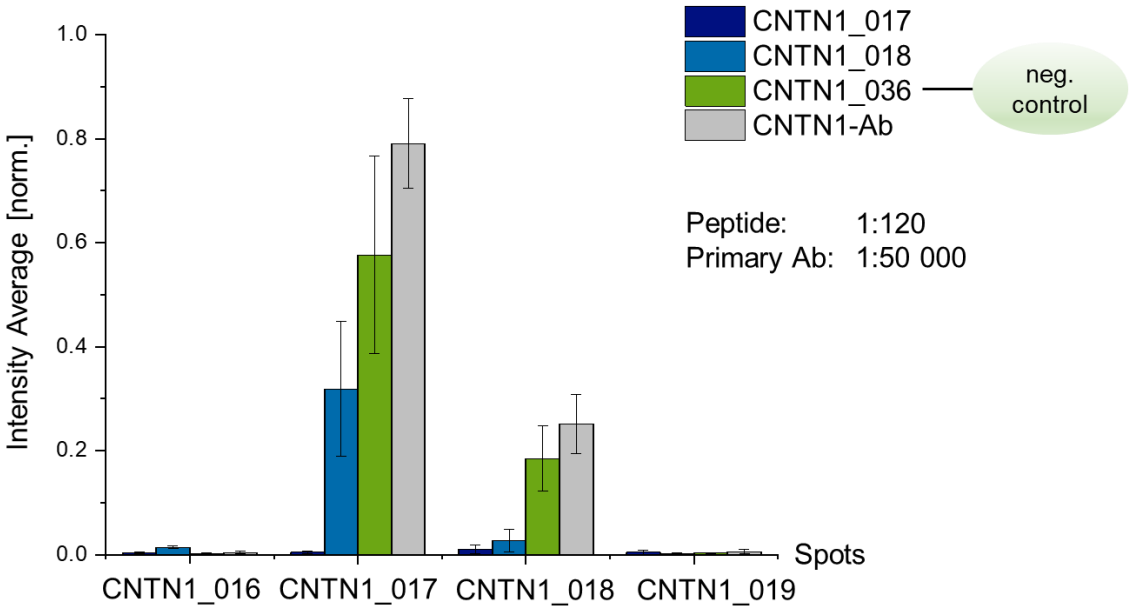

Figure 18 Chart of Anti-CNTN1 (ab66265) Neutralization

The results shown in Figure 17 are represented in a chart, with the standard deviation from n=3 measurements symbolized by bars. The intensity average is normalized to one and demonstrated for four spots of the library.

3.3.2 Neutralization of Anti-Caspr1 (ab34151)

Anti-Caspr1 (ab34151) binds to the C-Terminus of the corresponding antigen, to Caspr1_090 and Caspr1_091 (see 3.2.2). Together with Caspr1_018 the peptides are synthesized with SPPS, the latter one acting as a negative control.

The results are distinct and visible in Figure 19: Caspr1_090 and Caspr1_091 interact with the antibody, the original signal disappears in total. Compared to the binding results

received by the exclusive incubation of anti-Caspr1, Caspr1_018 leads to no change of the signal intensity. No bindings were detected on the control slide.

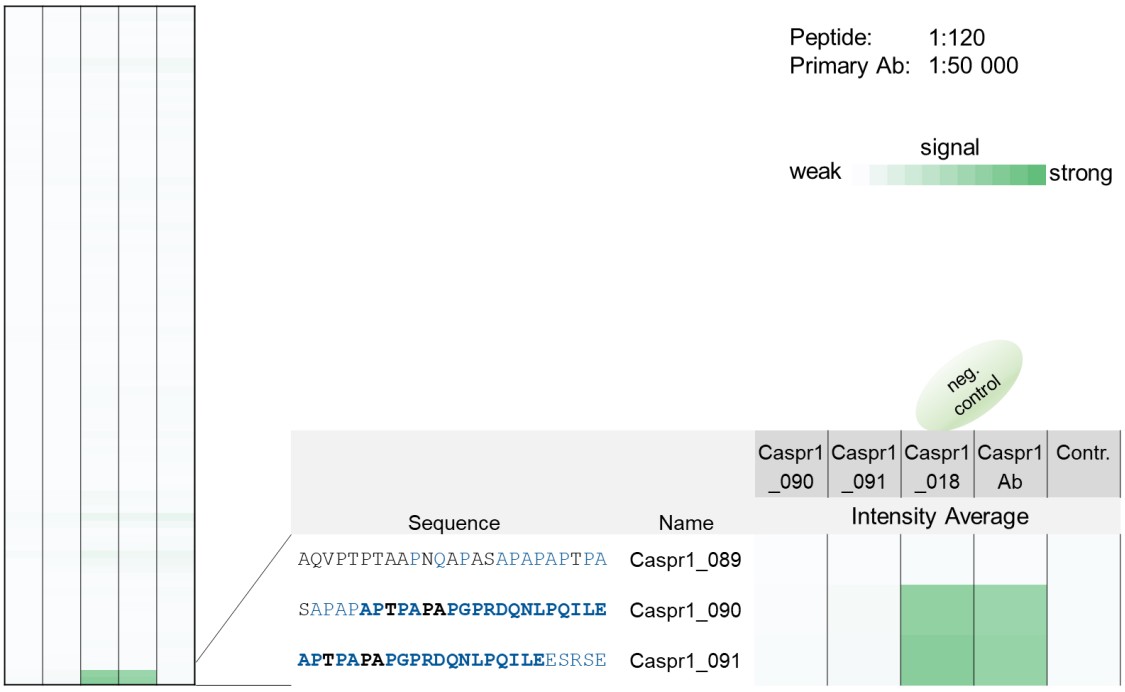

Figure 19 Neutralization of Caspr1 Binding Events

The left part of the figure illustrates the Caspr1 library (Table A2), each row standing for one epitope, each column shows the incubation results of primary antibody with different reagents (from left to right): with Caspr1_090, Caspr1_091, Caspr1_018 (negative control), no peptide (just primary antibody). The very right column represents the control slide, with no primary antibody, just secondary antibody. The end of the library is shown enlarged on the right. The blue written AA are the ones the primary antibody was raised against, the ones written in bold are essential for binding.

Figure 20 shows a chart of the neutralization results. The intensity average of the signals stays mainly the same with or without incubation of the negative control peptide Caspr1_018. Opposed to the results of incubation with Caspr1_090 and Caspr1_091: binding signals stay mainly away.

The raw data of this experimental series are displayed in Figure 21. The five slides of one pass are shown. On the blue marked spots, the epitopes Caspr1_090 and Caspr1_091 are localized, giving the strongest signal for the antibody. When they get incubated with anti-Caspr1 as soluble peptides, no binding to the corresponding peptides on the microarray can be detected anymore. In contrast to the incubation with Caspr1_018: The signal is as strong as without peptide.

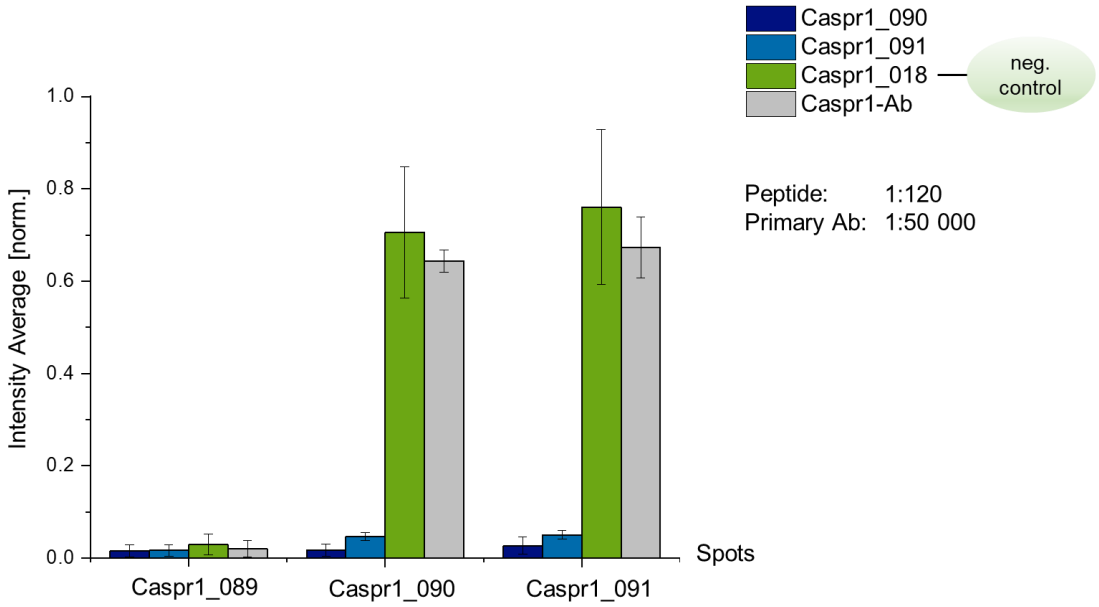

Figure 20 Chart of Anti-Caspr1 (ab34151) Neutralization

The chart shows the results of neutralization for the spots Caspr1_089, Caspr1_090 and Caspr1_091. Incubation was done with primary antibody and the relative peptides (see caption). Bars stand for standard deviation.

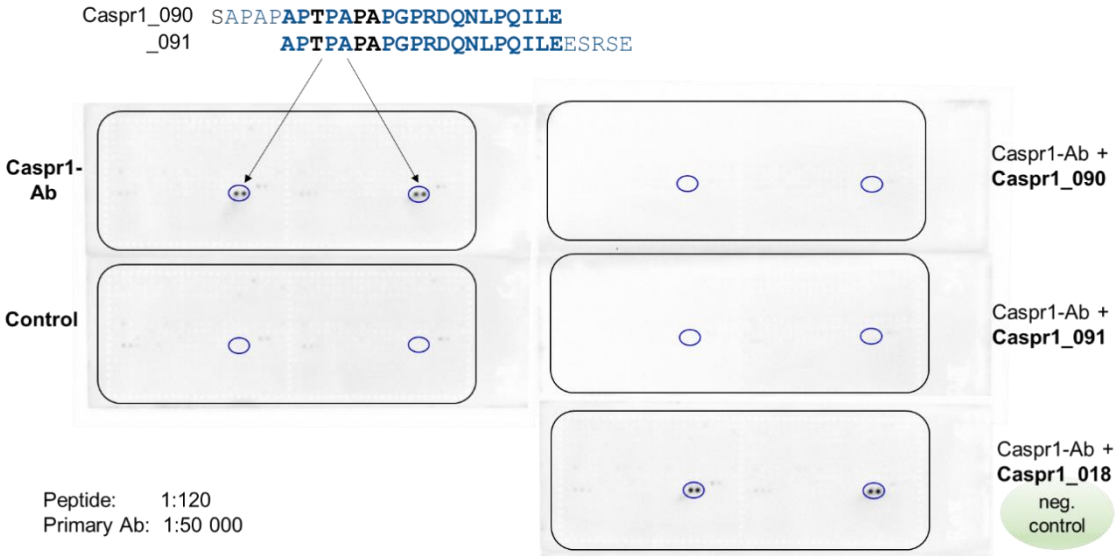

Figure 21 Raw data of Anti-Caspr1 (ab34151) Neutralization.

This figure shows the raw data of neutralization experiments with anti-Caspr1. The slides are constructed like described in Figure 4 with 2 x 384 spots in the framed regions. The two slides on the left were incubated with primary and secondary antibody (upper one) or just with secondary antibody as a control (lower one). The slides on the right were additionally incubated with the peptide labeled alongside, at which the lowermost acts as a negative control peptide. Primary antibody concentration is chosen 1:50 000, peptide concentration 1:120. Caspr1_090 and Caspr1_091 are localized in the blue framed region, their sequence is written down. The blue marked letters are the AA the primary antibody was raised against, the bold ones show the epitope responsible for binding.

3.3.3 Neutralization of Anti-NF (ab31457)

Five peptides were synthesized and taken for anti-NF neutralization, including one negative control: NF183_083, NF140_065, NF155_071, NF155_072 and NF155_032. Figure 22 gives an overview of the results, details are demonstrated in Figure 23.

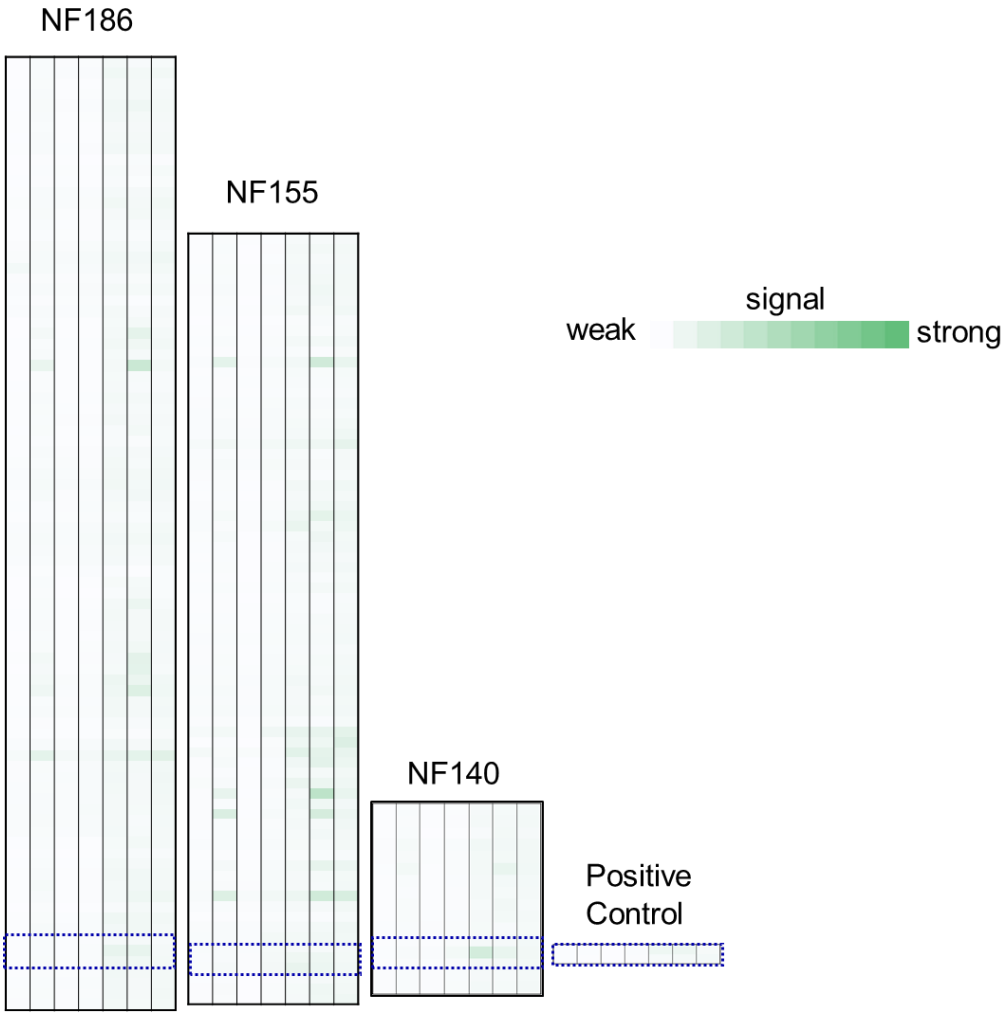

Figure 22 Overview of NF Binding Events Neutralization

An overview of the neutralization results is given, showing the whole NF libraries (Table A3 - Table A5). Each row stands for one specific epitope, the columns display the results of (from left to right): incubation with NF186_083, NF140_065, NF155_071, NF155_072 and NF155_032, no incubation of peptide, control slide. The blue marked regions are shown more detailed in Figure 23.

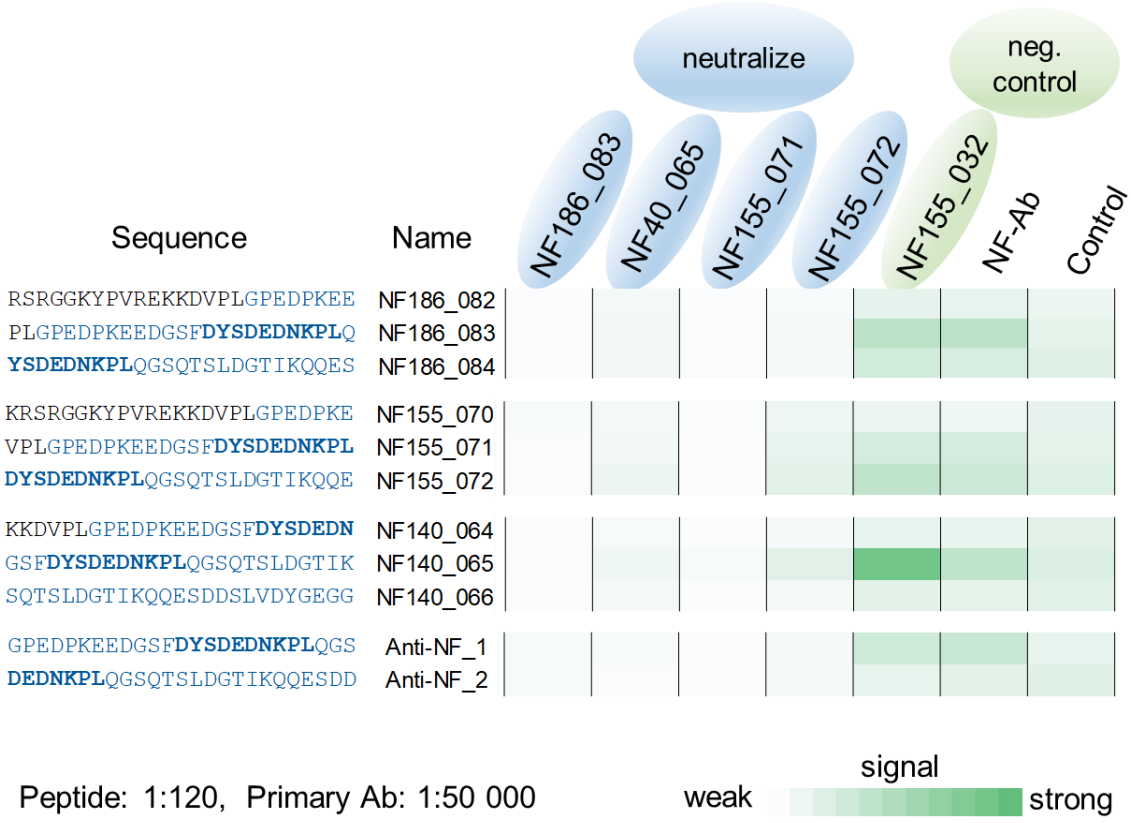

Figure 23 Details of NF Binding Events Neutralization

The relevant regions for binding are displayed, every NF isoform is included with three epitopes, in addition the positive control (Anti-NF_1, Anti-NF_2) is shown. Above the columns the peptides used for incubation are denoted. The two columns on the right show the control slides without peptide incubation, but with primary antibody, respectively on the very right just with secondary antibody. The overview in Figure 22 represents the original intensity of the binding signal. As the primary antibody concentration 1:50 000 gives weak signal for NF in general, the colors in this figure are intensified to see the results clearer.

Compared to the slides with no soluble peptide put on, the ones with incubation of NF186_083, NF140_065, NF155_071 or NF155_072 showed less signal. The negative control NF155_032 did not weaken the intensity; in case of spot NF140_065, the signal even gets stronger. A possible explanation for this could be a blocking of unspecific bindings by the negative control peptide, the resulting concentration of the primary antibody is higher and thus, signal gets stronger.

Another presentation of the output is given with Figure 24. The prior mentioned higher signal intensity received from spot NF140_065 by incubation with NF155_032 can be recognized. On the other spots, the signal does not extenuate under these conditions compared to the incubation with only primary antibody without soluble peptide. All the other peptides weaken the binding.

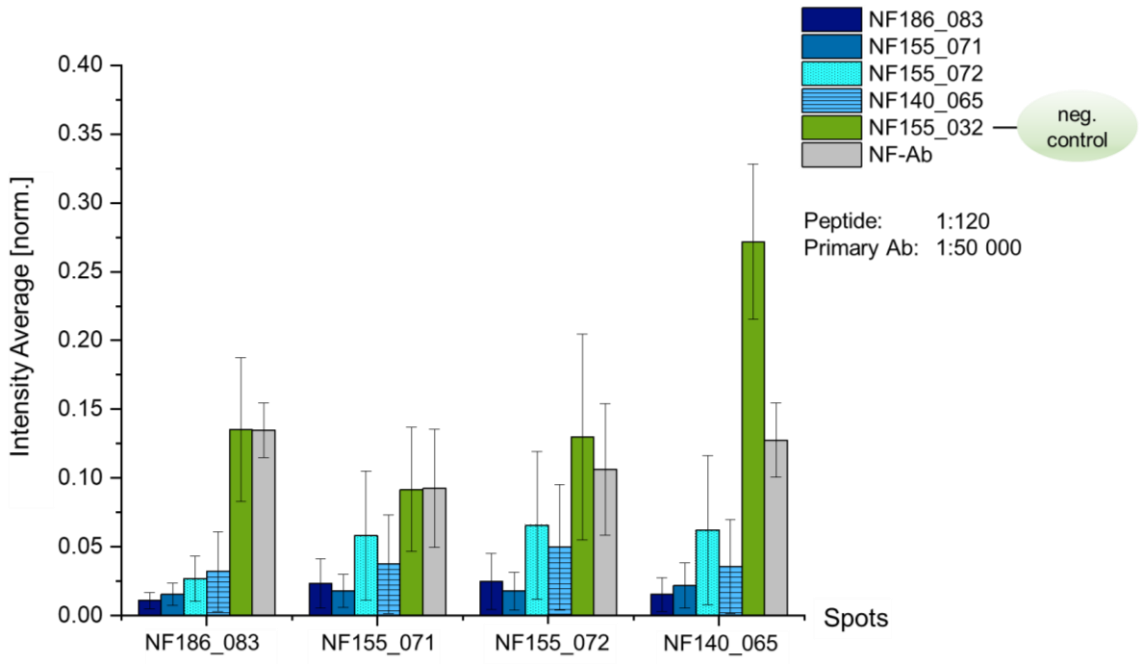

Figure 24 Chart of Anti-NF (ab31457) Neutralization

The results of anti-NF neutralization are demonstrated by dint of a chart. Normalized intensity average on the y-scale, spots on the x-scale. Primary antibody concentration is 1:50 000, peptide concentration 1:120. The peptides taken for neutralization are described in the caption, the negative control peptide is marked. Standard deviation is shown by bars.

3.3.4 Neutralization of Anti-Cortactin (TA590298)

To validate Cortactin binding events, Cort_008, Cort_012, Cort_013, Cort_018 and Cort_027 were chosen for neutralization experiments. The findings are stated in the following.

The control slide with no primary antibody, just secondary antibody, gives no signal at all. By incubation of the negative control Cort_027 no decrease was detected compared to the signals received from primary antibody (TA590298) on its own. The other four peptides extenuated the binding signals (Figure 25). On closer inspection a specific signal pattern for each incubated peptide is recognizable: they weaken especially their respective spot. In this connection it should be recalled that there are many repeats with only slightly variances within the Cortactin sequence, inclusively within the four marked epitopes chosen and synthesized for this validation. The assay reflects such diminutive differences.

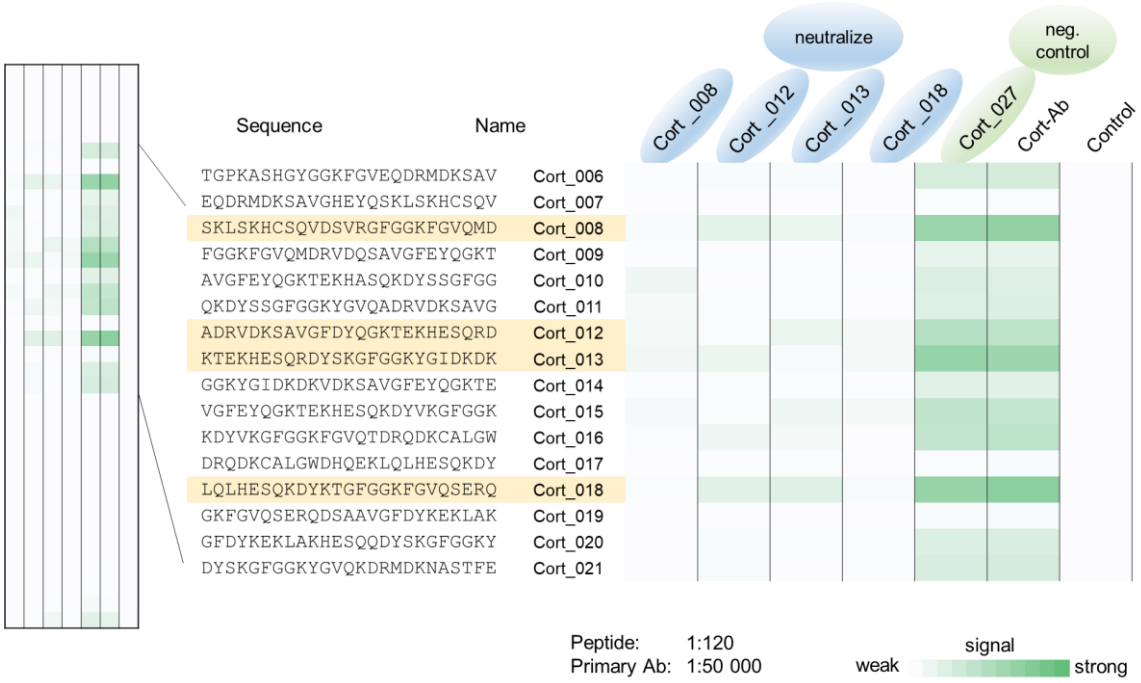

Figure 25 Neutralization of Cortactin Binding Events

The whole Cortactin library (Table A6) is shown on the left, with every row standing for one specific epitope, every column for incubation with a distinct peptide or the control slides, like it is described in the cutout on the right. The spots with the strongest signal and therefore chosen for neutralization are highlighted in the library.

Figure 26 highlights the different signal patterns for incubation with Cort_012 and Cort_013. Both peptides weaken the intensity in general. The binding signal for spot Cort_012 is extenuated more through the corresponding peptide Cort_012 than through Cort_013. For the following epitope in the library, Cort_013, the results are analogy the other way around: peptide Cort_013 weakens the signal more than Cort_012. Their sequence is compared in Figure 26, with the overlapping AA marked blue.

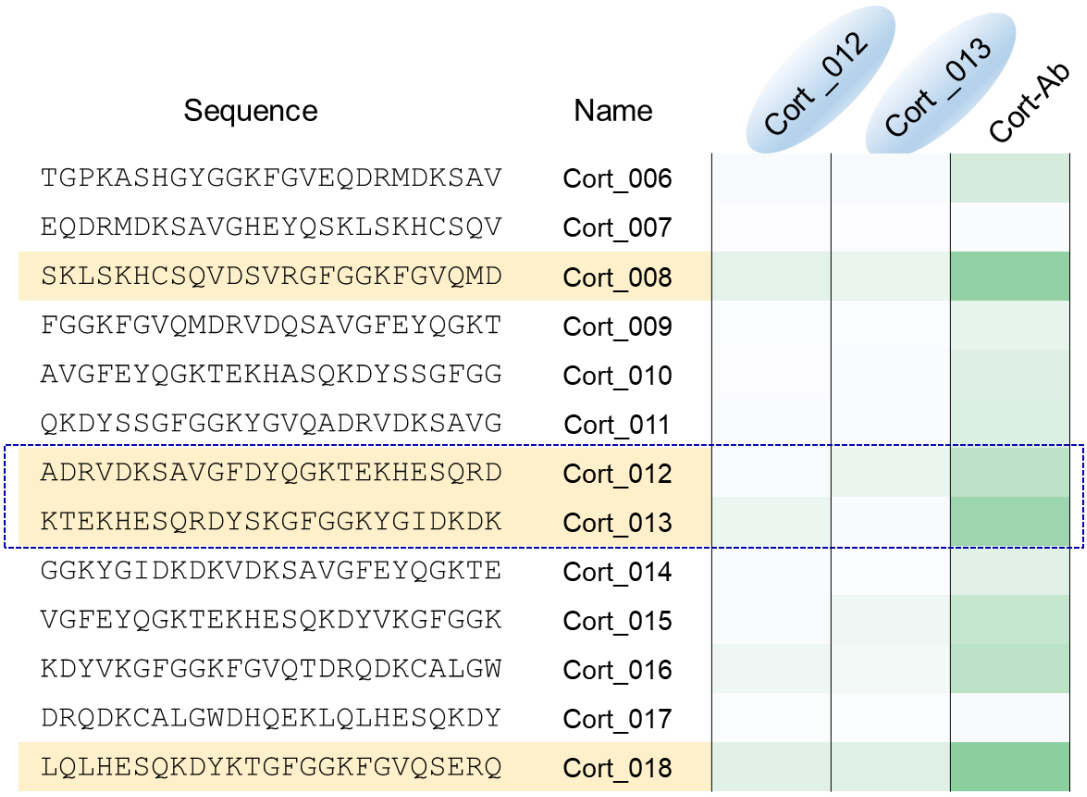

Cort_012 ADRVDKSAVGFDYQGKTEKHESQRD

Cort_013.....KTEKHESQRDYSKGFGGKYGIDKDK

Figure 26 Comparison of Cort_012 and Cort_013 Incubation

This figure shows the results for anti-Cortactin neutralization with focus on incubation with Cort_012 and Cort_013. The slightly differences between the signal patterns received from these two experimental settings become clear, especially by looking at the region framed by the blue dots.

A chart of the results is illustrated in Figure 27. Green and grey bars, representing incubation with the negative control, respectively signals received without any incubated peptide, show a similar level of intensity average. The blue balks demonstrate lower signals, having the maximum decrease on the corresponding spot for each peptide fragment.

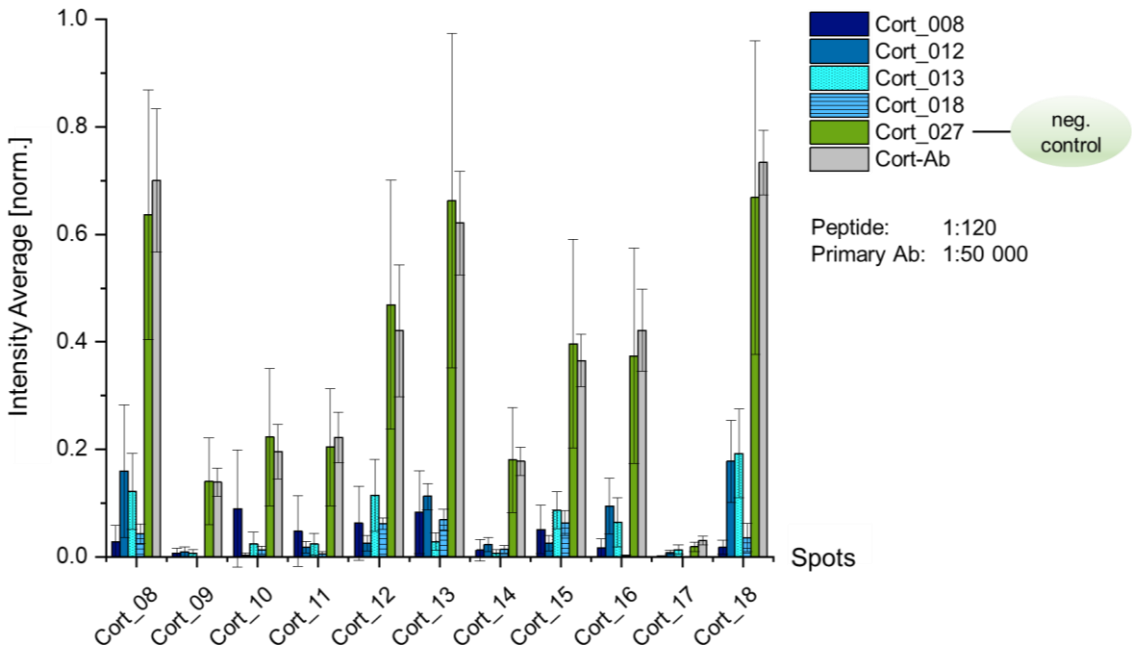

Figure 27 Chart of Anti-Cortactin (TA590298) Neutralization

Neutralization results for Cortactin are shown by a chart, with the normalized intensity average on y-scale and the spots on x-scale. Standard deviation is demonstrated by bars. The caption shows the peptides taken for incubation or rather where no peptide was used.

3.3.5 Dose-dependent On-chip Neutralization

The results of the NF155_072 dilution series can be seen in Figure 28 (for raw data see Figure A19). Incubation with the highest concentrated peptide leads to an extenuated signal, whereas with higher dilution it shows up again until to the full extent by using a 1:125 000 dilution of NF155_072. No binding was detected on the control slide.

Another presentation of the output is displayed in Figure 29. The same trend can be observed for each illustrated spot. Whereas with a peptide concentration of 1:50 the signal gets weaker, the results received from the highest diluted peptide show almost no difference compared to the results getting from primary antibody with no peptide at all. The soluble peptide has to be available in a sufficient amount to block the interaction between primary antibody and the immobilized peptides on the microarrays.

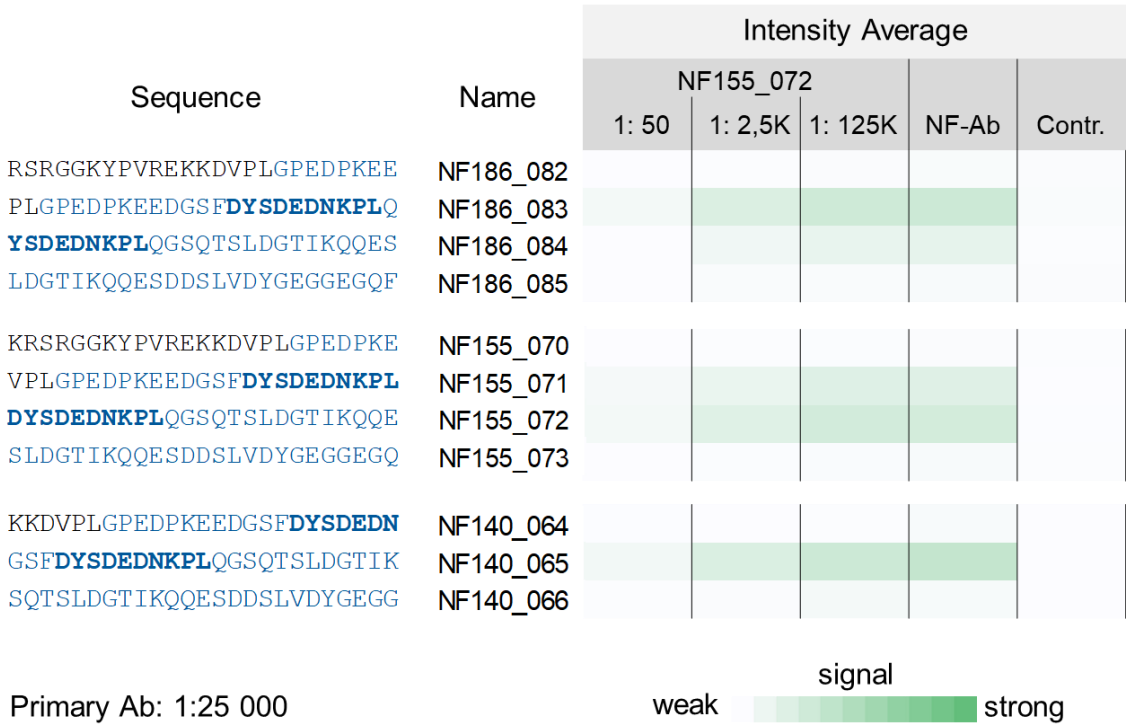

Figure 28 Neutralizing Dilution Series with Anti-NF (ab31457)

The epitopes of the binding sites are given on the left for each NF isoform. The intensity of the signals received for these spots under the respective conditions is shown on the right. The last two columns show the results with no incubated peptide, the very right column additional without primary antibody, acting as a control.

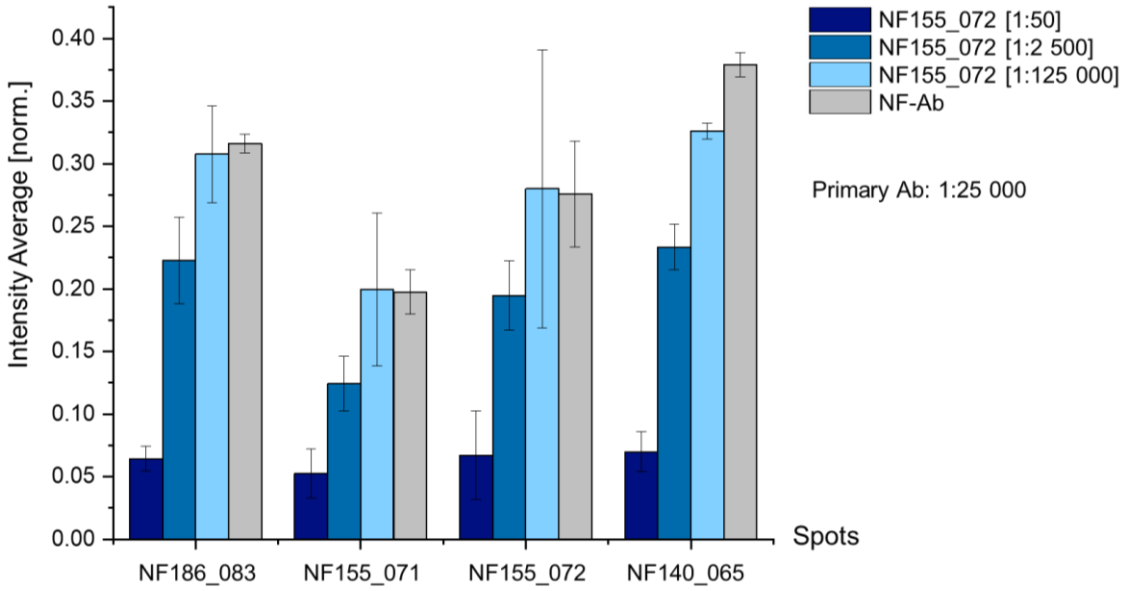

Figure 29 Chart of Neutralizing Dilution Series

The results shown in Figure 28 are here demonstrated in a chart. On the x-scale the spots are labeled, on the y-scale the normalized intensity average is shown. The caption gives information about the peptide concentration used for incubation. As this experiment was done n=1, the error bars show in this case the deviation between the duplicates on the respective slides.

4 Discussion

4.1 Method Approach Validation

In the first part of this thesis, the methodological approach was validated and fine mapping of commercial antibodies was conducted. Hereby, binding sites could be closer specified. Applied to patient sera, detailed information about the autoantibody binding epitope could give an insight into the molecular mode of action behind the pathomechanism of autoimmune mediated diseases. In 2016, Sinmaz et al. (39) already proposed that interest has increasingly focused on identification of the target epitopes of autoantibodies. Hereby, diagnosis improvement, more precise testing and development of epitope-specific therapies is aspired.

4.2 Establishment of On-chip Neutralization

Special attention was paid to the second part: a new method of validation was established. On-chip neutralization of previously detected binding events allows confirmation of the antibody specificity as well as estimations of the binding affinity and neutralization potency of antibody and peptide fragment. Neutralization potency depends on binding affinity as well as on accordance of the used peptide with the binding epitope. If it fits and the affinity is high enough, the soluble peptide binds to the antibody and therefore, neutralizes it, as the antibody cannot bind anymore to the immobilized peptides on the slides. Especially the neutralization experiments underlined the high resolution of the peptide microarrays, as even slightly differences in the amino acid sequence were recognized and displayed.

Furthermore, it is a way to identify overlapping epitopes and to have a closer look on the isoform specificity, e.g. for NF. Epitope-specific clinical phenotypes of patients with anti-NF autoantibodies were described, depending on the recognition of only NF155 or of the three NF isoforms (NF155, NF186, NF140) by the autoantibodies (36). Accordingly, investigation of autoantibody isoform specificity provides useful clinical information and will safeguard precise testing (39).

Briefly, with this validation of binding events within the same method, the biological significance of the binding signals received from the arrays is given.

4.3 Advantages of Microarrays

Using peptide microarrays for the introduced issues provides several advantages compared to ELISA (57). Fine mapping as well as on-chip neutralization can be done in

high-throughput. Peptides for both procedures are synthesized independently in our lab within the same method, with automated SPPS. Consequently, none of them is reliant on another company, providing flexibility as well as economic and time advantages. In addition, the produced peptides are very stable and can be stored over long periods (57, 58). Sample consumption is relatively low compared to ELISA, as the sensitivity of microarrays is proposed to be notably higher and clear results are still obtained with high dilutions (58, 59). Moreover, peptide microarrays can be used for multiplex analysis, further explained in 4.5.

A method against the initial high false-positive rate of peptide microarrays was established in this thesis by conducting on-chip neutralization. This validation allows an expanding of application areas of microarray-based approaches with all the described advantages.

4.4 Critical Reflection

4.4.1 Standard Deviation

Signal intensity deviation between different slides of the same experimental setting may be the major source of deviation in this thesis. Such slight variabilities are evidence of the sensitivity of this method, reacting on minimal changes during different passes. Global normalization is not possible in this case, as at fine mapping only one certain signal is received, being eliminated by on-chip neutralization. This explains why standard deviation may be relatively high for some spots. Nevertheless, if there are deviations between slides, it is mainly a general higher or lower signal intensity level, not changing anything regarding comparison of different spots for the respective slides. Consequently, each experimental run evaluated on its own shows clear results, being consistent to the ones with the same experimental setting.

4.4.2 Epitope Size

It has to be acknowledged that discontinuous epitopes cannot be detected with the library design used in this thesis, but therefore the linear ones with high precision. Contiguous stretches of antigen contact residues with a length of 2 up to 12 AA are described as a part of binding sites in a large analyze of antibody-antigen x-ray crystal structures (68). This shows that also small linear epitopes participate in antibody-antigen binding events. Their detection and further validation is covered by the introduced methods, as one spot of the library consists of 25 AA with an offset at 15 AA to the next one.

4.5 Future Application

Further development of this project can be a transfer of the gained skills to the analysis of patient sera. As a diagnostic tool, assays with sera can be performed in the same way as described for fine mapping in this thesis, in order to detect autoantibodies that may be present in patients. Validation via on-chip neutralization, using resynthesized peptides containing the detected binding epitope, could be conducted as per description, too. Usage of the in many cases limited available sera is low by comparison, like it was described (58, 59). Depending on the library design, high density peptide microarrays up to a single amino acid resolution can be constructed (57). Consequently, as the epitope of the binding site can be displayed in detail for every patient, a personalized medicine would be possible (40, 41). A correlation between specific epitope patterns and therapy response has already been hypothesized (39). Therapeutic investigations could start at the circumstances of antibody neutralization with the knowledge of the exact epitope responsible for the binding, due to the participation in the pathomechanism (9, 23, 39-41). In addition, with continuing tests over the time for the same patient, a possible epitope spreading during disease progression could be detected and the therapy if applicable adapted (40, 41, 57, 58).

As currently existing diagnostic methods likely only cover a certain fraction of all autoantigens (9, 39), multiplex analysis may follow. Various antigens printed on the slides enable a testing regarding several autoantibody targets simultaneously. Thereby, also rare or even novel autoantigens could be explored and identified. In further steps, multiplex analysis settings could not only be expanded to the whole nodal proteome in case of e.g. CIDP or GBS, but could also be applied for any other autoimmune disease. The field of described autoantigens will surely continue to extend (39).

In the distant future, there may be perhaps a fully automatic diagnostic device, requiring only a small amount of patient blood and quickly delivering a specific autoantibody profile of the patient, including possible consistent diagnosis.

5 Summary

5.1 Summary

Immune-mediated polyneuropathies like chronic inflammatory demyelinating polyradiculoneuropathy or Guillain-Barré syndrome are rare diseases of the peripheral nervous system. A subgroup of patients harbors autoantibodies against nodal or paranodal antigens, associated with a distinct phenotype and treatment response. In a part of patients with pathologic paranodal or nodal immunoreactivity the autoantigens remain difficult or impossible to determine owing to limitations of the used detection approach - usually ELISAs (enzyme-linked-immunosorbent-assays) - and incomplete knowledge of the possible autoantigens. Due to their high-throughput, low sample consumption and high sensitivity as well as the possibility to display many putative nodal and paranodal autoantigens simultaneously, peptide microarray-based approaches are prime candidates for the discovery of novel autoantigens, point-of-care diagnostics and, in addition, monitoring of pathologic autoimmune response. Current applications of peptide microarrays are however limited by high false-positive rates and the associated need for detailed follow-up studies and validation. Here, robust peptide microarray-based detection of antibodies and the efficient validation of binding signals by on-chip neutralization is demonstrated. First, autoantigens were displayed as overlapping peptide libraries in microarray format. Copies of the biochips were used for the fine mapping of antibody epitopes. Next, binding signals were validated by antibody neutralization in solution. Since neutralizing peptides are obtained in the process of microarray fabrications, neither throughput nor costs are significantly altered. Similar in-situ validation approaches could contribute to future autoantibody characterization and detection methods as well as to therapeutic research. Areas of application could be expanded to any autoimmune-mediated neurological disease as a long-term vision.

5.2 Zusammenfassung

Immunvermittelte Polyneuropathien wie die chronisch-inflammatorische demyelinisierende Polyradikuloneuropathie oder das Guillain-Barré-Syndrom sind seltene Erkrankungen des peripheren Nervensystems. Bei einem Teil dieser Patienten lassen sich Autoantikörper gegen nodale oder paranodale Antigene nachweisen, was mit einem bestimmten Phänotyp und Therapienansprechen assoziiert ist. Aufgrund der Einschränkungen verwendeter Detektionsansätze – üblicherweise ELISAs (Enzyme-linked Immunosorbent Assays) – sowie der unvollständigen Kenntnis potenzieller Autoantigene bleibt es bisher zum Teil schwierig bis unmöglich bei nachgewiesener pathologischer paranodaler bzw. nodaler Immunreaktivität die entsprechenden Autoantigene zu identifizieren. Die hohe Durchsatzleistung, der geringe Verbrauch an Probenmaterial, die hohe Sensitivität sowie die Möglichkeit zahlreiche mutmaßliche nodale und paranodale Autoantigene zeitgleich darzustellen machen Peptid-Microarray-basierte Ansätze zu wesentlichen Kandidaten für die Entdeckung neuer Autoantigene, für Point-of-Care-Diagnostik und darüber hinaus für das Monitoring pathologischer Autoimmunantworten. Durch die hohe Rate falsch positiver Ergebnisse sowie die damit verbundene Notwendigkeit detaillierter Folgestudien und Validierungen sind die gegenwärtigen Anwendungen von Peptid-Microarrays jedoch limitiert. In dieser Arbeit wird eine robuste, Peptid-Microarray-basierte Detektion von Antikörpern sowie eine effiziente Validierung der Bindungssignale mittels On-chip Neutralisation demonstriert. Zuerst wurden die Autoantigene als überlappende Peptidbüchereien im Microarray-Format dargestellt. Kopien der Biochips wurden für die Feinkartierung der Antikörper-Epitope verwendet. Mittels Antikörperneutralisation in Lösung wurden die Bindungssignale anschließend validiert. Da die neutralisierenden Peptide im Microarray- Herstellungsprozess gewonnen werden, ergeben sich weder beim Durchsatz noch bei den Kosten signifikante Änderungen. Vergleichbare In-situ-Validierungsansätze könnten zu künftigen Autoantikörper Charakterisierungen, Detektionsmethoden sowie zu therapeutischen Forschungsansätzen beitragen. Als langfristige Vision könnten die Anwendungsgebiete auf jede beliebige autoimmun-vermittelte neurologische Krankheit ausgeweitet werden.

6 References

1. Heuß D. et al. Diagnostik bei Polyneuropathien, Leitlinien für Diagnostik und Therapie in der Neurologie, S1-Leitlinie. Deutsche Gesellschaft für Neurologie. 2019.
2. Schlotter-Weigel B, Senderek J. Immune-mediated / inflammatory and hereditary neuropathies - overview and diagnostic algorithm. Fortschritte der Neurologie Psychiatrie. 2018;86(9):566-74.
3. Lehmann HC, Burke D, Kuwabara S. Chronic inflammatory demyelinating polyneuropathy: update on diagnosis, immunopathogenesis and treatment. Journal of neurology, neurosurgery, and psychiatry. 2019;90:981-7.
4. Sejvar JJ, Kohl KS, Gidudu J, Amato A, Bakshi N, Baxter R, et al. Guillain-Barre syndrome and Fisher syndrome: case definitions and guidelines for collection, analysis, and presentation of immunization safety data. Vaccine. 2011;29(3):599-612.
5. Richter T, Nestler-Parr S, Babela R, Khan ZM, Tesoro T, Molsen E, et al. Rare Disease Terminology and Definitions-A Systematic Global Review: Report of the ISPOR Rare Disease Special Interest Group. Value Health. 2015;18(6):906-14.
6. Song BH, Yun SI, Woolley M, Lee YM. Zika virus: History, epidemiology, transmission, and clinical presentation. J Neuroimmunol. 2017;308:50-64.
7. Van den Bergh PYK, Hadden RDM, Bouche P, Cornblath DR, Hahn A, Illa I, et al. European Federation of Neurological Societies/Peripheral Nerve Society Guideline on management of chronic inflammatory demyelinating polyradiculoneuropathy: report of a joint task force of the European Federation of Neurological Societies and the Peripheral Nerve Society--First Revision. J Peripher Nerv Syst. 2010;15(1):1-9.
8. Doppler K, Sommer C. Neue Entität der Paranodopathien: eine Zielstruktur mit therapeutischen Konsequenzen. Aktuelle Neurologie. 2017;44(03):194-9.
9. Devaux JJ, Odaka M, Yuki N. Nodal proteins are target antigens in Guillain-Barre syndrome. J Peripher Nerv Syst. 2012;17(1):62-71.
10. Querol L, Nogales-Gadea G, Rojas-Garcia R, Martinez-Hernandez E, Diaz-Manera J, Suarez-Calvet X, et al. Antibodies to contactin-1 in chronic inflammatory demyelinating polyneuropathy. Ann Neurol. 2013;73(3):370-80.
11. Doppler K, Appeltshauser L, Villmann C, Martin C, Peles E, Kramer HH, et al. Auto-antibodies to contactin-associated protein 1 (Caspr) in two patients with painful inflammatory neuropathy. Brain. 2016;139(Pt 10):2617-30.
12. Ng JK, Malotka J, Kawakami N, Derfuss T, Khademi M, Olsson T, et al. Neurofascin as a target for autoantibodies in peripheral neuropathies. Neurology. 2012;79(23):2241-8.
13. Delmont E, Manso C, Querol L, Cortese A, Berardinelli A, Lozza A, et al. Autoantibodies to nodal isoforms of neurofascin in chronic inflammatory demyelinating polyneuropathy. Brain. 2017;140(7):1851-8.

14. Devaux JJ, Miura Y, Fukami Y, Inoue T, Manso C, Belghazi M, et al. Neurofascin-155 IgG4 in chronic inflammatory demyelinating polyneuropathy. Neurology. 2016;86(9):800-7.

15. Kira JI, Yamasaki R, Ogata H. Anti-neurofascin autoantibody and demyelination. Neurochemistry international. 2019;130:104360.

16. Salzer JL. Schwann cell myelination. Cold Spring Harb Perspect Biol. 2015;7(8):a020529.

17. Kriebel M, Wuchter J, Trinks S, Volkmer H. Neurofascin: a switch between neuronal plasticity and stability. Int J Biochem Cell Biol. 2012;44(5):694-7.

18. Zhang A, Desmazieres A, Zonta B, Melrose S, Campbell G, Mahad D, et al. Neurofascin 140 is an embryonic neuronal neurofascin isoform that promotes the assembly of the node of Ranvier. J Neurosci. 2015;35(5):2246-54.

19. Lüllmann-Rauch R, Esther A. Taschenlehrbuch Histologie. Stuttgart; New York: Georg Thieme Verlag; 2015. 184-237 p.

20. Vural A, Doppler K, Meinl E. Autoantibodies Against the Node of Ranvier in Seropositive Chronic Inflammatory Demyelinating Polyneuropathy: Diagnostic, Pathogenic, and Therapeutic Relevance. Front Immunol. 2018;9:1029.

21. Sherman DL, Tait S, Melrose S, Johnson R, Zonta B, Court FA, et al. Neurofascins are required to establish axonal domains for saltatory conduction. Neuron. 2005;48(5):737-42.

22. Manso C, Querol L, Lleixa C, Poncelet M, Mekaouche M, Vallat JM, et al. Anti-Neurofascin-155 IgG4 antibodies prevent paranodal complex formation in vivo. The Journal of clinical investigation. 2019;129(6):2222-36.

23. Stathopoulos P, Alexopoulos H, Dalakas MC. Autoimmune antigenic targets at the node of Ranvier in demyelinating disorders. Nat Rev Neurol. 2015;11(3):143-56.

24. Doppler K, Schuster Y, Appeltshauser L, Biko L, Villmann C, Weishaupt A, et al. Anti-CNTN1 IgG3 induces acute conduction block and motor deficits in a passive transfer rat model. J Neuroinflammation. 2019;16(1):73.

25. Manso C, Querol L, Mekaouche M, Illa I, Devaux JJ. Contactin-1 IgG4 antibodies cause paranode dismantling and conduction defects. Brain. 2016;139(Pt 6):1700-12.

26. Doppler K, Appeltshauser L, Wilhelmi K, Villmann C, Dib-Hajj SD, Waxman SG, et al. Destruction of paranodal architecture in inflammatory neuropathy with anti-contactin-1 autoantibodies. Journal of neurology, neurosurgery, and psychiatry. 2015;86(7):720-8.

27. Miura Y, Devaux JJ, Fukami Y, Manso C, Belghazi M, Wong AH, et al. Contactin 1 IgG4 associates to chronic inflammatory demyelinating polyneuropathy with sensory ataxia. Brain. 2015;138(Pt 6):1484-91.

28. Mathey EK, Garg N, Park SB, Nguyen T, Baker S, Yuki N, et al. Autoantibody responses to nodal and paranodal antigens in chronic inflammatory neuropathies. J Neuroimmunol. 2017;309:41-6.

29. Querol L, Nogales-Gadea G, Rojas-Garcia R, Diaz-Manera J, Pardo J, Ortega-Moreno A, et al. Neurofascin IgG4 antibodies in CIDP associate with disabling tremor and poor response to IVIg. Neurology. 2014;82(10):879-86.

30. Burnor E, Yang L, Zhou H, Patterson KR, Quinn C, Reilly MM, et al. Neurofascin antibodies in autoimmune, genetic, and idiopathic neuropathies. Neurology. 2018;90(1):e31-e8.

31. Ogata H, Yamasaki R, Hiwatashi A, Oka N, Kawamura N, Matsuse D, et al. Characterization of IgG4 anti-neurofascin 155 antibody-positive polyneuropathy. Ann Clin Transl Neurol. 2015;2(10):960-71.

32. Querol L, Rojas-Garcia R, Diaz-Manera J, Barcena J, Pardo J, Ortega-Moreno A, et al. Rituximab in treatment-resistant CIDP with antibodies against paranodal proteins. Neurol Neuroimmunol Neuroinflamm. 2015;2(5):e149.

33. Labasque M, Hivert B, Nogales-Gadea G, Querol L, Illa I, Faivre-Sarrailh C. Specific contactin N-glycans are implicated in neurofascin binding and autoimmune targeting in peripheral neuropathies. J Biol Chem. 2014;289(11):7907-18.

34. Uncini A, Susuki K, Yuki N. Nodo-paranodopathy: beyond the demyelinating and axonal classification in anti-ganglioside antibody-mediated neuropathies. Clin Neurophysiol. 2013;124(10):1928-34.

35. Uncini A. A common mechanism and a new categorization for anti-ganglioside antibody-mediated neuropathies. Experimental neurology. 2012;235(2):513-6.

36. Stengel H, Vural A, Brunder AM, Heinius A, Appeltshauser L, Fiebig B, et al. Anti-pan-neurofascin IgG3 as a marker of fulminant autoimmune neuropathy. Neurol Neuroimmunol Neuroinflamm. 2019;6(5):e603.

37. Vallat JM, Mathis S, Magy L, Bounolleau P, Skarzynski M, Heitzmann A, et al. Subacute nodopathy with conduction blocks and anti-neurofascin 140/186 antibodies: an ultrastructural study. Brain. 2018;141(7):e56.

38. Fujita A, Ogata H, Yamasaki R, Matsushita T, Kira JI. Parallel fluctuation of anti-neurofascin 155 antibody levels with clinico-electrophysiological findings in patients with chronic inflammatory demyelinating polyradiculoneuropathy. Journal of the neurological sciences. 2018;384:107-12.

39. Sinmaz N, Nguyen T, Tea F, Dale RC, Brilot F. Mapping autoantigen epitopes: molecular insights into autoantibody-associated disorders of the nervous system. J Neuroinflammation. 2016;13(1):219.

40. Balboni I, Chan SM, Kattah M, Tenenbaum JD, Butte AJ, Utz PJ. Multiplexed protein array platforms for analysis of autoimmune diseases. Annu Rev Immunol. 2006;24:391-418.

41. Robinson WH, Steinman L, Utz PJ. Protein arrays for autoantibody profiling and fine-specificity mapping. Proteomics. 2003;3(11):2077-84.

42. Gilhus NE. Myasthenia Gravis. The New England journal of medicine. 2016;375(26):2570-81.

43. Illa I, Cortes-Vicente E, Martinez MA, Gallardo E. Diagnostic utility of cortactin antibodies in myasthenia gravis. Ann N Y Acad Sci. 2018;1412(1):90-4.

44. Huijbers MG, Lipka AF, Plomp JJ, Niks EH, van der Maarel SM, Verschuuren JJ. Pathogenic immune mechanisms at the neuromuscular synapse: the role of specific antibody-binding epitopes in myasthenia gravis. J Intern Med. 2014;275(1):12-26.

45. Cortes-Vicente E, Gallardo E, Martinez MA, Diaz-Manera J, Querol L, Rojas-Garcia R, et al. Clinical Characteristics of Patients With Double-Seronegative Myasthenia Gravis and Antibodies to Cortactin. JAMA Neurol. 2016;73(9):1099-104.

46. Gallardo E, Martinez-Hernandez E, Titulaer MJ, Huijbers MG, Martinez MA, Ramos A, et al. Cortactin autoantibodies in myasthenia gravis. Autoimmun Rev. 2014;13(10):1003-7.

47. Yalow RS, Berson SA. Immunoassay of endogenous plasma insulin in man. The Journal of clinical investigation. 1960;39:1157-75.

48. Engvall E, Perlmann P. Enzyme-linked immunosorbent assay, Elisa. 3. Quantitation of specific antibodies by enzyme-labeled anti-immunoglobulin in antigen-coated tubes. J Immunol. 1972;109(1):129-35.

49. Engvall E, Perlmann P. Enzyme-linked immunosorbent assay (ELISA). Quantitative assay of immunoglobulin G. Immunochemistry. 1971;8(9):871-4.

50. Lequin RM. Enzyme immunoassay (EIA)/enzyme-linked immunosorbent assay (ELISA). Clin Chem. 2005;51(12):2415-8.

51. Hornbeck PV. Enzyme-Linked Immunosorbent Assays. Curr Protoc Immunol. 2015;110:2.1.-2.1.23.

52. Fodor SP, Read JL, Pirrung MC, Stryer L, Lu AT, Solas D. Light-directed, spatially addressable parallel chemical synthesis. Science. 1991;251(4995):767-73.

53. Frank R. Spot-Synthesis : An Easy Technique for the Positionally Addressable, Parallel Chemical Synthesis on a Membrane Support. Tetrahedron. 1992;48(42):9217-32.

54. Foong YM, Fu J, Yao SQ, Uttamchandani M. Current advances in peptide and small molecule microarray technologies. Curr Opin Chem Biol. 2012;16(1-2):234-42.

55. Cerecedo I, Zamora J, Shreffler WG, Lin J, Bardina L, Dieguez MC, et al. Mapping of the IgE and IgG4 sequential epitopes of milk allergens with a peptide microarray-based immunoassay. J Allergy Clin Immunol. 2008;122(3):589-94.

56. Katz C, Levy-Beladev L, Rotem-Bamberger S, Rito T, Rudiger SG, Friedler A. Studying protein-protein interactions using peptide arrays. Chemical Society reviews. 2011;40(5):2131-45.

57. Ayoglu B, Schwenk JM, Nilsson P. Antigen arrays for profiling autoantibody repertoires. Bioanalysis. 2016;8(10):1105-26.

58. Robinson WH, DiGennaro C, Hueber W, Haab BB, Kamachi M, Dean EJ, et al. Autoantigen microarrays for multiplex characterization of autoantibody responses. Nat Med. 2002;8(3):295-301.

59. Quintana FJ, Farez MF, Viglietta V, Iglesias AH, Merbl Y, Izquierdo G, et al. Antigen microarrays identify unique serum autoantibody signatures in clinical and

pathologic subtypes of multiple sclerosis. Proc Natl Acad Sci U S A. 2008;105(48):18889-94.

60. Ayoglu B, Haggmark A, Khademi M, Olsson T, Uhlen M, Schwenk JM, et al. Autoantibody profiling in multiple sclerosis using arrays of human protein fragments. Mol Cell Proteomics. 2013;12(9):2657-72.

61. Ayoglu B, Mitsios N, Kockum I, Khademi M, Zandian A, Sjoberg R, et al. Anoctamin 2 identified as an autoimmune target in multiple sclerosis. Proc Natl Acad Sci U S A. 2016;113(8):2188-93.

62. Hecker M, Fitzner B, Wendt M, Lorenz P, Flechtner K, Steinbeck F, et al. High-Density Peptide Microarray Analysis of IgG Autoantibody Reactivities in Serum and Cerebrospinal Fluid of Multiple Sclerosis Patients. Mol Cell Proteomics. 2016;15(4):1360-80.

63. Hecker M, Lorenz P, Steinbeck F, Hong L, Riemekasten G, Li Y, et al. Computational analysis of high-density peptide microarray data with application from systemic sclerosis to multiple sclerosis. Autoimmun Rev. 2012;11(3):180-90.

64. The UniProt Consortium. UniProt: a worldwide hub of protein knowledge. Nucleic Acids Res. 2019;47(D1):D506-D15.

65. McBride R, Head SR, Ordoukhanian P, Law M. Low-Cost Peptide Microarrays for Mapping Continuous Antibody Epitopes. Methods Mol Biol. 2016;1352:67-83.

66. Frank R. The SPOT-synthesis technique. Synthetic peptide arrays on membrane supports--principles and applications. J Immunol Methods. 2002;267(1):13-26.

67. Wang C, Xiao R, Dong P, Wu X, Rong Z, Xin L, et al. Ultra-sensitive, high-throughput detection of infectious diarrheal diseases by portable chemiluminescence imaging. Biosens Bioelectron. 2014;57:36-40.

68. Stave JW, Lindpaintner K. Antibody and antigen contact residues define epitope and paratope size and structure. J Immunol. 2013;191(3):1428-35.

I Appendix

Table A1 Peptide sequences: Overlapping library for CNTN1

Peptide Sequence	Name	Spot
EFTWYRRYGHGVSEEDKGFGPIFEE	CNTN1_001	A01
DKGFGPIFEEQPINTIYPEESLEGK	CNTN1_002	A02
IYPEESLEGKVSLNCRARASPFPVY	CNTN1_003	A03
RARASPFPVYKWRMNNGDVDLTSDR	CNTN1_004	A04
NGDVDLTSDRYSMVGGNLVINNPDK	CNTN1_005	A05
GNLVINNPDKQKDAGIYYCLASNNY	CNTN1_006	A06
IYYCLASNNYGMVRSTEATLSFGYL	CNTN1_007	A07
TEATLSFGYLDPFPPEERPEVRVKE	CNTN1_008	A08
EERPEVRVKEGKGMVLLCDPPYHFP	CNTN1_009	A09
LLCDPPYHFPDDLSYRWLLNEFPVF	CNTN1_010	A10
RWLLNEFPVFITMDKRRFVSQTNGN	CNTN1_011	A11
RRFVSQTNGNLYIANVEASDKGNYS	CNTN1_012	A12
VEASDKGNYSCFVSSPSITKSVFSK	CNTN1_013	A13
PSITKSVFSKFIPLIPIPERTTKPY	CNTN1_014	A14
PIPERTTKPYPADIVVQFKDVYALM	CNTN1_015	A15
VQFKDVYALMGQNVTLECFALGNPV	CNTN1_016	A16
LECFALGNPVPDIRWRKVLEPMPST	CNTN1_017	A17
RKVLEPMPSTAEISTSGAVLKIFNI	CNTN1_018	A18
SGAVLKIFNIQLEDEGIYECEAENI	CNTN1_019	A19
GIYECEAENIRGKDKHQARIYVQAF	CNTN1_020	A20
HQARIYVQAFPEWVEHINDTEVDIG	CNTN1_021	A21
HINDTEVDIGSDLYWPCVATGKPIP	CNTN1_022	A22
PCVATGKPIPTIRWLKNGYAYHKGE	CNTN1_023	A23
KNGYAYHKGELRLYDVTFENAGMYQ	CNTN1_024	A24
VTFENAGMYQCIAENTYGAIYANAE	CNTN1_025	B01
TYGAIYANAELKILALAPTFEMNPM	CNTN1_026	B02
LAPTFEMNPMKKKILAAKGGRVIIE	CNTN1_027	B03
AAKGGRVIIECKPKAAPKPKFSWSK	CNTN1_028	B04
APKPKFSWSKGTEWLVNSSRILIWE	CNTN1_029	B05
VNSSRILIWEDGSLEINNITRNDGG	CNTN1_030	B06

INNITRNDGGIYTCFAENNRGKANS	CNTN1_031	B07
AENNRGKANSTGTLVITDPTRIILA	CNTN1_032	B08
ITDPTRIILAPINADITVGENATMQ	CNTN1_033	B09
ITVGENATMQCAASFDPALDLTFVW	CNTN1_034	B10
DPALDLTFVWSFNGYVIDFNKENIH	CNTN1_035	B11
VIDFNKENIHYQRNFMLDSNGELLI	CNTN1_036	B12
MLDSNGELLIRNAQLKHAGRYTCTA	CNTN1_037	B13
KHAGRYTCTAQTIVDNSSASADLVV	CNTN1_038	B14
NSSASADLVVRGPPGPPGGLRIEDI	CNTN1_039	B15
PPGGLRIEDIRATSVALTWSRGSDN	CNTN1_040	B16
ALTWSRGSDNHSPISKYTIQTKTIL	CNTN1_041	B17
KYTIQTKTILSDDWKDAKTDPPIIE	CNTN1_042	B18
DAKTDPPIIEGNMEAARAVDLIPWM	CNTN1_043	B19
ARAVDLIPWMEYEFRVVATNTLGRG	CNTN1_044	B20
VVATNTLGRGEPSIPSNRIKTDGAA	CNTN1_045	B21
SNRIKTDGAAPNVAPSDVGGGGGRN	CNTN1_046	B22
SDVGGGGGRNRELTITWAPLSREYH	CNTN1_047	B23
TWAPLSREYHYGNNFGYIVAFKPFD	CNTN1_048	B24
GYIVAFKPFDGEEWKKVTVTNPDTG	CNTN1_049	C01
KVTVTNPDTGRYVHKDETMSPSTAF	CNTN1_050	C02
DETMSPSTAFQVKVKAFNNKGDGPY	CNTN1_051	C03
AFNNKGDGPYSLVAVINSAQDAPSE	CNTN1_052	C04
INSAQDAPSEAPTEVGVKVLSSSEI	CNTN1_053	C05
GVKVLSSSEISVHWEHVLEKIVESY	CNTN1_054	C06
HVLEKIVESYQIRYWAAHDKEEAAN	CNTN1_055	C07
AAHDKEEAANRVQVTSQEYSARLEN	CNTN1_056	C08
SQEYSARLENLLPDTQYFIEVGACN	CNTN1_057	C09
QYFIEVGACNSAGCGPPSDMIEAFT	CNTN1_058	C10
PPSDMIEAFTKKAPPSQPPRIISSV	CNTN1_059	C11
SQPPRIISSVRSGSRYIITWDHVVA	CNTN1_060	C12
YIITWDHVVALSNESTVTGYKVLYR	CNTN1_061	C13
TVTGYKVLYRPDGQHDGKLYSTHKH	CNTN1_062	C14
DGKLYSTHKHSIEVPIPRDGEYVVE	CNTN1_063	C15
IPRDGEYVVEVRAHSDGGDGVVSQV	CNTN1_064	C16

DGGDGVVSQVKISGAPTLSPSLLGL	CNTN1_065	C17
GAPTLSPSLLGLLLPAFGILVYLEF	CNTN1_066	C18
IYTMMGQNVTLECFALGNPVPDIRW	Positive Control 1 (Anti-CNTN1_1)	E01
PDIRWRKVLEPMPSTAEISTSGAVL	Positive Control 2 (Anti-CNTN1_2)	E02

Table A2 Peptide sequences: Overlapping library for Caspr1

Peptide Sequence	Name	Spot
WGYYGCDEELVGPLYARSLGASSYY	Caspr1_001	G01
ARSLGASSYYSLLTAPRFARLHGIS	Caspr1_002	G02
PRFARLHGISGWSPRIGDPNPWLQI	Caspr1_003	G03
IGDPNPWLQIDLMKKHRIRAVATQG	Caspr1_004	G04
HRIRAVATQGSFNSWDWVTRYMLLY	Caspr1_005	G05
DWVTRYMLLYGDRVDSWTPFYQRGH	Caspr1_006	G06
SWTPFYQRGHNSTFFGNVNESAVVR	Caspr1_007	G07
GNVNESAVVRHDLHFHFTARYIRIV	Caspr1_008	G08
HFTARYIRIVPLAWNPRGKIGLRLG	Caspr1_009	G09
PRGKIGLRLGLYGCPYKADILYFDG	Caspr1_010	G10
YKADILYFDGDDAISYRFPRGVSRS	Caspr1_011	G11
YRFPRGVSRSLWDVFAFSFKTEEKD	Caspr1_012	G12
AFSFKTEEKDGLLLHAEGAQGDYVT	Caspr1_013	G13
AEGAQGDYVTLELEGAHLLLHMSLG	Caspr1_014	G14
AHLLLHMSLGSSPIQPRPGHTTVSA	Caspr1_015	G15
PRPGHTTVSAGGVLNDQHWHYVRVD	Caspr1_016	G16
DQHWHYVRVDRFGRDVNFTLDGYVQ	Caspr1_017	G17
VNFTLDGYVQRFILNGDFERLNLDT	Caspr1_018	G18
GDFERLNLDTEMFIGGLVGAARKNL	Caspr1_019	G19
GLVGAARKNLAYRHNFRGCIENVIF	Caspr1_020	G20
FRGCIENVIFNRVNIADLAVRRHSR	Caspr1_021	G21
ADLAVRRHSRITFEGKVAFRCLDPV	Caspr1_022	G22
KVAFRCLDPVPHPINFGGPHNFVQV	Caspr1_023	G23
FGGPHNFVQVPGFPRRGRLAVSFRF	Caspr1_024	G24
RGRLAVSFRFRTWDLTGLLLFSRLG	Caspr1_025	H01

TGLLLFSRLGDGLGHVELTLSEGQV	Caspr1_026	H02
VELTLSEGQVNVSIAQSGRKKLQFA	Caspr1_027	H03
QSGRKKLQFAAGYRLNDGFWHEVNF	Caspr1_028	H04
NDGFWHEVNFVAQENHAVISIDDVE	Caspr1_029	H05
HAVISIDDVEGAEVRVSYPLLIRTG	Caspr1_030	H06
VSYPLLIRTGTSYFFGGCPKPASRW	Caspr1_031	H07
GGCPKPASRWDCHSNQTAFHGCMEL	Caspr1_032	H08
QTAFHGCMELLKVDGQLVNLTLVEG	Caspr1_033	H09
QLVNLTLVEGRRLGFYAEVLFDTCG	Caspr1_034	H10
YAEVLFDTCGITDRCSPNMCEHDGR	Caspr1_035	H11
SPNMCEHDGRCYQSWDDFICYCELT	Caspr1_036	H12
DDFICYCELTGYKGETCHTPLYKES	Caspr1_037	H13
TCHTPLYKESCEAYRLSGKTSGNFT	Caspr1_038	H14
LSGKTSGNFTIDPDGSGPLKPFVVY	Caspr1_039	H15
SGPLKPFVVYCDIRENRAWTVVRHD	Caspr1_040	H16
NRAWTVVRHDRLWTTRVTGSSMERP	Caspr1_041	H17
RVTGSSMERPFLGAIQYWNASWEEV	Caspr1_042	H18
QYWNASWEEVSALANASQHCEQWIE	Caspr1_043	H19
ASQHCEQWIEFSCYNSRLLNTAGGY	Caspr1_044	H20
SRLLNTAGGYPYSFWIGRNEEQHFY	Caspr1_045	H21
IGRNEEQHFYWGGSQPGIQRCACGL	Caspr1_046	H22
PGIQRCACGLDRSCVDPALYCNCDA	Caspr1_047	H23
DPALYCNCDADQPQWRTDKGLLTFV	Caspr1_048	H24
RTDKGLLTFVDHLPVTQVVIGDTNR	Caspr1_049	I01
TQVVIGDTNRSTSEAQFFLRPLRCY	Caspr1_050	I02
QFFLRPLRCYGDRNSWNTISFHTGA	Caspr1_051	I03
WNTISFHTGAALRFPPIRANHSLDV	Caspr1_052	I04
PIRANHSLDVSFYFRTSAPSGVFLE	Caspr1_053	I05
TSAPSGVFLENMGGPYCQWRRPYVR	Caspr1_054	I06
YCQWRRPYVRVELNTSRDVVFAFDV	Caspr1_055	I07
SRDVVFAFDVGNGDENLTVHSDDFE	Caspr1_056	I08
NLTVHSDDFEFNDDEWHLVRAEINV	Caspr1_057	I09
WHLVRAEINVKQARLRVDHRPWVLR	Caspr1_058	I10
RVDHRPWVLRPMPLQTYIWMEYDQP	Caspr1_059	I11

TYIWMEYDQPLYVGSAELKRRPFVG	Caspr1_060	I12
AELKRRPFVGCLRAMRLNGVTLNLE	Caspr1_061	I13
RLNGVTLNLEGRANASEGTSPNCTG	Caspr1_062	I14
SEGTSPNCTGHCAHPRLPCFHGGRC	Caspr1_063	I15
RLPCFHGGRCVERYSYYTCDCDLTA	Caspr1_064	I16
YYTCDCDLTAFDGPYCNHDIGGFFE	Caspr1_065	I17
CNHDIGGFFEPGTWMRYNLQSALRS	Caspr1_066	I18
RYNLQSALRSAAREFSHMLSRPVPG	Caspr1_067	I19
SHMLSRPVPGYEPGYIPGYDTPGYV	Caspr1_068	I20
IPGYDTPGYVPGYHGPGYRLPDYPR	Caspr1_069	I21
PGYRLPDYPRPGRPVPGYRGPVYNV	Caspr1_070	I22
PGYRGPVYNVTGEEVSFSFSTSSAP	Caspr1_071	I23
SFSFSTSSAPAVLLYVSSFVRDYMA	Caspr1_072	I24
VSSFVRDYMAVLIKDDGTLQLRYQL	Caspr1_073	J01
DGTLQLRYQLGTSPYVYQLTTRPVT	Caspr1_074	J02
VYQLTTRPVTDGQPHSINITRVYRN	Caspr1_075	J03
SINITRVYRNLFIQVDYFPLTEQKF	Caspr1_076	J04
DYFPLTEQKFSLLVDSQLDSPKALY	Caspr1_077	J05
SQLDSPKALYLGRVMETGVIDPEIQ	Caspr1_078	J06
ETGVIDPEIQRYNTPGFSGCLSGVR	Caspr1_079	J07
GFSGCLSGVRFNNVAPLKTHFRTPR	Caspr1_080	J08
PLKTHFRTPRPMTAELAEALRVQGE	Caspr1_081	J09
LAEALRVQGELSESNCGAMPRLVSE	Caspr1_082	J10
CGAMPRLVSEVPPELDPWYLPPDFP	Caspr1_083	J11
DPWYLPPDFPYYHDEGWVAILLGFL	Caspr1_084	J12
GWVAILLGFLVAFLLLGLVGMLVLF	Caspr1_085	J13
LGLVGMLVLFYLQNHRYKGSYHTNE	Caspr1_086	J14
RYKGSYHTNEPKAAHEYHPGSKPPL	Caspr1_087	J15
EYHPGSKPPLPTSGPAQVPTPTAAP	Caspr1_088	J16
AQVPTPTAAPNQAPASAPAPAPTPA	Caspr1_089	J17
SAPAPAPTPAPAPGPRDQNLPQILE	Caspr1_090	J18
APTPAPAPGPRDQNLPQILEESRSE	Caspr1_091	J19

Table A3 Peptide sequences: Overlapping library for NF186

Peptide Sequence	Name	Spot
IEIPMDPSIQNELTQPPTITKQSAK	NF186_001	A01
PPTITKQSAKDHIVDPRDNILIECE	NF186_002	A02
PRDNILIECEAKGNPAPSFHWTRNS	NF186_003	A03
APSFHWTRNSRFFNIAKDPRVSMRR	NF186_004	A04
AKDPRVSMRRRSGTLVIDFRSGGRP	NF186_005	A05
VIDFRSGGRPEEYEGEYQCFARNKF	NF186_006	A06
EYQCFARNKFGTALSNRIRLQVSKS	NF186_007	A07
NRIRLQVSKSPLWPKENLDPVVVQE	NF186_008	A08
ENLDPVVVQEGAPLTLQCNPPPGLP	NF186_009	A09
LQCNPPPGLPSPVIFWMSSSMEPIT	NF186_010	A10
WMSSSMEPITQDKRVSQGHNGDLYF	NF186_011	A11
SQGHNGDLYFSNVMLQDMQTDYSCN	NF186_012	A12
QDMQTDYSCNARFHFTHTIQQKNPF	NF186_013	A13
THTIQQKNPFTLKVLTTRGVAERTP	NF186_014	A14
TTRGVAERTPSFMYPQGTASSQMVL	NF186_015	A15
QGTASSQMVLRGMDLLLECIASGVP	NF186_016	A16
LLECIASGVPTPDIAWYKKGGDLPS	NF186_017	A17
WYKKGGDLPSDKAKFENFNKALRIT	NF186_018	A18
ENFNKALRITNVSEEDSGEYFCLAS	NF186_019	A19
DSGEYFCLASNKMGSIRHTISVRVK	NF186_020	A20
IRHTISVRVKAAPYWLDEPKNLILA	NF186_021	A21
LDEPKNLILAPGEDGRLVCRANGNP	NF186_022	A22
RLVCRANGNPKPTVQWMVNGEPLQS	NF186_023	A23
WMVNGEPLQSAPPNPNREVAGDTII	NF186_024	A24
NREVAGDTIIFRDTQISSRAVYQCN	NF186_025	B01
ISSRAVYQCNTSNEHGYLLANAFVS	NF186_026	B02
GYLLANAFVSVLDVPPRMLSPRNQL	NF186_027	B03
PRMLSPRNQLIRVILYNRTRLDCPF	NF186_028	B04
YNRTRLDCPFFGSPIPTLRWFKNGQ	NF186_029	B05
PTLRWFKNGQGSNLDGGNYHVYENG	NF186_030	B06
GGNYHVYENGSLEIKMIRKEDQGIY	NF186_031	B07
MIRKEDQGIYTCVATNILGKAENQV	NF186_032	B08

NILGKAENQVRLEVKDPTRIYRMPE	NF186_033	B09
DPTRIYRMPEDQVARRGTTVQLECR	NF186_034	B10
RGTTVQLECRVKHDPSLKLTVSWLK	NF186_035	B11
SLKLTVSWLKDDEPLYIGNRMKKED	NF186_036	B12
YIGNRMKKEDDSLTIFGVAERDQGS	NF186_037	B13
FGVAERDQGSYTCVASTELDQDLAK	NF186_038	B14
STELDQDLAKAYLTVLADQATPTNR	NF186_039	B15
LADQATPTNRLAALPKGRPDRPRDL	NF186_040	B16
KGRPDRPRDLELTDLAERSVRLTWI	NF186_041	B17
AERSVRLTWIPGDANNSPITDYVVQ	NF186_042	B18
NSPITDYVVQFEEDQFQPGVWHDHS	NF186_043	B19
FQPGVWHDHSKYPGSVNSAVLRLSP	NF186_044	B20
VNSAVLRLSPYVNYQFRVIAINEVG	NF186_045	B21
FRVIAINEVGSSHPSLPSERYRTSG	NF186_046	B22
LPSERYRTSGAPPESNPGDVKGEGT	NF186_047	B23
NPGDVKGEGTRKNNMEITWTPMNAT	NF186_048	B24
EITWTPMNATSAFGPNLRYIVKWRR	NF186_049	C01
NLRYIVKWRRRETREAWNNVTVWGS	NF186_050	C02
AWNNVTVWGSRYVVGQTPVYVPYEI	NF186_051	C03
QTPVYVPYEIRVQAENDFGKGPEPE	NF186_052	C04
NDFGKGPEPESVIGYSGEDYPRAAP	NF186_053	C05
SGEDYPRAAPTEVKVRVMNSTAISL	NF186_054	C06
RVMNSTAISLQWNRVYSDTVQGQLR	NF186_055	C07
YSDTVQGQLREYRAYYWRESSLLKN	NF186_056	C08
YWRESSLLKNLWVSQKRQQASFPGD	NF186_057	C09
KRQQASFPGDRLRGVVSRLFPYSNY	NF186_058	C10
VSRLFPYSNYKLEMVVVNGRGDGPR	NF186_059	C11
VVNGRGDGPRSETKEFTTPEGVPSA	NF186_060	C12
FTTPEGVPSAPRRFRVRQPNLETIN	NF186_061	C13
VRQPNLETINLEWDHPEHPNGIMIG	NF186_062	C14
PEHPNGIMIGYTLKYVAFNGTKVGK	NF186_063	C15
VAFNGTKVGKQIVENFSPNQTKFTV	NF186_064	C16
FSPNQTKFTVQRTDPVSRYRFTLSA	NF186_065	C17
VSRYRFTLSARTQVGSGEAVTEESP	NF186_066	C18

SGEAVTEESPAPPNEATPTAAPPTL	NF186_067	C19
ATPTAAPPTLPPTTVGATGAVSSTD	NF186_068	C20
GATGAVSSTDATAIAATTEATTVPI	NF186_069	C21
ATTEATTVPIIPTVAPTTIATTTTV	NF186_070	C22
PTTIATTTTVATTTTTTAAATTTTE	NF186_071	C23
TTAAATTTTESPPTTTSGTKIHESA	NF186_072	C24
TSGTKIHESAPDEQSIWNVTVLPNS	NF186_073	D01
IWNVTVLPNSKWANITWKHNFGPGT	NF186_074	D02
TWKHNFGPGTDFVVEYIDSNHTKKT	NF186_075	D03
YIDSNHTKKTVPVKAQAQPIQLTDL	NF186_076	D04
QAQPIQLTDLYPGMTYTLRVYSRDN	NF186_077	D05
YTLRVYSRDNEGISSTVITFMTSTA	NF186_078	D06
TVITFMTSTAYTNNQADIATQGWFI	NF186_079	D07
ADIATQGWFIGLMCAIALLVLILLI	NF186_080	D08
IALLVLILLIVCFIKRSRGGKYPVR	NF186_081	D09
RSRGGKYPVREKKDVPLGPEDPKEE	NF186_082	D10
PLGPEDPKEEDGSFDYSDEDNKPLQ	NF186_083	D11
YSDEDNKPLQGSQTSLDGTIKQQES	NF186_084	D12
LDGTIKQQESDDSLVDYGEGGEGQF	NF186_085	D13
DYGEGGEGQFNEDGSFIGQYTVKKD	NF186_086	D14
FIGQYTVKKDKEETEGNESSEATSP	NF186_087	D15
KDKEETEGNESSEATSPVNAIYSLA	NF186_088	D16

Table A4 Peptide sequences: Overlapping library for NF140

Peptide Sequence	Name	Spot
NDFGKGPEPESVIGYSGEDLPSAPR	NF140_053	E01
SGEDLPSAPRRFRVRQPNLETINLE	NF140_054	E02
QPNLETINLEWDHPEHPNGIMIGYT	NF140_055	E03
HPNGIMIGYTLKYVAFNGTKVGKQI	NF140_056	E04
FNGTKVGKQIVENFSPNQTKFTVQR	NF140_057	E05
PNQTKFTVQRTDPVSRYRFTLSART	NF140_058	E06
RYRFTLSARTQVGSGEAVTEESPAP	NF140_059	E07
EAVTEESPAPPNEAYTNNQADIATQ	NF140_060	E08
TNNQADIATQGWFIGLMCAIALLVL	NF140_061	E09

LMCAIALLVLILLIVCFIKRSRGGK	NF140_062	E10
CFIKRSRGGKYPVREKKDVPLGPED	NF140_063	E11
KKDVPLGPEDPKEEDGSFDYSDEDN	NF140_064	E12
GSFDYSDEDNKPLQGSQTSLDGTIK	NF140_065	E13
SQTSLDGTIKQQESDDSLVDYGEGG	NF140_066	E14
DSLVDYGEGGEGQFNEDGSFIGQYT	NF140_067	E15
EDGSFIGQYTVKKDKEETEGNESSE	NF140_068	E16

Table A5 Peptide sequences: Overlapping library for NF155 and positive control

Peptide Sequence	Name	Spot
IEIPMDLTQPPTITKQSAKDHIVDP	NF155_001	F01
QSAKDHIVDPRDNILIECEAKGNPA	NF155_002	F02
IECEAKGNPAPSFHWTRNSRFFNIA	NF155_003	F03
TRNSRFFNIAKDPRVSMRRRSGTLV	NF155_004	F04
SMRRRSGTLVIDFRSGGRPEEYEGE	NF155_005	F05
GGRPEEYEGEYQCFARNKFGTALSN	NF155_006	F06
RNKFGTALSNRIRLQVSKSPLWPKE	NF155_007	F07
VSKSPLWPKENLDPVVVQEGAPLTL	NF155_008	F08
VVQEGAPLTLQCNPPPGLPSPVIFW	NF155_009	F09
PGLPSPVIFWMSSSMEPITQDKRVS	NF155_010	F10
EPITQDKRVSQGHNGDLYFSNVMLQ	NF155_011	F11
DLYFSNVMLQDMQTDYSCNARFHFT	NF155_012	F12
YSCNARFHFTHTIQQKNPFTLKVLT	NF155_013	F13
KNPFTLKVLTNHPYNDSSLRNHPDM	NF155_014	F14
DSSLRNHPDMYSARGVAERTPSFMY	NF155_015	F15
VAERTPSFMYPQGTASSQMVLRGMD	NF155_016	F16
SSQMVLRGMDLLLECIASGVPTPDI	NF155_017	F17
IASGVPTPDIAWYKKGGDLPSDKAK	NF155_018	F18
GGDLPSDKAKFENFNKALRITNVSE	NF155_019	F19
KALRITNVSEEDSGEYFCLASNKMG	NF155_020	F20
YFCLASNKMGSIRHTISVRVKAAPY	NF155_021	F21
ISVRVKAAPYWLDEPKNLILAPGED	NF155_022	F22
KNLILAPGEDGRLVCRANGNPKPTV	NF155_023	F23
RANGNPKPTVQWMVNGEPLQSAPPN	NF155_024	F24

GEPLQSAPPNPNREVAGDTIIFRDT	NF155_025	G01
AGDTIIFRDTQISSRAVYQCNTSNE	NF155_026	G02
AVYQCNTSNEHGYLLANAFVSVLDV	NF155_027	G03
ANAFVSVLDVPPRMLSPRNQLIRVI	NF155_028	G04
SPRNQLIRVILYNRTRLDCPFFGSP	NF155_029	G05
RLDCPFFGSPIPTLRWFKNGQGSNL	NF155_030	G06
WFKNGQGSNLDGGNYHVYENGSLEI	NF155_031	G07
HVYENGSLEIKMIRKEDQGIYTCVA	NF155_032	G08
EDQGIYTCVATNILGKAENQVRLEV	NF155_033	G09
KAENQVRLEVKDPTRIYRMPEDQVA	NF155_034	G10
IYRMPEDQVARRGTTVQLECRVKHD	NF155_035	G11
VQLECRVKHDPSLKLTVSWLKDDEP	NF155_036	G12
TVSWLKDDEPLYIGNRMKKEDDSLT	NF155_037	G13
RMKKEDDSLTIFGVAERDQGSYTCV	NF155_038	G14
ERDQGSYTCVASTELDQDLAKAYLT	NF155_039	G15
DQDLAKAYLTVLGRPDRPRDLELTD	NF155_040	G16
DRPRDLELTDLAERSVRLTWIPGDA	NF155_041	G17
VRLTWIPGDANNSPITDYVVQFEED	NF155_042	G18
TDYVVQFEEDQFQPGVWHDHSKYPG	NF155_043	G19
VWHDHSKYPGSVNSAVLRLSPYVNY	NF155_044	G20
VLRLSPYVNYQFRVIAINEVGSSHP	NF155_045	G21
AINEVGSSHPSLPSERYRTSGAPPE	NF155_046	G22
RYRTSGAPPESNPGDVKGEGTRKNN	NF155_047	G23
VKGEGTRKNNMEITWTPMNATSAFG	NF155_048	G24
TPMNATSAFGPNLRYIVKWRRRETR	NF155_049	H01
IVKWRRRETREAWNNVTVWGSRYVV	NF155_050	H02
VTVWGSRYVVGQTPVYVPYEIRVQA	NF155_051	H03
YVPYEIRVQAENDFGKGPEPESVIG	NF155_052	H04
KGPEPESVIGYSGEDYPRAAPTEVK	NF155_053	H05
YPRAAPTEVKVRVMNSTAISLQWNR	NF155_054	H06
STAISLQWNRVYSDTVGQLREYRAY	NF155_055	H07
VGQLREYRAYYWRESSLLKNLWVSQ	NF155_056	H08
SLLKNLWVSQKRQQASFPGDRLRGV	NF155_057	H09
SFPGDRLRGVVSRLFPYSNYKLEMV	NF155_058	H10

PYSNYKLEMVVVNGRGDGPRSETKE	NF155_059	H11
GDGPRSETKEFTTPEGVPSAPRRFR	NF155_060	H12
GVPSAPRRFRVRQPNLETINLEWDH	NF155_061	H13
LETINLEWDHPEHPNGIMIGYTLKY	NF155_062	H14
GIMIGYTLKYVAFNGTKVGKQIVEN	NF155_063	H15
TKVGKQIVENFSPNQTKFTVQRTDP	NF155_064	H16
TKFTVQRTDPVSRYRFTLSARTQVG	NF155_065	H17
FTLSARTQVGSGEAVTEESPAPPNE	NF155_066	H18
TEESPAPPNEAYTNNQADIATQGWF	NF155_067	H19
QADIATQGWFIGLMCAIALLVLILL	NF155_068	H20
AIALLVLILLIVCFIKRSRGGKYPV	NF155_069	H21
KRSRGGKYPVREKKDVPLGPEDPKE	NF155_070	H22
VPLGPEDPKEEDGSFDYSDEDNKPL	NF155_071	H23
DYSDEDNKPLQGSQTSLDGTIKQQE	NF155_072	H24
SLDGTIKQQESDDSLVDYGEGGEGQ	NF155_073	I01
VDYGEGGEGQFNEDGSFIGQYTVKK	NF155_074	I02
SFIGQYTVKKDKEETEGNESSEATS	NF155_075	I03
GPEDPKEEDGSFDYSDEDNKPLQGS	**Positive Control 1** (Anti-NF_1)	K01
DEDNKPLQGSQTSLDGTIKQQESDD	**Positive Control 2** (Anti-NF_2)	K02

Table A6 Peptide sequences: Overlapping library for Cortactin

Peptide Sequence	Name	Spot
MWKASAGHAVSIAQDDAGADDWETD	Cort_001	M01
DAGADDWETDPDFVNDVSEKEQRWG	Cort_002	M02
DVSEKEQRWGAKTVQGSGHQEHINI	Cort_003	M03
GSGHQEHINIHKLRENVFQEHQTLK	Cort_004	M04
NVFQEHQTLKEKELETGPKASHGYG	Cort_005	M05
TGPKASHGYGGKFGVEQDRMDKSAV	Cort_006	M06
EQDRMDKSAVGHEYQSKLSKHCSQV	Cort_007	M07
SKLSKHCSQVDSVRGFGGKFGVQMD	Cort_008	M08
FGGKFGVQMDRVDQSAVGFEYQGKT	Cort_009	M09
AVGFEYQGKTEKHASQKDYSSGFGG	Cort_010	M10

QKDYSSGFGGKYGVQADRVDKSAVG	Cort_011	M11
ADRVDKSAVGFDYQGKTEKHESQRD	Cort_012	M12
KTEKHESQRDYSKGFGGKYGIDKDK	Cort_013	M13
GGKYGIDKDKVDKSAVGFEYQGKTE	Cort_014	M14
VGFEYQGKTEKHESQKDYVKGFGGK	Cort_015	M15
KDYVKGFGGKFGVQTDRQDKCALGW	Cort_016	M16
DRQDKCALGWDHQEKLQLHESQKDY	Cort_017	M17
LQLHESQKDYKTGFGGKFGVQSERQ	Cort_018	M18
GKFGVQSERQDSAAVGFDYKEKLAK	Cort_019	M19
GFDYKEKLAKHESQQDYSKGFGGKY	Cort_020	M20
DYSKGFGGKYGVQKDRMDKNASTFE	Cort_021	M21
RMDKNASTFEDVTQVSSAYQKTVPV	Cort_022	M22
SSAYQKTVPVEAVTSKTSNIRANFE	Cort_023	M23
KTSNIRANFENLAKEKEQEDRRKAE	Cort_024	M24
KEQEDRRKAEAERAQRMAKERQEQE	Cort_025	N01
RMAKERQEQEEARRKLEEQARAKTQ	Cort_026	N02
LEEQARAKTQTPPVSPAPQPTEERL	Cort_027	N03
PAPQPTEERLPSSPVYEDAASFKAE	Cort_028	N04
YEDAASFKAELSYRGPVSGTEPEPV	Cort_029	N05
PVSGTEPEPVYSMEAADYREASSQQ	Cort_030	N06
ADYREASSQQGLAYATEAVYESAEA	Cort_031	N07
TEAVYESAEAPGHYPAEDSTYDEYE	Cort_032	N08
AEDSTYDEYENDLGITAVALYDYQA	Cort_033	N09
TAVALYDYQAAGDDEISFDPDDIIT	Cort_034	N10
ISFDPDDIITNIEMIDDGWWRGVCK	Cort_035	N11
DDGWWRGVCKGRYGLFPANYVELRQ	Cort_036	N12

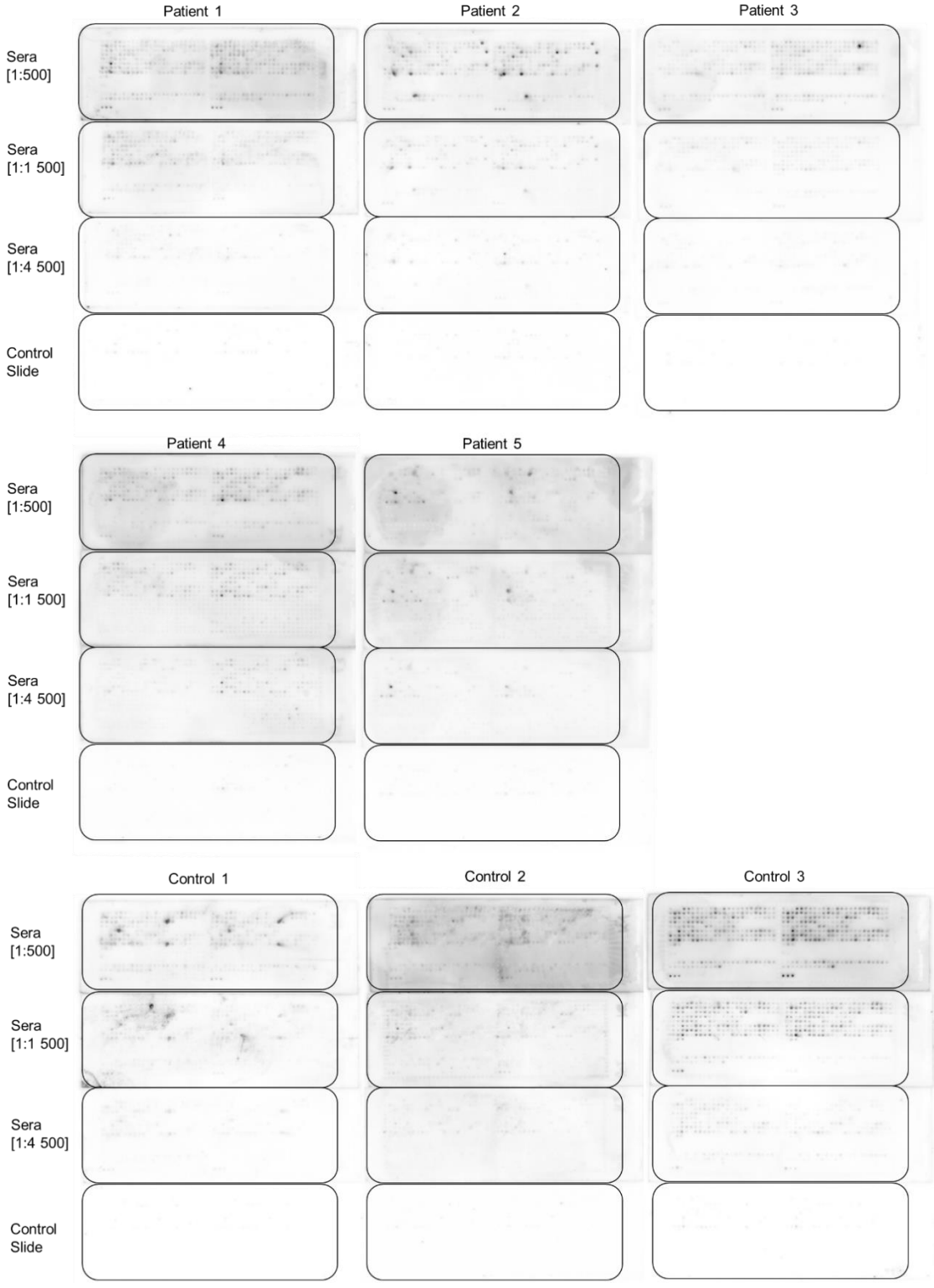

Figure A1 Studying Sera of Patients and Healthy Controls in Microarray Format (Raw Data)

For each patient sample as well as for each healthy control four slides were prepared. The upper three slides show the respective results for sera in descending concentration, the lower one is the control slide, with no sera incubated, only secondary antibody. The received patterns are reproducible and sample specific.

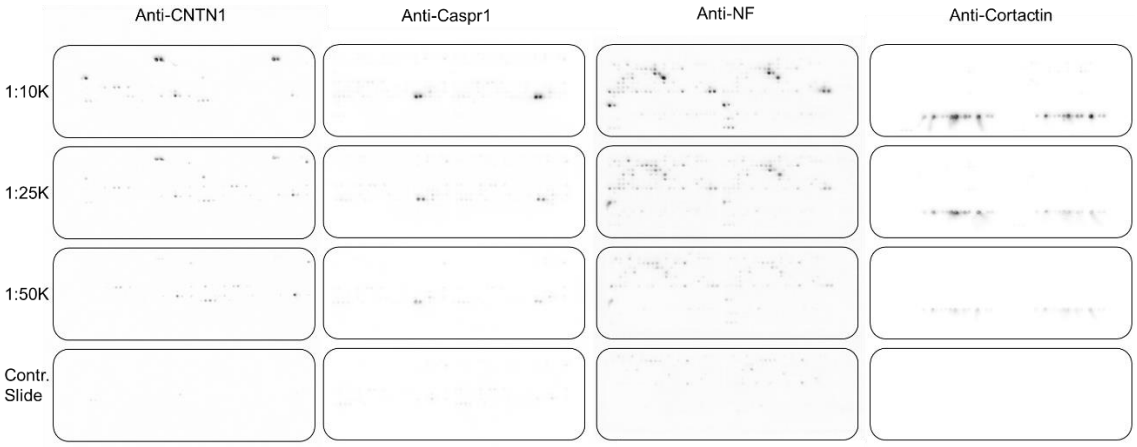

Figure A2 Overview of Fine Mapping of Anti-CNTN1, Anti-Caspr1, Anti-NF and Anti-Cortactin (Raw Data)

Results of dilution series of anti-CNTN11 (ab66265), anti-Caspr1 (ab34151), anti-NF (ab31457) and anti-Cortactin (TA590298) was done (n=3). Control slides are included. Anti-CNTN1 and anti-Caspr1 were tested on “CC” microarrays, anti-NF and anti-Cortactin on “NC” microarrays (see Table 5).

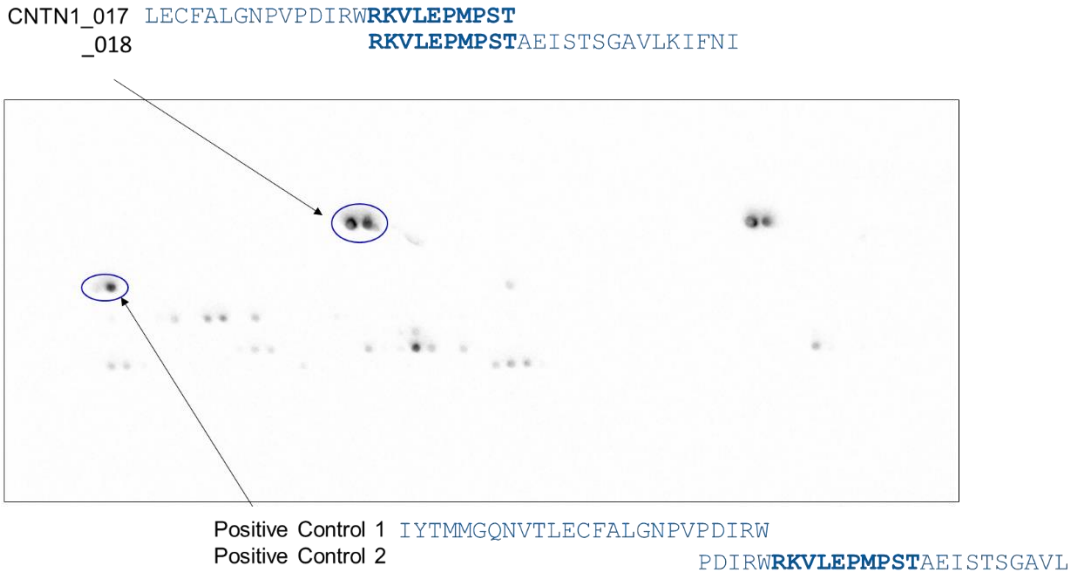

Figure A3 Details of Anti-CNTN1 (ab66265) Fine Mapping (Raw Data)

The slide shows the results received from 1:10 000 diluted anti-CNTN1. Spots of the binding epitopes are marked and labeled, the essential amino acid fragment for the interplay is written in bold.

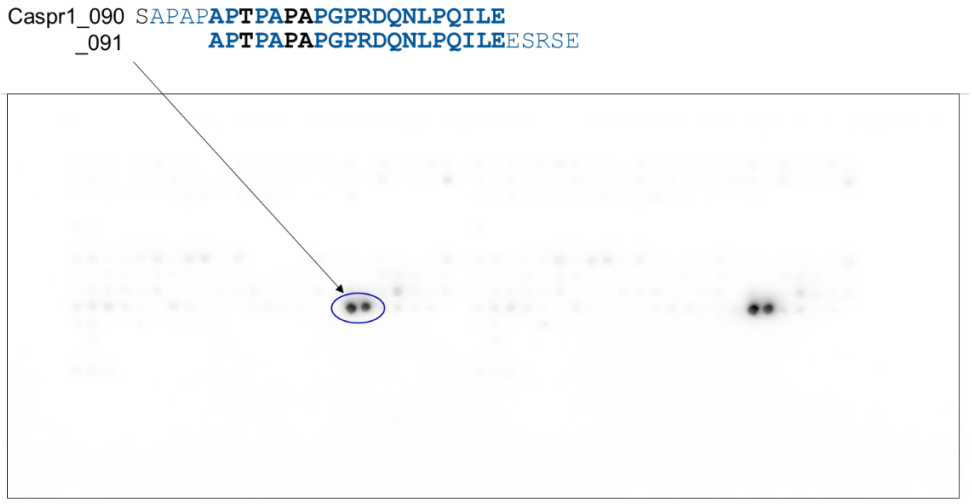

Figure A4 Details of Anti-Caspr1 (ab34151) Fine Mapping (Raw Data)

The slide shows the results received from 1:10 000 diluted anti-Caspr1. The two marked spots show the highest signal intensity by far, the epitope essential for binding is written in bold.

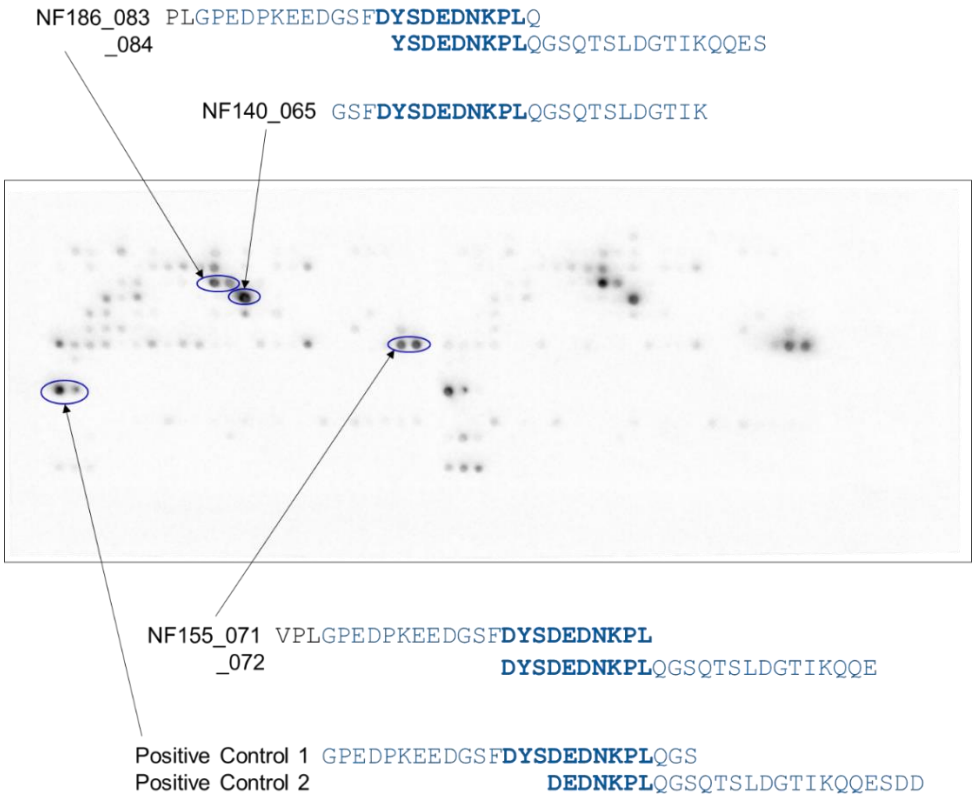

Figure A5 Details of Anti-NF (ab31457) Fine Mapping (Raw Data)

The slide shows the results received from 1:10 000 diluted anti-NF. The peptide fragments of the framed spots are displayed, with the common sequence being crucial for binding written in bold.

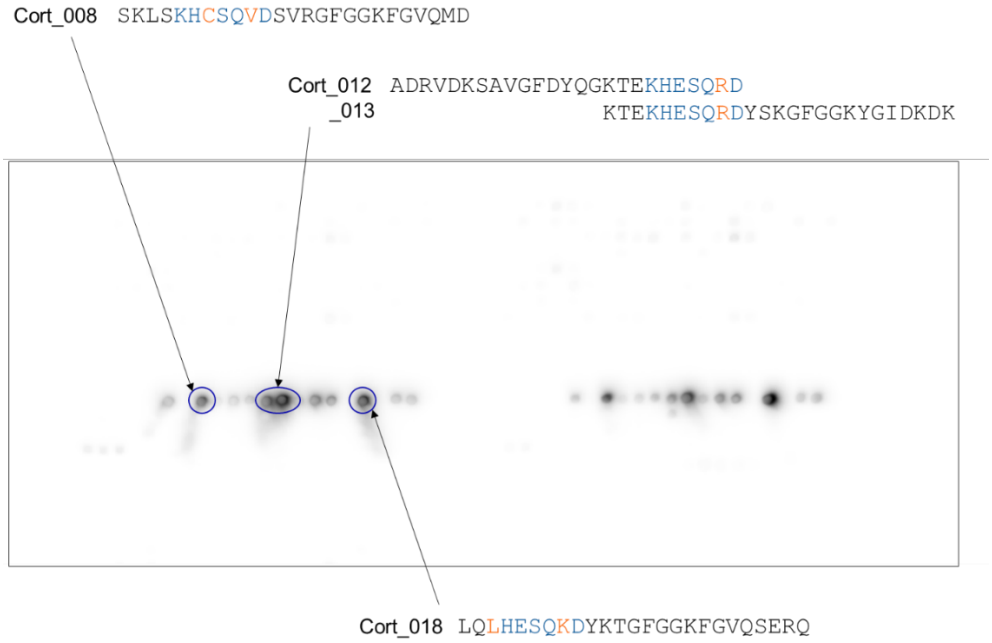

Figure A6 Details of Anti-Cortactin (TA590298) Fine Mapping (Raw Data)

The slide shows the results received from 1:10 000 diluted anti-Cortactin. The four spots with the strongest signal are marked, their amino acid sequence is compared.

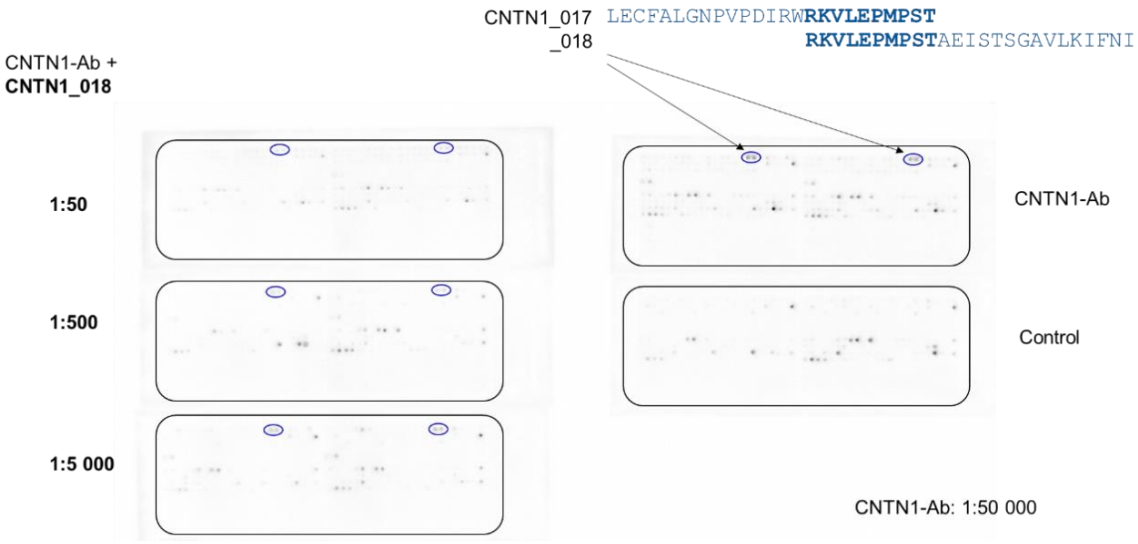

Figure A7 Neutralization of CNTN1 Binding Events with CNTN1_018 (Raw Data)

Preincubation of anti-CNTN1 (ab66265) with soluble peptide fragment CNTN1_018 in different concentrations is shown on the left, incubation of primary antibody without peptide fragment as well as a control slide on the right. The region of interest is marked blue.

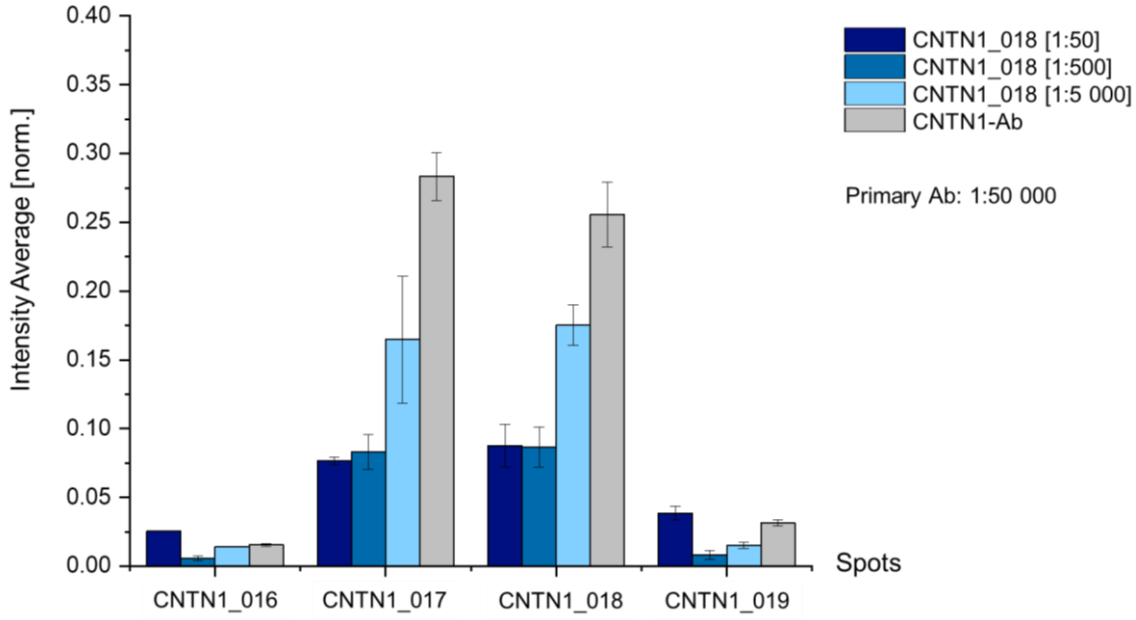

Figure A8 Chart of Anti-CNTN1 (ab66265) Neutralization with CNTN1_018

Results shown in Figure A7 are transferred to a bar graph. Normalized intensity average on y-scale, spots on x-scale. Error bars show the deviations between the duplicates of the respective slides.

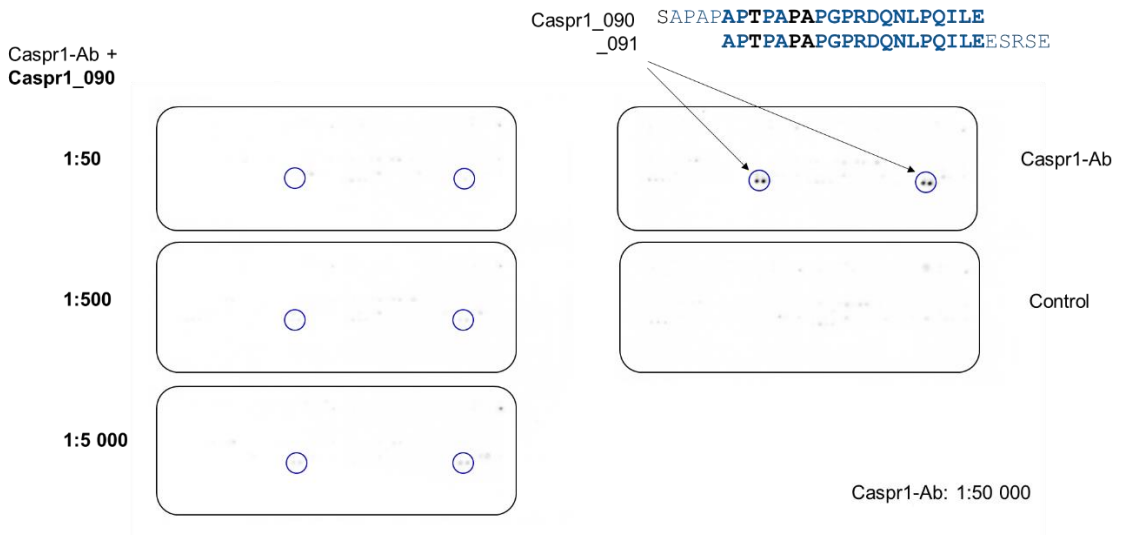

Figure A9 Neutralization of Caspr1 Binding Events with Caspr1_090 (Raw Data)

Anti-Caspr1 (ab34151) got incubated with soluble peptide fragment CNTN1_018 in descending concentrations (shown on the left). Incubation without peptide fragment as well as a control slide is displayed on the right. The blue marked spots show the binding epitope.

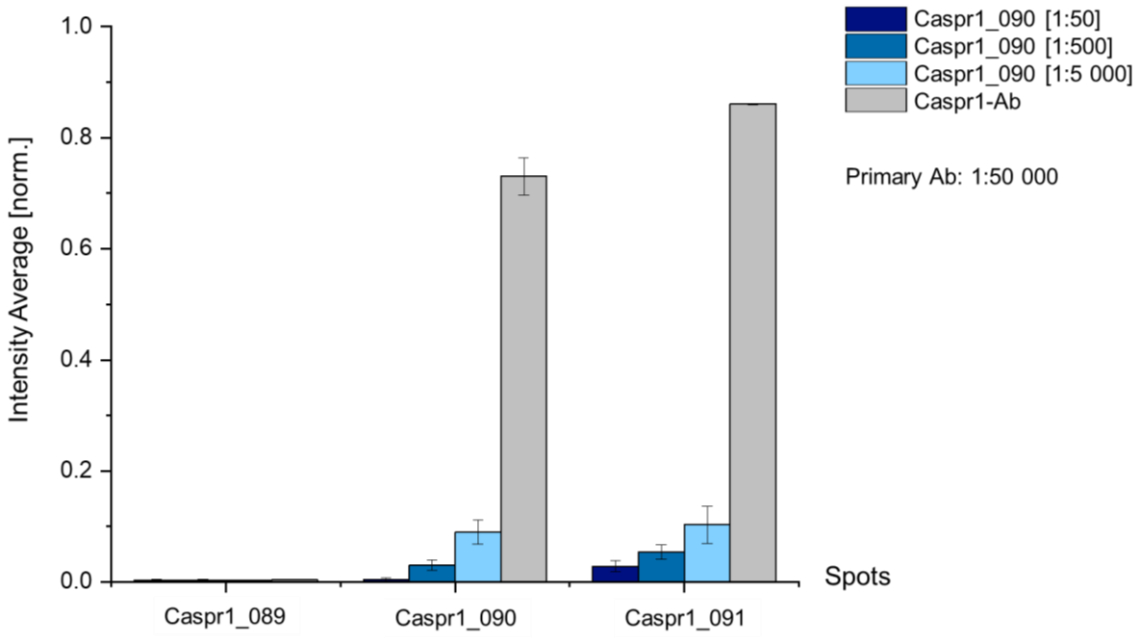

Figure A10 Chart of Anti-Caspr1 (ab34151) Neutralization with Caspr1_090

This bar chart shows the results of Figure A9. Normalized intensity average on y scale, spots on x-scale. Error bars show the deviations between the duplicates of the respective slides.

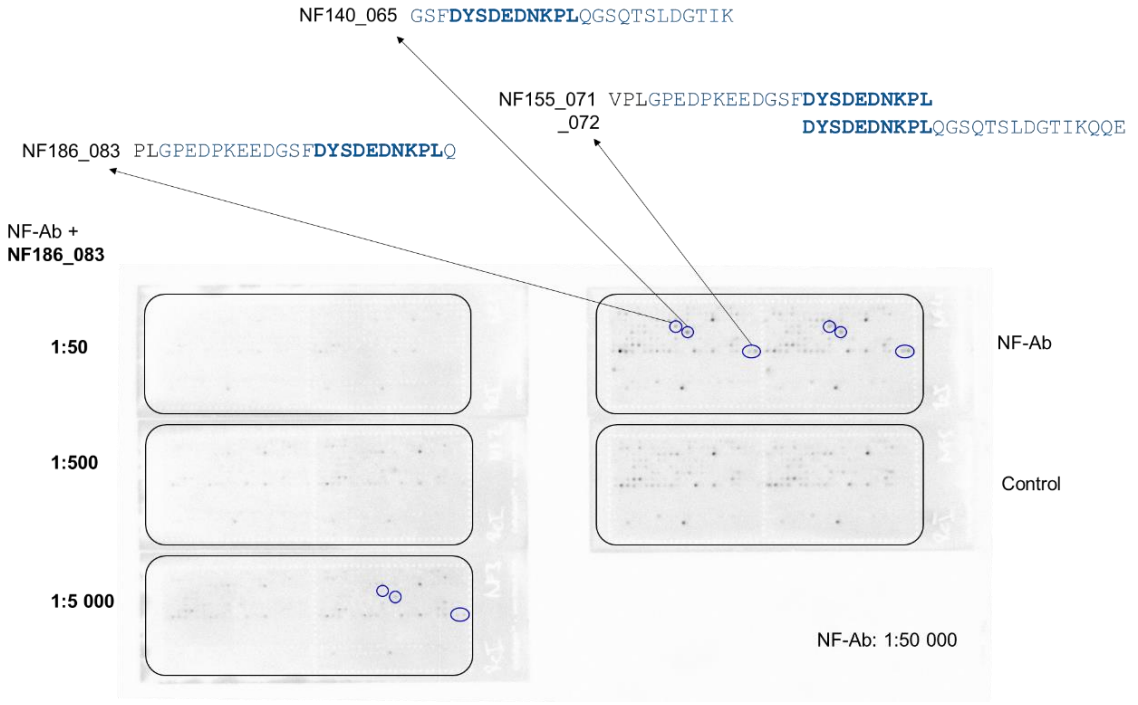

Figure A11 Neutralization of NF Binding Events with NF186_083 (Raw Data)

NF186_083 in different dilutions got incubated with primary antibody (anti-NF, ab31457), corresponding slides are displayed on the left. Signals received from primary antibody without peptide as well as signals received from control slide are shown on the right. The binding spots are marked.

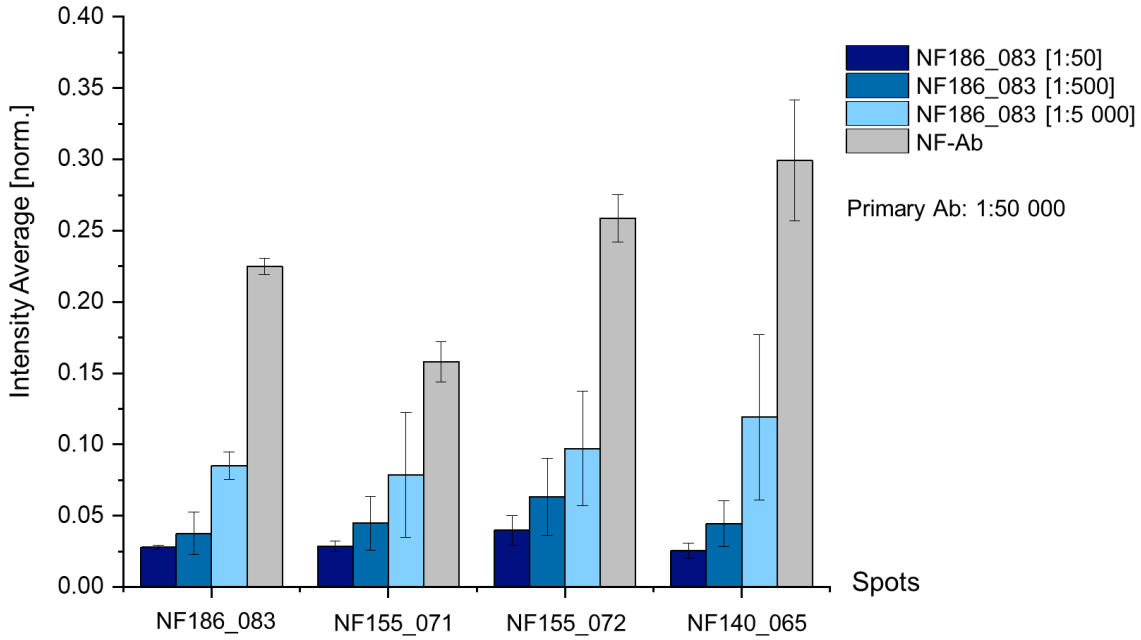

Figure A12 Chart of Anti-NF (ab31457) Neutralization with NF186_083

This bar chart shows the results of Figure A11. Normalized intensity average on y scale, spots on x-scale. Error bars show the deviations between the duplicates of the respective slides.

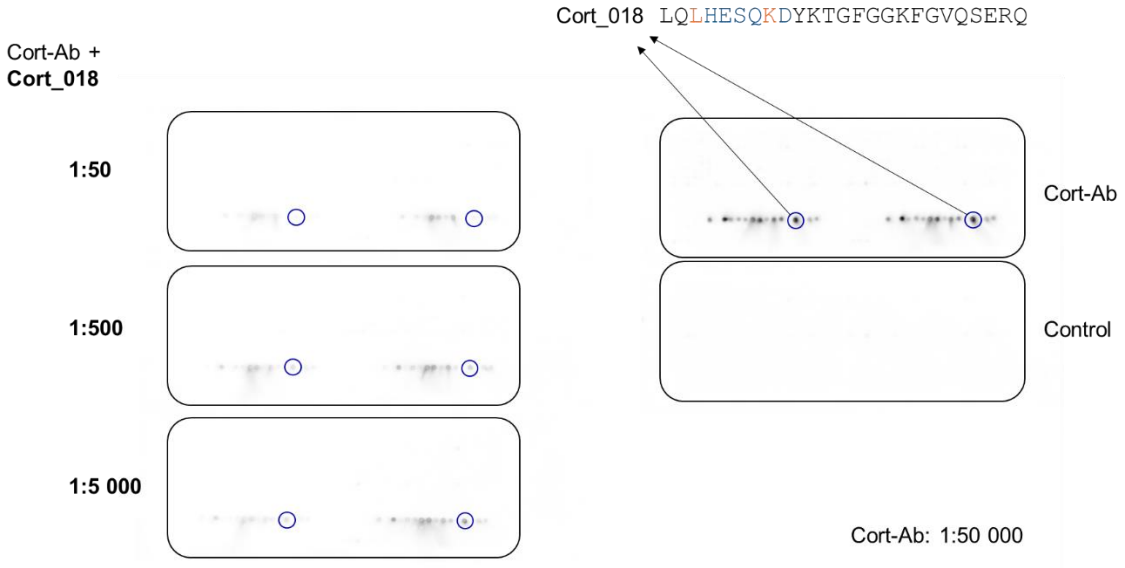

Figure A13 Neutralization of Cortactin Binding Events with Cort_018 (Raw Data)

Incubation of anti-Cortactin (TA590298) with Cort_018 in different concentration. For comparing, signals received from primary antibody without peptide as well as a control slide are included on the right. The peptide used for neutralization is marked on the slides.

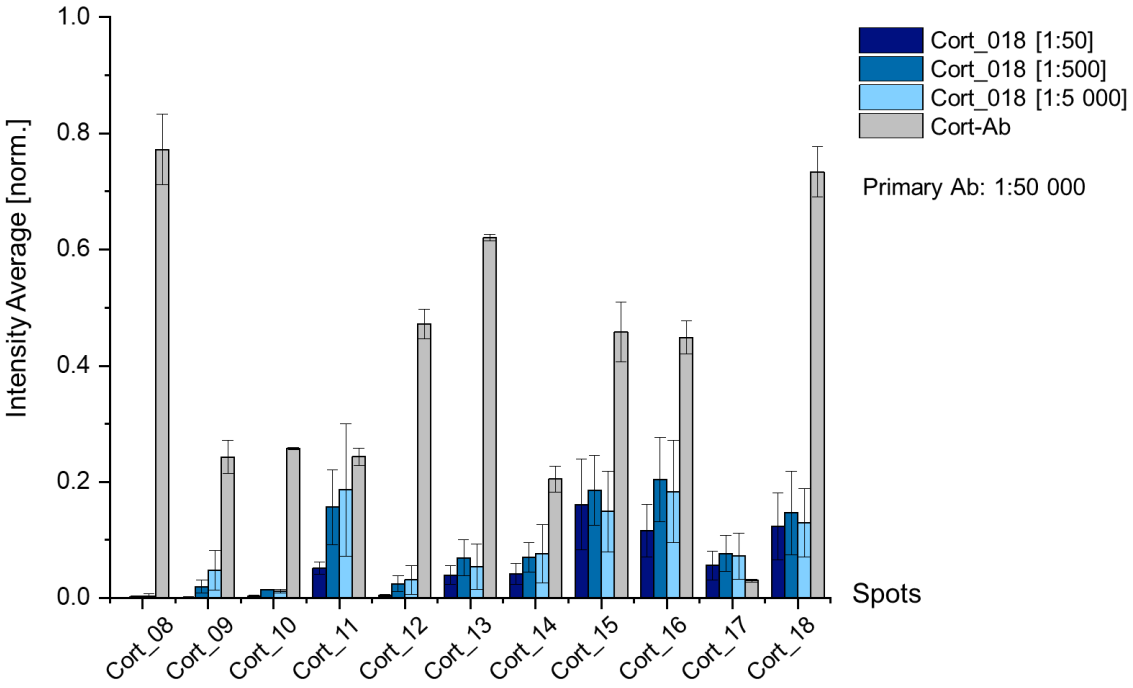

Figure A14 Chart of Anti-Cortactin (TA590298) Neutralization with Cort_018

This bar chart shows the results of Figure A13. Normalized intensity average on y scale, spots on x-scale. Error bars show the deviations between the duplicates of the respective slides.

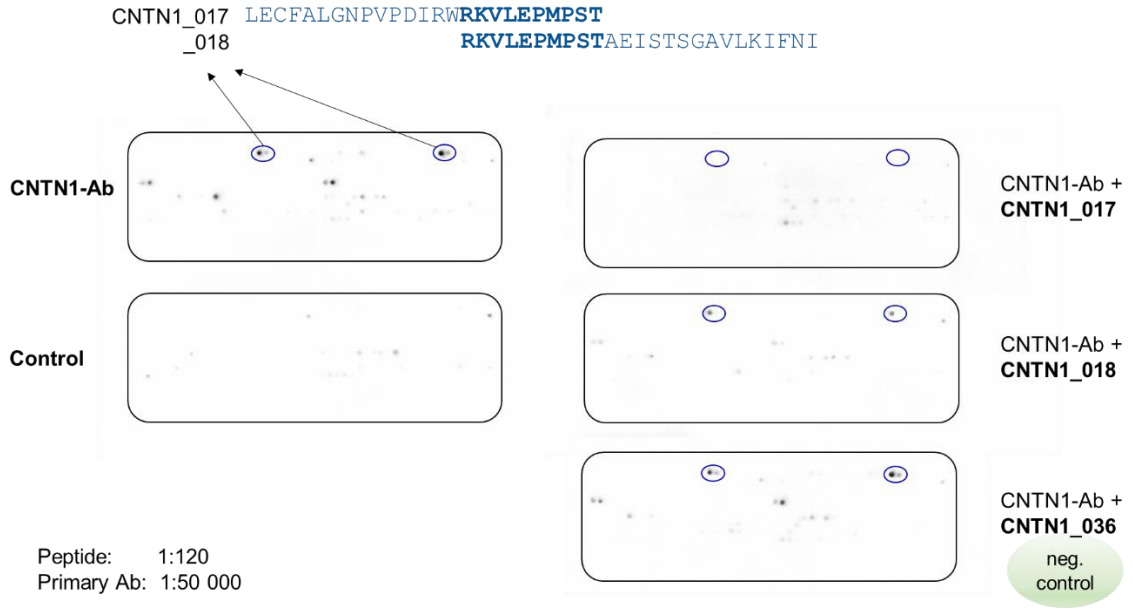

Figure A15 Validation of Anti-CNTN1 (ab66265) Neutralization (Raw Data)

Three different soluble peptides got incubated with anti-CNTN1, CNTN1_036 acts as a negative control (slides shown on the right side). On the left a slide incubated with no peptide, just primary antibody, as well as a control slide is included. The framed spots show the region of interest.

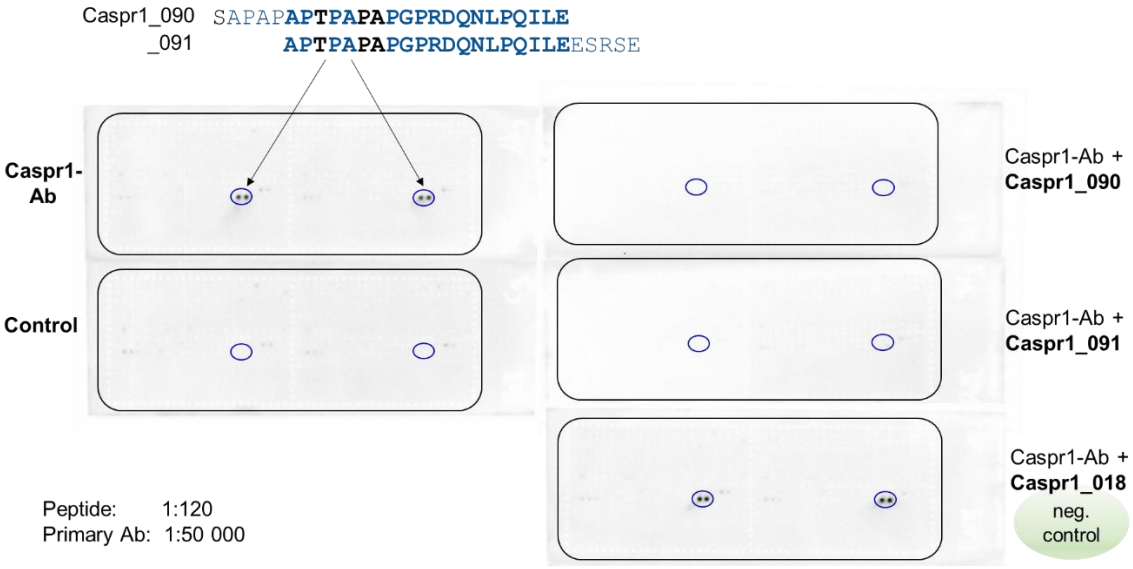

Figure A16 Validation of Anti-Caspr1 (ab34151) Neutralization (Raw Data)

Incubation of anti-Caspr1 without peptide as well as a control slide is shown on the left. The right part of the picture displays the results of incubation with Caspr1_090, Caspr1_091 or Caspr1_018, the last one acting as a negative control. The last two spots of the Caspr1 library (see Table A2) are marked.

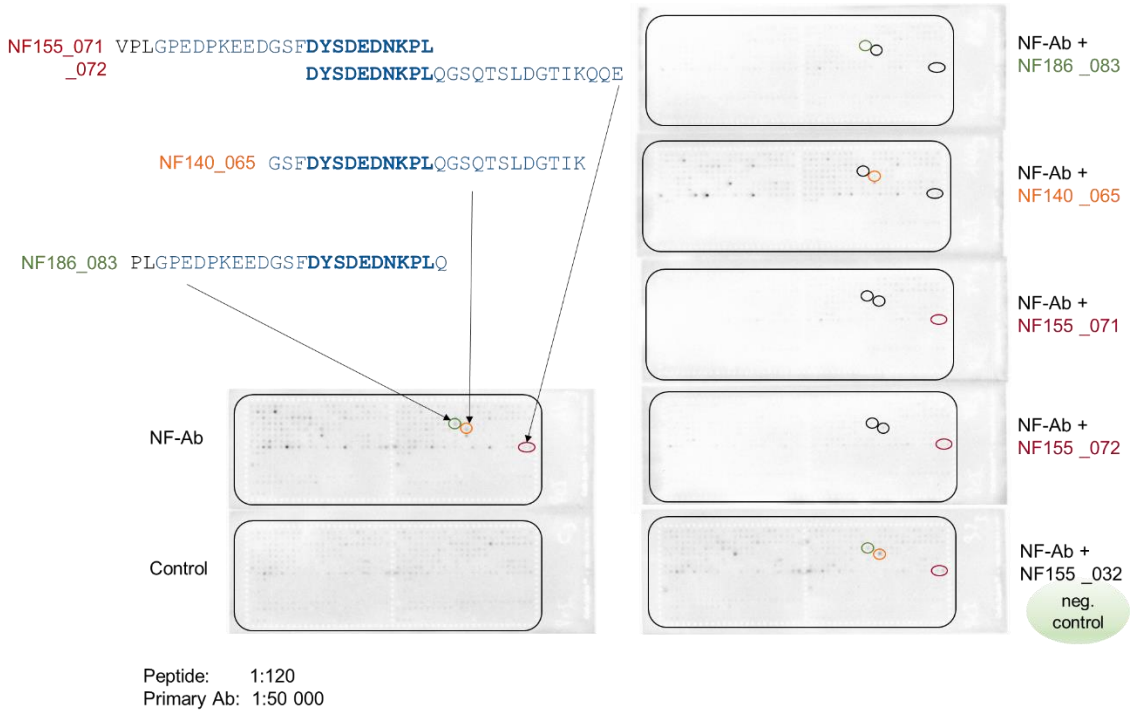

Figure A17 Validation of Anti-NF (ab31457) Neutralization (Raw Data)

The slides on the left show incubation with anti-NF or rather with only secondary antibody (control slide). On the right sight the microarrays incubated with distinct peptide fragments are represented. The lower slide is a negative control. The respective spots of the peptides synthesized again and taken for neutralization are marked.

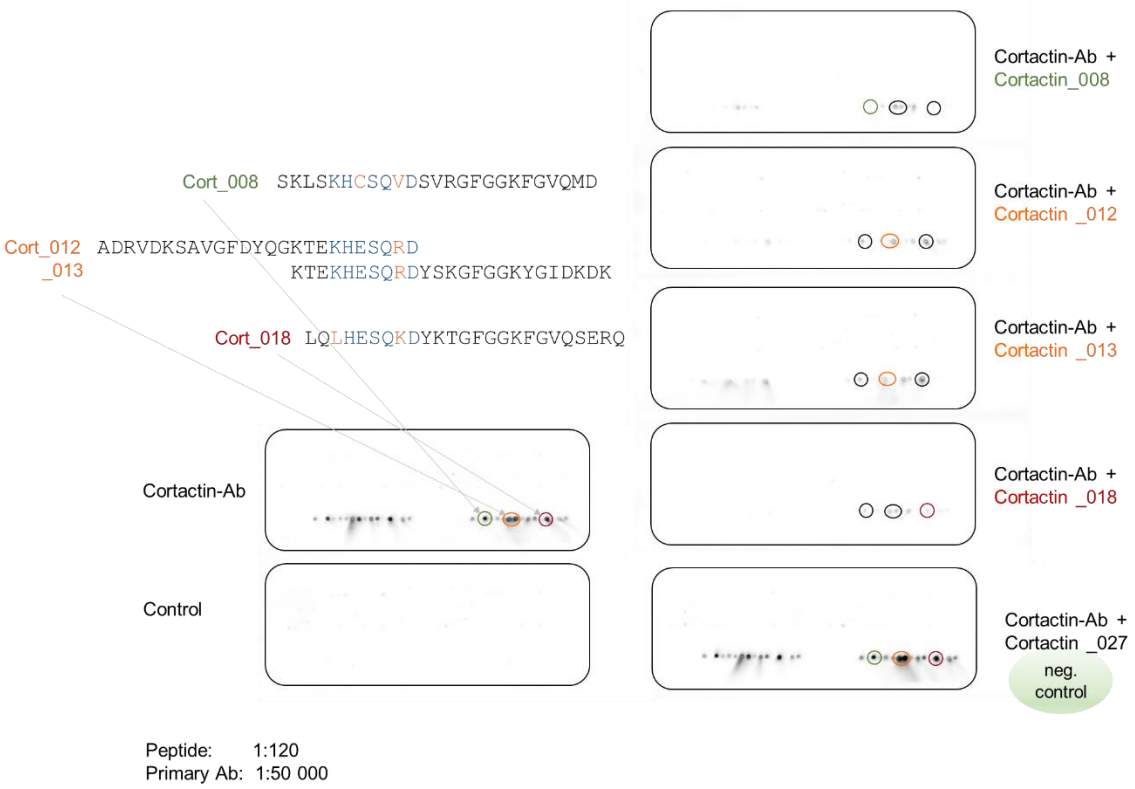

Figure A18 Validation of Anti-Cortactin (TA590298) Neutralization (Raw Data)

Incubation with anti-Cortactin together with five different peptides, one acting as a negative control, is shown on the right. Results received from primary antibody on its own as well as a control slide are displayed on the left. Peptides chosen for neutralization are marked on the microarrays.

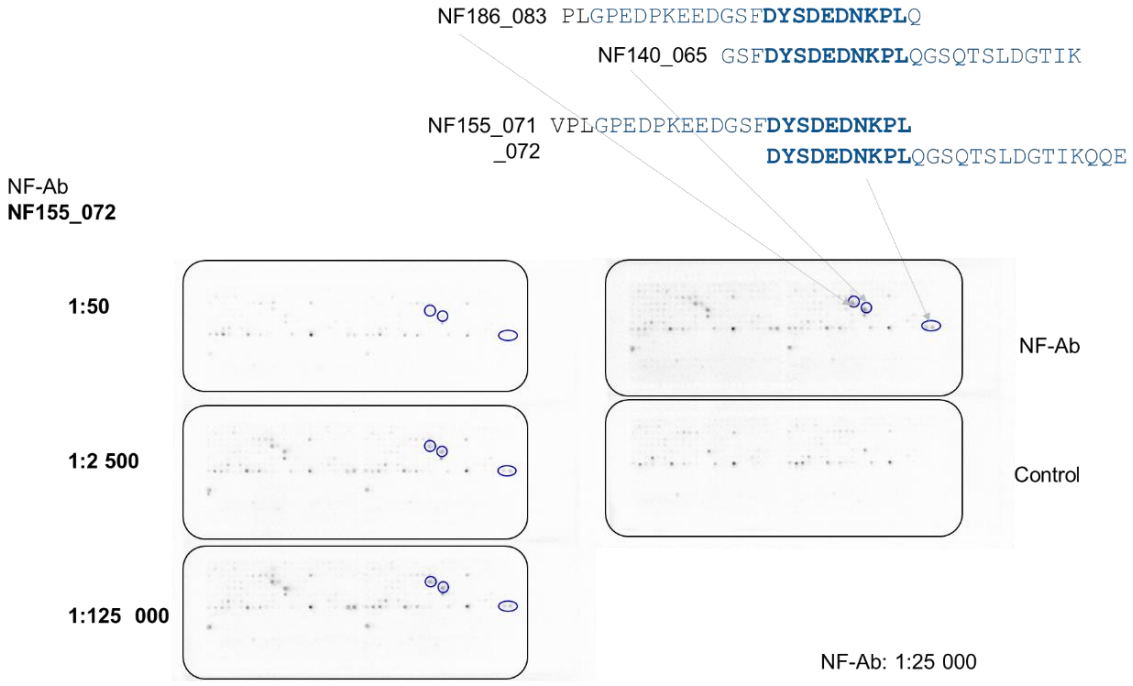

Figure A19 Neutralizing Dilution Series with NF155_072 (Raw Data)

NF155_072 was diluted in three steps up to 1:125 000, each dilution got incubated with anti-NF (ab31457) (slides shown on the left). Anti-NF on its own as well as a control slide are included on the right. The epitopes essential for binding are framed.

II List of Abbreviations

AA	Amino acid(s)
ACh	Acetylcholine
AChR	Acetylcholine receptor
APC	Adenomatous polyposis coli
BSA	Bovine serum albumin
Caspr1	Contactin associated protein 1
CIDP	Chronic inflammatory demyelinating polyradiculoneuropathy
CNTN1	Contactin 1
Dok7	Downstream of tyrosine kinase 7
dSNMG	Double-seronegative myasthenia gravis
ELISA	Enzyme-linked immunosorbent assay
Fmoc	9-Fluorenylmethyloxycarbonyl
GBS	Guillain-Barré syndrome
HRP	Horseradish peroxidase
K_v	Potassium channel
LRP4	Lipoprotein receptor-related protein 4
MG	Myasthenia gravis
MS	Multiple sclerosis
MuSK	Muscle-specific kinase
Na_v	Voltage-gated sodium channel
NF	Neurofascin
NrCAM	Neuronal cell adhesion molecule
PBS	Phosphate-buffered saline
PCC	Peptide-cellulose conjugate
PE	Plasma exchange
PNP	Polyneuropathy
PNS	Peripheral nervous system
RT	Room temperature
SPPS	Solid-phase peptide synthesis
Tid1	Tumorous imaginal disc 1
Tris	Tris(hydroxymethyl)-aminomethan
Tween 20	Polysorbat 20
VGCC	Voltage gated calcium channel

III List of Figures

Figures - Appendix

IV List of Tables

Tables - Appendix

V Acknowledgements

VI Curriculum Vitae